Anonymous Referee #1

Received and published: 3 June 2015

Overall comments:

This study investigates the results of five-year sampling measurements of long-lived greenhouse gases (i.e. CO_2, CH_4, N_2O, and SF_6) and trace gases (i.e. CO and H_2) at three stations (Hanle, Pondicherry, and Port Blair) located in India. By the compounds in the collected air samples that measured by different analytical techniques, many approaches are made to investigate the regional features of the target compounds. The authors have characterized these trace gases with delta value ratios at these stations in different seasons. The data at numeric stations over Europe and the United States are also estimated and discussed.

My overall feeling to this manuscript is that all the target compounds are put together for discussion but little is mentioned regarding the relationship between them, especially for N_2O, SF_6, and H_2. What are the integrated findings that these compounds can together indicate? The authors are required to make more efforts to describe the scientific connections between these compounds. If the authors cannot adequately find major contribution of N_2O, SF_6, and H_2 that are relevant with other compounds, I would suggest remove them from this manuscript.

In addition, from the description and data presented in this manuscript, the PON site seemed to be easily influenced by local emissions, e.g. Pondicherry city with a population of ~240,00 at a distance of 8 km southward and a four-lane highway at ~80 m to the station. These can make the station not able to act as the regional background representative for the trace gases, especially for CO. I would suggest filter out the data that are possibly polluted significantly by local emissions at PON.

I suggest that this manuscript can get warranty for publication if these issues can be carefully revised or improved.

[Response] Thanks very much for your careful review and comments.

For the first general comment, in this study, we present the flask measurements of four GHG species (CO_2, CH_4, N_2O, SF_6) and two additional trace gases (CO, H_2) at three Indian stations. We put them together for several reasons. First, emissions of all the four GHG species contribute to global warming, and regularly reporting emissions and removals of these gases is required by the United Nations Framework Convention on Climate Change (UNFCCC). Although CO and H_2 are not greenhouse gas by themselves, both of them play critical roles in the CH_4 budget as products of CH_4 oxidation and as competitors through reaction with the free OH radicals (Ehhalt and Rohrer, 2009). Besides, CO and H_2 are good tracers for

biomass/biofuel burning (Andreae and Merlet, 2001), an important source of GHG emissions that is quite extensive in India (Streets et al., 2003; Yevich and Logan, 2003).

Second, the importance of N_2O and SF_6 also rests in the fact that their emission patterns in India notably differ from those of the USA and Western Europe, where estimates of GHG budgets are better known and more accurate. As suggested by *Section 3.1.3*, there are substantial N_2O emission sources in the Indian subcontinent, most of which contributed by agricultural activities. SF_6 is widely considered as a good tracer for anthropogenic activities because it is extremely stable with purely anthropogenic sources (Maiss et al., 1996). While India ranked as the world's third largest GHG emitter in 2010 (EDGAR v4.2), unlike the USA and EU countries, its SF_6 emissions are rather weak as suggested by *Section 3.1.4*.

Last but not least, for all the trace gases, the variations of concentrations are influenced by atmospheric transport, including circulation of the monsoon system. For example, as shown in *Section 3.1.2* and *Section 3.1.3*, the summer maximum observed at HLE for both CH_4 and N_2O are likely related to the deep convection that is associated with the SW monsoon and mixes surface emissions of both species (and probably others) into the mid-to-upper troposphere. Following your suggestions, we revised the manuscript and clarify the importance of the trace gases we investigated in the study, especially for N_2O, SF_6, CO and H_2 (Lines 500–508, 587–594, 642–652, 716–722).

For the second general comment, we agree that PON can be influenced by local emissions. Although the highway nearby has a low traffic flow, in-situ measurements at PON (not presented in this paper) do show that this site is heavily polluted by local emissions during nighttime. Therefore, we used two approaches to minimize the influences of local GHG sources/sinks. First, we took flask air samples at PON between 12:00 and 18:00 local time (actually 97% between 12:00 and 14:00 local time), when the sea breeze moves towards land and the boundary layer air is well mixed (see *Section 2.1* for details). The recirculation of continental air mass during the sea breeze period should average regional influences, even though the footprint of PON is less than those of HLE and PBL. Second, when we performed the CCGVU curve-fitting, any data lying outside 3 SD of the residuals were regarded as outliers and discarded from the time series, and this procedure was repeated until no outliers remained (Harris et al., 2000; Zhang et al., 2007) (see *Section 2.3.1* for details). These outliers were likely a result of pollution by local emissions and not representative of regional background concentrations (denoted by crosses in each panel of Fig. 2, 4, 6, 8, 10 and 12). We believe that through these two approaches the local influences at PON should be sufficiently minimized.

Further, following your suggestion, we also tried to use CO as a tracer for local emissions and filtered time series of other species by CO outliers. That means, for each species (other than CO), we removed the samples with abnormal CO values before the curve-fitting procedures. As shown in Table R1 and Fig. R1, filtering time series by CO outliers does not make significant difference to the trends, seasonal cycles and mean annual gradients (relative to

HLE) for other species at this station. On the other hand, however, this filtering approach may substantially decrease the number of samples used to fit the smooth curve (e.g. ~38% for CH_4) and result in larger data gaps (Table R1, Fig. R1), probably compromising reliability of the analyses. Therefore finally we didn't use CO as a tracer of local emissions for additional filtering.

Specific comments:

Introduction: The authors have clearly indicated their research motivation on studying the GHGs in the introduction section. However, little is discussed about the additional trace gases (i.e. CO and H_2). What are the relationships between the GHGs and the additional trace gases scientifically? Please also address the importance of CO and H_2 for this study.

[Response] As we replied to your general comment #1, although CO and H_2 are not greenhouse gas by themselves, both of them play critical roles in the CH_4 budget as products of CH_4 oxidation and as competitors through reaction with the free OH radicals (Ehhalt and Rohrer, 2009). Besides, CO and H_2 are good tracers for biomass/biofuel burning (Andreae and Merlet, 2001), an important source of GHG emissions that is quite extensive in India (Streets et al., 2003; Yevich and Logan, 2003). Following your suggestions, we revised the manuscript and clarify the importance of CO and H_2 at the beginning of *Section 3.1.5* and *Section 3.1.6* (Lines 642–652, 716–722)

Section 2: Please provide the data availability. For example, the website of the data provided by LSCE, NOAA, aircraft measurements, etc.

[Response] Following your suggestion, we added in the manuscript the websites for the data from the NOAA and ICOS networks, as well as the CONTRAIL and CARIBIC projects. The dataset of flask measurements at Hanle, Pondicherry and Port Blair will be made available in the near future on the World Date Centre for Greenhouse Gases (WDCGG) website (http://ds.data.jma.go.jp/gmd/wdcgg/).

Figure 1: Not just CO_2 being discussed in this manuscript. Therefore I think the elevation of a trajectory is more important than its CO_2 level in this figure. By doing so, the 3-D traveling routes of air masses can be clearly viewed, which also can provide useful information for other trace gases. The authors can try to merge the vertical data of the trajectories in Figure S5 into Figure 1.

[Response] Follow your suggestion, we revised Fig. 1 and colored the back-trajectories by elevations of air masses instead of CO_2 levels. Additionally, following Reviewer #2's suggestion, we also added an extra panel (Fig. 1b) zoomed over India to show locations of the three stations and terrain.

Section 2.2.2: It seems that there were three channels for separating respective compound pairs (i.e. channel #1: CO_2 and CH_4, channel #2: N_2O and SF_6, channel #3: CO and H_2). However, the descriptions are given based on different part of a GC technique (e.g. sample loop, column, detector, etc.), which is quite easy to get readers confused. In order to improve the readability, the authors are encouraged to rephrase this paragraph based on different compound pairs.

[Response] Following your suggestion, we revised the second paragraph of *Section 2.2.2* to improve readability (Lines 259–272).

Page 7181 Line 24: stemmed

[Response] Follow your suggestion, we revised it.

Figure 2: The 4 subplots are recommended to be merged into 1 or 2 plots. This comment also applies to Figure 4, 6, 8, 10, and 12.

[Response] Thanks a lot for your suggestion. We did this previously as you suggested. However, in this way data points and smoothed curves from different stations overlap heavily. To better display contrasts between pairs of stations in trends, annual gradients and seasonal cycles, we didn't revise the plots.

Figure 3: The CO_2 levels are shown in relative scales. What are those "zeros" on the y-scale representing? Please clarify. Furthermore, the mean seasonal variations can contain some errors obtained from the increasing trends. In order to avoid this, the authors can estimate the detrended seasonal curves by subtracting the growth rates.

[Response] As we mentioned in *Section 2.3.1* (Lines 333–337), a smoothed function was fitted to the retained data, consisting of a first-order polynomial for the growth rate and two harmonics for the annual cycle (Levin et al., 2002; Ramonet et al., 2002), as well as a low pass filter with 80 and 667 days as short-term and long-term cutoff values, respectively (Bakwin et al., 1998). The mean seasonal cycles we present at Fig. 3 (and many others) are already detrended by removing the growth rates. That's why we have "zeros" on the y-axes. We revised the caption to make it more clear and precise.

Figure 3(b): There are three lines in the figure, but only two are shown in the legend.

[Response] Following your suggestion, we revised it.

Page 7186 Line 11: How good is the agreement between the flask measurements at HLE and aircraft measurements over New Delhi? Please quantify.

[Response] The correlation coefficients between harmonics of the mean seasonal cycles derived from the flask measurements at HLE and the CONTRAIL measurements over Delhi are 0.98–0.99 ($p<0.001$). We also added this information in the text (Line 395).

Page 7186 Line 29: than those at HLE by . . .

[Response] Following your suggestion, we revised it.

Page 7188 Line 24 “The annual mean N_2O mole fraction at HUN was higher than at Mauna Loa (MLO) and Mace Head (MHD) by only 1.6 and 1.3 ppb, respectively.”: I think this sentence is referring the study at HUN and is irrelevant to this study.

[Response] The HUN (46.95 °N, 16.65 °W, 248 m a.s.l.) station is a rural monitoring station located in Hungary in Central Europe (Haszpra et al., 2008). Here we would like to compare the N_2O gradients observed between PON, PBL and HLE with the typical gradients observed in Europe and the US. As shown in *Section 3.1.3*, results showed that the N_2O gradients between PON, PBL and HLE are larger than typical N_2O gradients observed between stations scattered in Europe or in North America, suggesting substantial N_2O in the Indian subcontinent. Following your suggestion, we removed the N_2O gradient between HUN and MLO. The HUN observations and its gradients to MHD serve as an example to indicate the magnitude of N_2O sources in Central Europe, therefore we think it is relevant to the study and didn’t remove it from the manuscript.

Page 7188 Line 25: I do not think it is necessary to use the data observed at so many stations in this manuscript. It is better to choose just one background station at similar latitude or in nearby region to be compared with the Indian sites. For instance, the authors may choose GMI or MLO as the reference to be compared with PON and PBL. Or use NWR and JUN (Jungfraujoch) as the background reference station for United States and Europe, respectively. This comment is not only for N_2O, but also for other compounds such as SF_6 discussed in other sections.

[Response] Here we chose HLE as a background station simply because it is located in India and closest to PON and PBL. Any gradient in trace gas concentrations between PON, PBL and HLE would suggest regional sources/sinks easily. The principle is also applicable to stations in the USA and Europe used in this study.

Page 7189 Line 17 “more noisy due to regional sources and synoptic variability”: Why is N_2O the only compound influenced by the regional sources and synoptic variability? Why are other compounds like CO_2 and CH_4 not influenced due to the same reasons?

[Response] When we argue that the seasonal cycle of N_2O is noisier compared to CO_2 and CH_4 in the manuscript, it means the N_2O seasonal cycle has a larger uncertainty (i.e. lower signal-to-noise ratio and precision, also indicated by the wide shaded area in Fig. 7). Given that the N_2O seasonal cycle is very small, synoptic events are more likely to mask the seasonal signal. As shown in Table 1, if we take the ratio of the seasonal cycle amplitude to the residual standard deviation (RSD, an indicator of synoptic variability) as a surrogate of the signal-to-noise ratio, we find that this ratio is significantly lower for N_2O (2.0, 1.5 and 2.0 for HLE, PON and PBL) than CO_2 (11.1, 1.9 and 7.1 for HLE, PON and PBL) and CH_4 (3.2, 3.6, 6.3 for HLE, PON and PBL). Following your suggestion, we revised the statement in the manuscript for clarification (Lines 541–542).

Page 7191 Line 14 “the SF_6 mole fractions at HUN over the years of 1997-2007 are higher than those at MLO and MHD by ...” Line 19 “At HFM, the SF_6 mole fractions are higher than those of the NWR on average by 0.15...”: I think these sentences are irrelevant to this study.

[Response] Thanks a lot for your careful review comments. As we replied to your general comment #1, SF_6 is widely considered as a good tracer for anthropogenic activities because it is extremely stable with purely anthropogenic sources (Maiss et al., 1996). As shown in *Section 3.1.4*, the SF_6 gradients between PON, PBL and HLE are slightly negative, whereas the stations in Europe or in North America show positive SF_6 gradients above the background. While India ranked as the world’s third largest GHG emitter in 2010 (EDGAR v4.2), unlike the USA and EU countries, its SF_6 emissions are rather weak. We think the comparisons with stations in the USA and Europe are relevant to this study and didn’t remove it from the manuscript.

Page 7193 Line 13 “The PON and PBL stations are influenced by CO regional emissions, mainly due to biofuel and agricultural burning over South and Southeast Asia.": As mentioned above, I think PON station can be easier affected by local emissions from the Pondicherry city or the four-lane high way nearby.

[Response] As we replied to your general comment #2, we agree that PON can be influenced by local emissions. Although the highway nearby has a low traffic flow, in-situ measurements at PON (not presented in this paper) do show that this site is heavily polluted by local emissions during nighttime. Therefore, we used two approaches to minimize the influences of local GHG sources/sinks. First, we took flask air samples at PON between 12:00 and 18:00 local time (actually 97% between 12:00 and 14:00 local time), when the sea breeze moves towards land and the boundary layer air is well mixed (see *Section 2.1* for details). The recirculation of continental air mass during the sea breeze period should average regional influences, even though the footprint of PON is less than those of HLE and PBL. Second, when we performed the CCGVU curve-fitting, any data lying outside 3SD of the residuals were regarded as outliers and discarded from the time series, and this procedure was repeated until no outliers were identified (Harris et al., 2000; Zhang et al., 2007) (see *Section 2.3.1* for details). These outliers were likely a result of pollution by local emissions and not representative of regional background concentrations (denoted by crosses in each panel of Fig. 2, 4, 6, 8, 10 and 12). We believe that through the two approaches the local influences at PON should be sufficiently minimized. Therefore the substantial and positive CO gradient between PON and HLE generally reflects regional sources rather than local influences.

Section 3.3: It seems that the PBL and PON site are at a similar location and elevation. Were CH_4 and CO elevated at PON due to the SW monsoon as well? How about the impacts of the monsoon prevails at PON? Please discuss that in this section.

[Response] Thanks a lot for your careful review and comments. We don’t know if PON also detected the two elevated CH_4 and CO events observed at PBL that could be related to

biomass burning emissions in Indonesia. We don't have enough data from flask measurements to test it. Besides, at PON this signal could be masked by influences of other CH_4 and CO sources (e.g. residential energy use, transportation, etc.) from South India. Note that the mechanisms we proposed for the abnormal CH_4 and CO events and the possible linkage between PBL and BKT during the SW monsoon season are speculative, and need further verification with model experiments.

References

Andreae, M. O., and Merlet, P.: Emission of trace gases and aerosols from biomass burning, Global Biogeochem. Cy., 15, 955-966, 10.1029/2000gb001382, 2001.

Ehhalt, D. H., and Rohrer, F.: The tropospheric cycle of H2: a critical review, Tellus B, 61, 500-535, 10.1111/j.1600-0889.2009.00416.x, 2009.

Haszpra, L., Barcza, Z., Hidy, D., Szilágyi, I., Dlugokencky, E., and Tans, P.: Trends and temporal variations of major greenhouse gases at a rural site in Central Europe, Atmos. Environ., 42, 8707-8716, http://dx.doi.org/10.1016/j.atmosenv.2008.09.012, 2008.

Maiss, M., Steele, L. P., Francey, R. J., Fraser, P. J., Langenfelds, R. L., Trivett, N. B. A., and Levin, I.: Sulfur hexafluoride—A powerful new atmospheric tracer, Atmos. Environ., 30, 1621-1629, http://dx.doi.org/10.1016/1352-2310(95)00425-4, 1996.

Streets, D. G., Yarber, K. F., Woo, J. H., and Carmichael, G. R.: Biomass burning in Asia: Annual and seasonal estimates and atmospheric emissions, Global Biogeochem. Cy., 17, 1099, 10.1029/2003gb002040, 2003.

Yevich, R., and Logan, J. A.: An assessment of biofuel use and burning of agricultural waste in the developing world, Global Biogeochem. Cy., 17, 1095, 10.1029/2002gb001952, 2003.

Tables

Table R1 Features of the smoothed fitting curves for flask measurements at PON (2007–2011). For each species, the smoothed curves are fitted to the data not filtered by CO outliers and the data filtered by CO outliers. The annual mean values and average peak-to-peak amplitude are calculated from the smoothed curve and mean season cycle, respectively. Uncertainty of each estimate is calculated from 1 s.d. of 1000 bootstrap replicates.

	Not CO filtered	CO filtered
CO_2 (ppm)		
N_{fit}	121	105
Annual mean 2007	386.6±0.9	386.5±1.1
Annual mean 2008	388.1±0.9	388.0±0.9
Annual mean 2009	389.0±0.6	388.4±0.8
Annual mean 2010	391.3±1.5	391.2±1.5
Annual gradient relative to HLE	2.9±1.2	2.6±1.4
Trend	1.7±0.1	1.7±0.1
RSD	4.0	4.1
Amplitude	7.6±1.4	7.8±1.6
D_{max}	111.0±13.4	116.0±14.1
D_{min}	327.0±54.3	327.0±55.8
CH_4 (ppb)		
N_{fit}	164	101
Annual mean 2007	1859.2±6.7	1854.2±5.9
Annual mean 2008	1856.1±10.4	1857.3±6.8
Annual mean 2009	1865.7±5.1	1855.5±6.2
Annual mean 2010	1876.9±9.1	1877.3±7.3
Annual gradient relative to HLE	37.4±10.7	34.0±11.0
Trend	9.4±0.1	9.0±0.1
RSD	34.4	19.8
Amplitude	124.1±10.2	127.8±11.4
D_{max}	337.0±6.1	331.0±5.4
D_{min}	189.0±10.7	192.0±9.8
N_2O (ppb)		
N_{fit}	137	110
Annual mean 2007	324.8±0.3	324.9±0.4
Annual mean 2008	326.3±0.3	326.3±0.3
Annual mean 2009	326.7±0.3	326.4±0.3
Annual mean 2010	327.1±0.5	327.0±0.5
Annual gradient relative to HLE	3.1±0.3	3.0±0.3
Trend	0.8±0.1	0.7±0.1
RSD	1.4	1.4
Amplitude	1.2±0.5	1.1±0.5

D_{max}	262.0±83.2	262.0±46.1
D_{min}	141.0±48.2	97.0±65.8
SF_6 (ppt)		
N_{fit}	174	139
Annual mean 2007	6.19±0.01	6.19±0.02
Annual mean 2008	6.49±0.02	6.49±0.02
Annual mean 2009	6.77±0.01	6.77±0.02
Annual mean 2010	7.08±0.02	7.08±0.02
Annual gradient relative to HLE	-0.06±0.03	-0.06±0.03
Trend	0.31±0.05	0.31±0.06
RSD	0.05	0.05
Amplitude	0.24±0.02	0.24±0.03
D_{max}	327.0±12.1	327.0±21.7
D_{min}	204.0±3.3	205.0±3.4
CO (ppb)		
N_{fit}	139	139
Annual mean 2007	200.5±7.8	200.5±7.8
Annual mean 2008	175.3±13.1	175.3±13.1
Annual mean 2009	174.3±4.8	174.3±4.8
Annual mean 2010	185.1±8.7	185.1±8.7
Annual gradient relative to HLE	82.4±10.7	82.4±10.7
Trend	0.4±0.1	0.4±0.1
RSD	32.0	32.0
Amplitude	78.2±11.6	78.2±11.6
D_{max}	4.0±160.2	4.0±160.2
D_{min}	238.0±46.1	238.0±46.1
H_2 (ppb)		
N_{fit}	140	120
Annual mean 2007	574.5±2.4	573.7±3.2
Annual mean 2008	558.2±5.3	558.3±5.1
Annual mean 2009	562.4±1.6	561.9±1.6
Annual mean 2010	563.9±2.3	563.0±2.5
Annual gradient relative to HLE	29.8±4.1	29.3±3.7
Trend	-1.3±0.1	-1.3±0.1
RSD	8.4	8.3
Amplitude	21.6±3.4	21.1±3.8
D_{max}	96.0±9.6	97.0±9.8
D_{min}	219.0±10.3	215.0±11.9

Figures

Figure R1 Time series of flask measurements at PON (2007–2011) with smoothed fitting curves for **(a)** CO_2, **(b)** CH_4, **(c)** N_2O, **(d)** SF_6 and **(e)** H_2. The open circles denote flask data used to fit the solid smoothed curves, while the crosses denote discarded flask data lying outside 3 times the residual standard deviations from the smoothed curve fits as well as those filtered by CO outliers. For PON, the solid (dotted) red line indicates the smoothed curve fitted to the data (not) filtered by CO outliers. The flask measurements at HLE and the corresponding smoothed fitting curve are also presented for comparison.

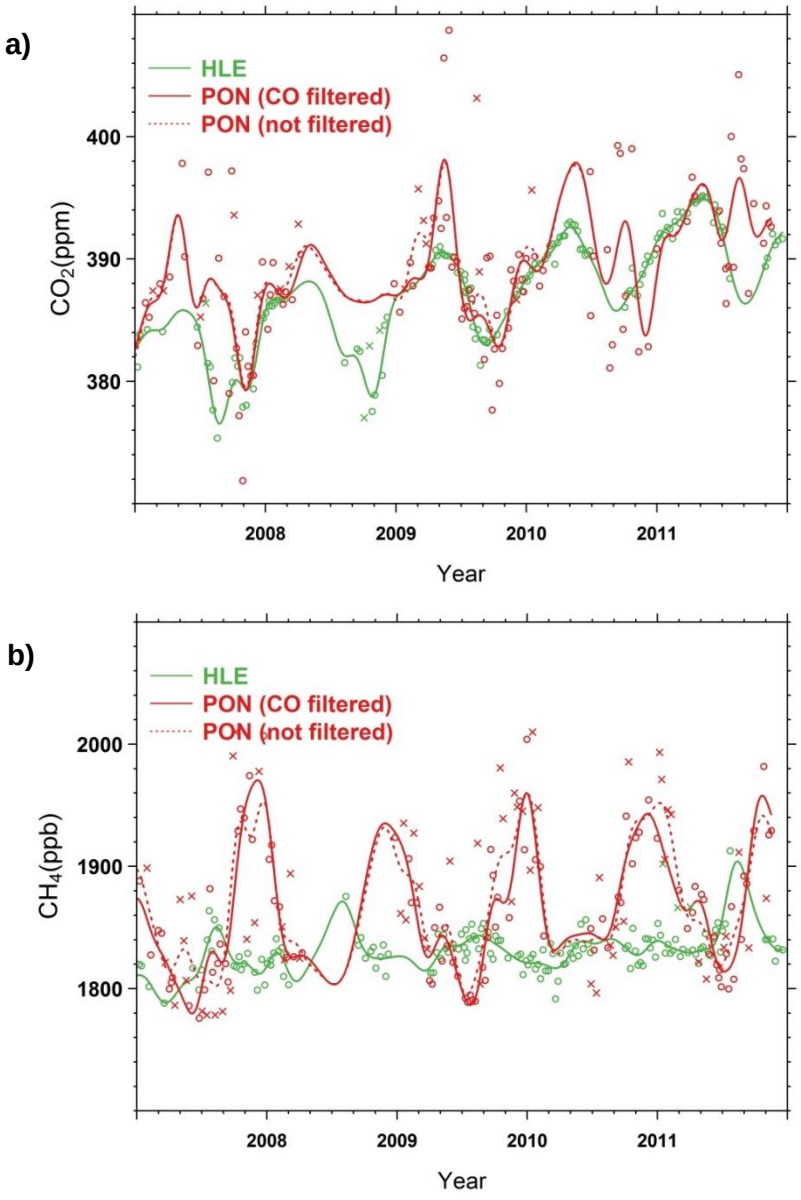

c)

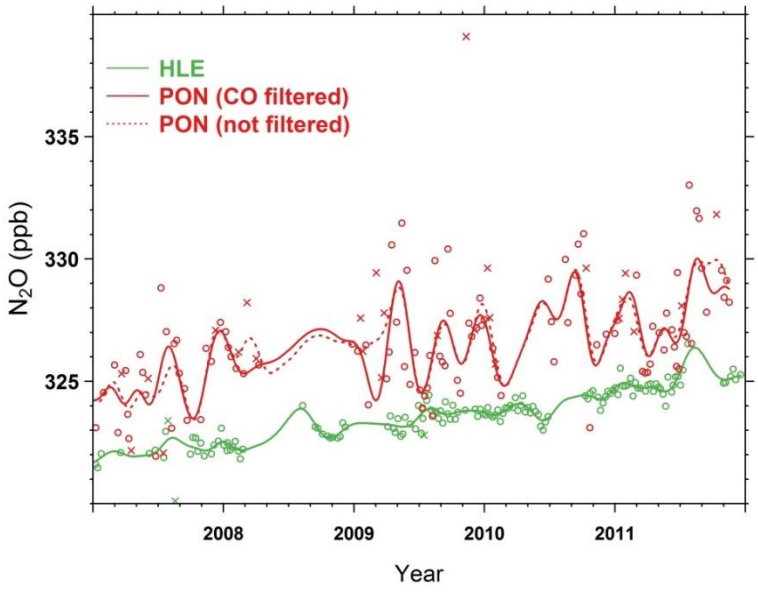
HLE
PON (CO filtered)
PON (not filtered)
335
330
325
N2O (ppb)
2008
2009
2010
2011
Year

d)

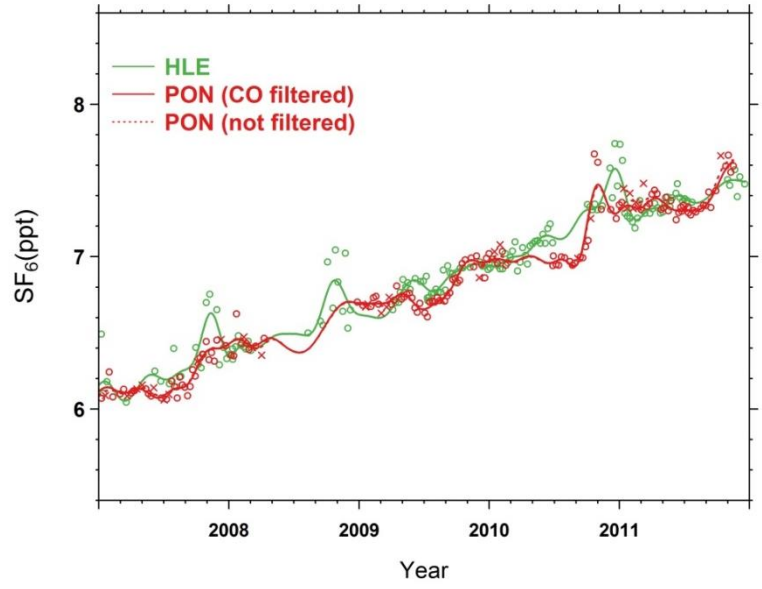
HLE
PON (CO filtered)
PON (not filtered)
8
7
6
SF6(ppt)
2008
2009
2010
2011
Year

e)

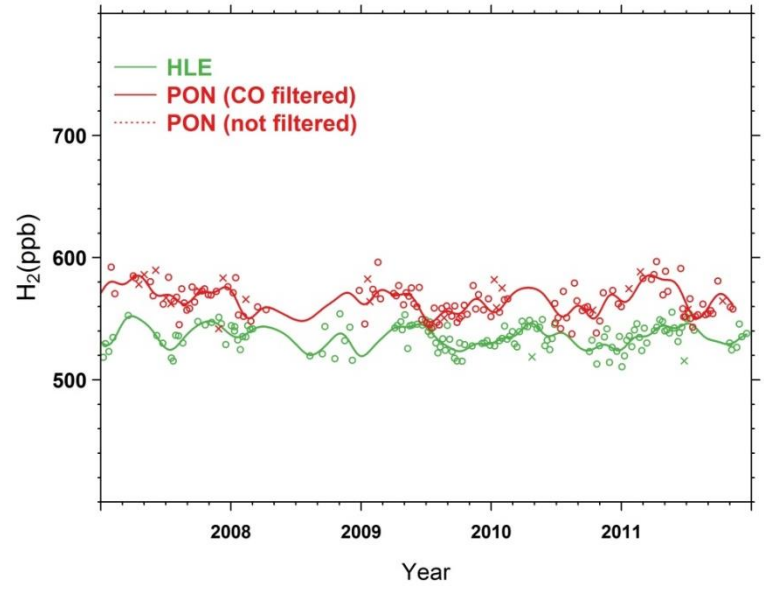
HLE
PON (CO filtered)
PON (not filtered)
700
600
500
H2(ppb)
2008
2009
2010
2011
Year

Anonymous Referee #2

General comments:

The paper presents a new record of flask sample observations of long-lived trace gases from two sites in mainland India and one site on the Andaman Islands. Data from the two mainland sites are presented from 2007 to 2011 and from the island site from 2009 to 2011. The target sampling frequency is weekly, though there are significant gaps in the record, sometimes weeks/months, due to bad weather and technical problems (see figure S2 in the supplement). The target compounds are CO_2, CH_4, N_2O, SF_6, CO and H_2. The paper describes in detail the sampling and analysis stages and the data processing techniques used to generate annual means, seasonal cycles and gradients between stations. The paper compares these new flask data with observations from stations in other countries such as Kazakhstan and China. An attempt is made to relate the seasonal cycles and gradients between stations to variations in natural GHG fluxes, anthropogenic emissions and monsoon circulations.

The Indian continent is currently experiencing rapid industrial development and as such is an important region globally for emissions of these long-lived trace gases. There appears to be a paucity of ground-based GHG measurements from this region and these observations go someway to filling the data gap. The authors should be encouraged to continue their observations and where possible improve future measurement frequency/reliability to avoid large data gaps. Have the authors considered analysing the flask samples for stable carbon isotope ratio which would be a big help in determining source apportionment especially for CH_4 and CO_2?

I recommend that this paper be published after consideration to the following minor specific comments and technical corrections.

An interactive comment indicated that a site in India at Sinhagad has been collecting samples for CO_2 and CH_4 analysis since 2009 (Y.K. Tiwari et al, 2014). The authors do refer to this paper in the conclusions (p 7204, line 23) but could also refer to it earlier in the CO_2/CH_4 discussion section.

[Response] Thanks a lot for your careful review and comments. Until now flask sampling at the three stations and analyses of the flask samples are still on-going for the trace gases we investigated here. The analyses of $^{13}CO_2$ for HLE have been started but data are not available at the moment. The in-situ measurements of CO_2 and CH_4 have been deployed at HLE, PON and PBL as well.

Following your suggestion, we referred to Tiwari et al., (2014) in *Section 3.1.1*. (Lines 432–434). We also referred to several other papers on Indian surface observations (Bhattacharya et al., 2009; Ganesan et al., 2013; Tiwari et al., 2011) and added more discussions in *Section 3.1* (Lines 429–434, 494–497, 534–535).

Specific comments (individual scientific questions/issues):

1 Introduction, page 7174, line 1: it would be useful to compare the estimated increase in GHG emissions from India (1.4 to 2.8 $GtCO_2$ eq) with the estimate from Europe or the USA.

[Response] Following your suggestion, we added this information in our manuscript (Lines 48–49). Between 1991 and 2010, anthropogenic GHG emissions in India increased by ~100% from 1.4 to 2.8 $GtCO_2$eq, much faster than rates of most developed countries and economies like the USA (9%) and EU (-14%) over the same period (EDGAR v4.2).

1 Introduction, page 7174, line 17: suggest to add a sentence defining what is meant by the top-down and bottom-up approaches.

[Response] Follow your suggestion, we revised this sentence to "Current estimates of GHG budgets in India, either from the top-down approaches (based on atmospheric inversions) or bottom-up approaches (based on emission inventories or biospheric models), have larger uncertainties than for other continents" (Lines 66–67).

1 Introduction, page 7174, line 24: suggest to extend the sentence starting 'Notably, these ...' to include a comparison of Indian bottom-up uncertainties with those from say Western Europe where inventories are more accurate.

[Response] Following your suggestion, we revised this sentence to "Notably, these estimates have uncertainties as high as 100–150%, much larger compared to those of Europe (~30%, see Luyssaert et al., 2012) and North America (~60%, see King et al., 2015), where observational networks are denser and emission inventories are more accurate" (Lines 72–75).

1 Introduction, page 7175, line 17: suggest add here an extra sentence describing key meteorological features of the NE winter monsoon.

[Response] During the winter monsoon period, little deep convection occurs over South Asia and the monsoon system carries less moisture than it does during the summer monsoon period (Lawrence and Lelieveld, 2010). Following your suggestion, we added a sentence describing key meteorological features of the NE winter monsoon to the manuscript (Lines 109–111).

2.1 Sampling stations, page 7176, line 15: I would like to see a map, possibly as an extra panel in Fig.1 centred and zoomed on India showing the three sampling stations and terrain.

[Response] Following your suggestion, we revised Fig. 1 and added an extra panel (Fig. 1b) zoomed over India to show locations of the three stations and terrain. Additionally, following other reviewers' suggestions, we also modified the color scheme of Fig. 1, with back-trajectories colored by elevations of air masses instead of CO_2 levels.

2.1 Sampling stations, page 7177, line 8: suggest add sentence somewhere here describing the inlet location, height above the ground, type of inlet tubing used etc.

[Response] For HLE, the flask sampling inlet is installed on the top of a 3m mast fixed on the roof of a 2m high building, and the ambient air is pumped through a Dekabon tubing with a diameter of 1/4". Following your suggestion, we added the sentence to the manuscript (Lines 159–161).

2.1 Sampling stations, page 7178, line 19: suggest add an extra sentence detailing the inlet location, inlet height above ground, type of tubing sed etc.

[Response] For PBL, The flask sampling inlet is located on the top of a 30 m high tower, and the ambient air is pumped through a Dekabon tubing with a diameter of 1/4". Following your suggestion, we added the sentence to the manuscript (Lines 203–204).

2.2.1 Flask sampling, page 7179, lines 10-14: is the loss correction the same for both valve types used? If so please state in text.

[Response] No, this correction is only applied to the Teflon sealed flasks. We revised the manuscript accordingly for clarification (Lines 225–229).

2.2.1 Flask sampling, page 7179, lines 15-17: has the magnesium perchlorate drier been tested for loss of the target compounds?

[Response] Yes, we have performed tests and didn't find any influence of the magnesium perchlorate drier on the target gases.

2.2.2 Flask analyses, page 7180, lines 2-4: is the pressure inside each flask on arrival at LSCE the same as it was after filling in India? Some concern about loss/leakage during air-freight.

[Response] We cannot guarantee that the pressure inside each flask on arrival at LSCE is the same as it was after filling in India. If the flask pressure is too low, we will flag the sample during the flask analyses.

2.2.2 Flask analyses, page 7180, line 6: is this the Agilent micro-cell ECD? If so please state.

[Response] No, it is a standard ECD.

2.2.2 Flask analyses, page 7180, line 14: are samples flushed through the sample loop under the pressure inside the flask or is a pump used? If so, is the pump upstream or downstream of the sample loops?

[Response] No pump is used. We use the overpressure of the flasks. We revised the manuscript accordingly for clarification (Line 256).

2.2.2 Flask analyses, page 7180, lines 17-22: please also state column flow rates, oven temperature, isothermal or oven program etc.

[Response] Following your suggestion, we revised the manuscript (Lines 259–268, also see Table S1).

2.2.2 Flask analyses, page 7180, line 25: please include more detail on the ECD detector temperature, make-up gas flow etc.

[Response] Following your suggestion, we added the temperature and flow rate in the manuscript (Lines 259– 268, also see Table S1). We don't use make-up gas here.

2.2.2 Flask analyses, page 7181, line 1: please include RGD detector temperature.

[Response] The oven temperature is kept at 105°C, and the catalytic chamber is heated to 265°C. Following your suggestion, we added this information to manuscript (Lines 268– 272, also see Table S1).

2.2.2 Flask analyses, page 7181, lines 2-7: are the working calibration cylinders filled with synthetic air or ambient air? Please state if they are filled by LSCE or purchased (then include supplier details). Also please state make and model of gas regulator used on the calibration cylinders.

[Response] The calibration and quality control cylinders are filled and spiked in a matrix of synthetic air containing N_2, O_2 and Ar prepared by Deuste Steininger (Germany). Following your suggestion, we added this information to the manuscript (Lines 275– 276).

2.2.2 Flask analyses, page 7181, line 10: please name the international calibration scale used.

[Response] Following your suggestion, we added the he international calibration scales used (Lines 282–285, also see Table S1).

2.3.2 Ratio of Species, page 7184, lines 2-7: please expand this section by adding a couple of sentences giving more detail of the procedure used.

[Response] Following your suggestion, we added a couple of sentences and references in *Section 2.3.2* to clarify the procedures we used to calculate the ratios of species and uncertainties (Lines 358–364).

3.1.2 CH_4, page 7187, line 1: the low observations of CH_4 at PBL in summer 2009 and 2011 are striking and should be mentioned here. Presumably the air arriving at PBL at this time of year has southern hemisphere origin, arriving on the SW monsoon flow.

[Response] As we mentioned in the paragraph describing the CH_4 mean seasonal cycles at PON and PBL (Lines 488–491), we attributed this summer minimum to influence of southern

hemispheric air transported at lower altitudes, the dilution effect by increased local planetary boundary layer height and higher rates of removal by OH.

3.1.3 N_2O, page 7188, lines 16-18: suggest compare the observed N_2O growth rate at HLE to say AGAGE northern hemisphere average growth rate.

[Response] Following your suggestion, here we compared the observed N_2O growth rate at HLE (0.8±0.0 ppb/yr) to that at MLO during the same period (1.0±0.0 ppb/yr). We revised the manuscript accordingly (Line 513).

3.1.4 SF_6, page 7192, lines 1-2: there is also a strong possibility that some of the episodic SF_6 pollution events originate in China.

[Response] Following your suggestion, we revised the manuscript (Lines 617, 639).

3.1.5 CO, page 7194, lines 26-28: China should also be considered as an influence on CO enriched air-masses arriving at PBL during NE monsoon.

[Response] Following your suggestion, we revised the manuscript (Line 711).

4 Conclusions, page 7203, lines 7-9: This sentence needs some qualification as it implies a five year history of observations at PBL when in fact only 2.5 years are available at that site with a long data break during 2010. The site at PBL is somewhat under-sampled in relation to HLE and PON.

[Response] Following your suggestion, we rephrased this sentence (Lines 948– 955).

4 Conclusions, page 7204, lines 17-26: In this paragraph the authors could mention any plans to continue flask sampling and if possible extend the measurement suite. Although in-situ continuous measurement techniques are hard to deploy reliably in these remote tropical locations this would add considerably to the value of the sites. The authors could also consider adding stable carbon isotope ratio analysis to the flask measurement process which help with source apportionment, especially for CO_2 and CH_4.

[Response] At present, analyses of $\delta^{13}C$-CO_2 have been started for HLE but data are not available yet. Isotopic measurements for CH_4 have not been started. Apart from the flask measurements of trace gases presented in this study for the three stations, in-situ measurements of CO_2 and CH_4 have also been deployed at HLE, PON and PBL in parallel, which would considerably contribute to the value of the stations through high-frequency air sampling. Following your suggestion, we revised the conclusions accordingly (Lines 986–996).

Figure 14, page 7235: I suggest also give in each panel the number of samples used to create each fitting line, there are noticeably fewer points available for PBL. Same also for Fig.15 and Fig. 16.

[Response] Following your suggestion, we revised Figs. 14–16 accordingly.

References

King, A. W., Andres, R. J., Davis, K. J., Hafer, M., Hayes, D. J., Huntzinger, D. N., de Jong, B., Kurz, W. A., McGuire, A. D., Vargas, R., Wei, Y., West, T. O. and Woodall, C. W.: North America's net terrestrial CO_2 exchange with the atmosphere 1990–2009, Biogeosciences, 12(2), 399–414, doi:10.5194/bg-12-399-2015, 2015.

Lawrence, M. G., and Lelieveld, J.: Atmospheric pollutant outflow from southern Asia: a review, Atmos. Chem. Phys., 10, 11017-11096, 10.5194/acp-10-11017-2010, 2010.

Luyssaert, S., Abril, G., Andres, R., Bastviken, D., Bellassen, V., Bergamaschi, P., Bousquet, P., Chevallier, F., Ciais, P., Corazza, M., Dechow, R., Erb, K.-H., Etiope, G., Fortems-Cheiney, A., Grassi, G., Hartmann, J., Jung, M., Lathière, J., Lohila, A., Mayorga, E., Moosdorf, N., Njakou, D. S., Otto, J., Papale, D., Peters, W., Peylin, P., Raymond, P., Rödenbeck, C., Saarnio, S., Schulze, E.-D., Szopa, S., Thompson, R., Verkerk, P. J., Vuichard, N., Wang, R., Wattenbach, M. and Zaehle, S.: The European land and inland water CO_2, CO, CH_4 and N_2O balance between 2001 and 2005, Biogeosciences, 9(8), 3357–3380, doi:10.5194/bg-9-3357-2012, 2012.

Technical corrections (typing errors, etc.):

1 Introduction, page 7173, line 24: '... during the recent decades ...'

[Response] Following your suggestion, we revised it.

1 Introduction, page 7174, line 5 to 7: remove brackets from '... (in 2010, the per capita...)' and make new sentence starting: 'For comparison, in 2010, the per capita GHG emission rates ...'

[Response] Following your suggestion, we revised it.

1 Introduction, page 7174, line 8: '... agriculture-related ...' replace with '... agricultural ...'

[Response] Following your suggestion, we revised it.

1 Introduction, page 7174, line 12: try to improve this sentence, e.g. 'Reducing emissions of these two non-CO_2 greenhouse gases may offer a more cost-effective way to mitigate future climate change than by attempting to directly reduce CO_2 emissions (Montzka et al., 2011)'

[Response] Following your suggestion, we revised it.

1 Introduction, page 7176, line 8: suggest to re-arrange this sentence to remove brackets, for e.g. 'We examine synoptic variations of CO_2, CH_4 and CO by analysing co-variances between species, using deviations from their smoothed fitting curves (Sect. 3.2).'

[Response] Following your suggestion, we revised it.

2.1 Sampling stations, page 7177, line 4: suggest to give HLE lat/lon co-ordinates to three decimal places. Same also for PON and PBL, with only two decimal places these two sites appear to be offshore.

[Response] Following your suggestion, we revised it.

2.1 Sampling stations, page 7177, line 15: suggest to re-arrange sentence for ease of reading, e.g ' ... background free tropospheric air masses in the northern mid-latitudes.'

[Response] Following your suggestion, we revised it.

2.1 Sampling stations, page 7177, line 26: suggest to modify sentence, e.g. 'The flask sampling inlet, was initially located on a 10m mast fixed on the roof of the University Guest House, was later moved to a 30 m high tower in June 2011.' Also give the type of inlet tubing used.

[Response] For PON, the ambient air is pumped from the top of the tower through a Dekabon tubing with a diameter of 1/4". Following your suggestion, we revised it and added the sentence to the manuscript (Lines 180–182).

2.1 Sampling stations, page 7178, line 7: suggest to combine the sentences starting 'Flask sampling ...' and 'Over the period ...', how about: 'Flask sampling began in September 2006 and over the period 2007–2011, a total of 185 flask sample pairs were collected at the site.'

[Response] Following your suggestion, we revised it.

2.2.2 Flask analyses, page 7180, line 4: '... HP86890 ...'

[Response] Following your suggestion, we revised it.

2.2.2 Flask analyses, page 7180, line 18: '... 3/16" ...', is this the internal or external column diameter? Please state. Same on line 19 and 20. Use either " or inches, both are used in text.

[Response] They all indicate external column diameters. We revised the manuscript accordingly.

3.1.2 CH_4, page 7188, line 7: 'This These not only ...'

[Response] Following your suggestion, we revised it.

3.1.3 N_2O, page 7188, line 25: 'We also analyze analyzed ...'

[Response] Following your suggestion, we revised it.

3.1.3 N_2O, page 7190, line 11-13: Improve sentence starting 'One reason may be ...', for example: 'One reason may be that air arriving at the site during the SW monsoon period is relatively enriched in N_2O compared to CH_4, reflecting differences in their relative emissions along the air mass history.'

[Response] Following your suggestion, we revised it.

3.1.4 SF_6, page 7192, line 22: delete 'southwesterly' which would otherwise imply winds from the SW. Also consider China as well as Southeast Asia to explain some of the polluted air masses.

[Response] Following your suggestion, we revised it.

3.1.6 H_2, page 7195, line 27: 'The mean H_2 seasonal cycle cycles ...'

[Response] Following your suggestion, we revised it.

3.2.1 $\Delta CH_4/\Delta CO$, page 7198, line 10: add 'that', so: '... estimates are 1.5 to 4 times that of the ...'

[Response] Following your suggestion, we revised it.

Table 1, page 7220: define RSD abbreviation in the caption, same for D_{max} and D_{min}. Consider also adding additional row after the trend row for each compound, giving northern hemisphere average trends say from the AGAGE network.

[Response] Following your suggestion, we revised the caption of Table 1. We also included in Table 1 the observed trends at MLO for CO_2, CH_4, N_2O, SF_6 and CO during the study period. The trend of H_2 is not presented because reliable data are not available yet at MLO for the study period.

Figure 2, page 7223: use "open circles" and "crosses" in the caption description rather than "o" and "x". Same throughout the text, figure captions and in supplement.

[Response] Following your suggestion, we revised it.

Figure 3, page 7224: all three panels are too small.

[Response] Following your suggestion, we enlarge the three panels.

Figure 4, page 7225: Needs full caption, not just 'same as Fig. 2 ...'

[Response] Following your suggestion, we revised it.

Figure 8, page 7229: Needs full caption, not just 'same as Fig. 6 ...'

[Response] Following your suggestion, we revised it.

Figure 9, page 7230: Needs full caption, not just 'same as Fig. 7 ...'. Also can the uncertainty shaded areas be made clearer?

[Response] Following your suggestion, we revised it. We also tried to make the uncertainty shaded areas of Fig. 7 clearer.

Figure 10, page 7231: Needs full caption, not just 'same as Fig. 2 ...'

[Response] Following your suggestion, we revised it.

Figure 12, page 7233: Needs full caption, not just 'same as Fig. 2 ...'

[Response] Following your suggestion, we revised it.

Figure 13, page 7233: Needs full caption, not just 'same as Fig. 11 ...'

[Response] Following your suggestion, we revised it.

Figure 15, page 7236: Needs full caption, not just ‘same as Fig. 14 ...’

[Response] Following your suggestion, we revised it.

Figure 16, page 7237: Needs full caption, not just ‘same as Fig. 14 ...’

[Response] Following your suggestion, we revised it.

Supplement, Table S5: what is the reason for the grey shaded columns? Different instrument network? Same for Table S7 and Table S9.

[Response] Here the grey shaded columns indicate results for the reference stations. We did this for better display of the data. We revised the captions to clarify it.

Supplement, Figure S3: can the shaded uncertainty areas be made clearer?

[Response] The uncertainties of the mean CO_2 seasonal cycles for HLE, KZM and WLG are too small (relative to scales of the plot) to be visible. Following your suggestion, we tried to revised it and make the uncertainty shaded area in Fig. S3 clearer.

Supplement, Figure S7 caption: ‘ MHD, BGU, FIK, ~~FIK~~ and LPO ...’

[Response] Following your suggestion, we revised it.

Anonymous Referee #3

Received and published: 9 June 2015

The authors present a multi-species time series of trace gas data from three flask stations in India. The data represent a very valuable contribution to this area of the world, which is currently poorly monitored, and the authors have analysed various aspects of the data (trends, gradients, etc) and covariance between species. However, the manuscript requires some revision to bolster some of the scientific conclusions that are made. If these comments can be addressed, the manuscript should be published.

General comments:

1. Introduction – There should be a comprehensive review of other measurement programs in South Asia – there is a description of CARIBIC and satellite-based studies, but there lacks a detailed description of other measurements (e.g., Bhattacharya et al., 2011, Ganesan et al, 2013 and Tiwari et al, 2014). At the moment it reads as though there are no other surface measurements (whether concurrently or previously) and while the authors discuss some very brief comparisons in the Results section, this needs to be brought forward into the Introduction. On page 7175 Line 9: 'Besides a lack of observation sites' should be written more accurately, which is that there are few observation sites in addition to those presented here, but this is not enough to constrain a large country like India.

[Response] Thanks a lot for your careful review and comments. Following your suggestions, we revised the second paragraph of the *Introduction* section and added a more detailed description of the surface atmospheric stations that have been recently established in India, including the stations in Sinhagad (18.35°N, 73.75°E, 1600m a.s.l.; Tiwari and Kumar, 2012; Tiwari et al., 2014), Mount Abu (24.60°N, 72.70°E, 1700m a.s.l.; S. Lal, personal communication), Ahmedabad (23.00°N, 72.50°E, 55m a.s.l.; Lal et al., 2015), Nainital (29.37°N, 79.45°E, 1958m a.s.l.; Kumar et al., 2010) and Darjeeling (27.03°N, 88.15°E, 2194m a.s.l.; Ganesan et al., 2013). Note that most of these stations started to measure GHG concentrations very recently (e.g. Sinhagad – since 2009; Ahmedabad – since 2013; Mount Abu – since 2013; Nainital – since 2006; Darjeeling – since 2011), and datasets are not always available. We also rephrased a few sentences in the second and third paragraphs accordingly (Lines 83–99, 101).

2. The authors compare their data to many other sites from NOAA and ICOS. While it is understandable that these measurements are directly linked to the authors and may overlap the time period of this study, there are measurements in India that should be compared to (see previous point), as these are very related to the conclusions made here (i.e. about regional sources, etc). Any comparisons made to other surface data are very minimal at present. The comparisons to CARIBIC, satellites, etc are important but to a lesser degree than other Indian surface observations.

[Response] Thanks a lot for your careful review and comments. In this study, we compared the flask measurements at HLE with KZM and WLG as well as those from the CONTRAIL and CARIBIC projects for several reasons: First, they all sample free-tropospheric air masses in northern mid-latitudes; Second, both HLE and the CARIBIC flights (and probably satellite measurements as well) show influences of the SW monsoon (and associated deep convection) on trace gas concentrations in the mid-to-high troposphere; Third, currently there is no ground station in India other than HLE that is representative of free tropospheric background concentrations over northern mid-latitudes. For N_2O and SF_6, we also compared gradients between PON, PBL and HLE to gradients between stations in Europe and the US, where GHG emissions are better known and relatively more accurate. Following your suggestions, we also referred to several previous papers on Indian surface observations (Bhattacharya et al., 2009; Ganesan et al., 2013; Tiwari et al., 2011, 2014) and added more discussions in *Section 3.1* (Lines 429–434, 494–497, 534–535).

3. The authors should be careful throughout the text to maintain that the mechanisms proposed for the various features in the data set are still speculative. This is a measurement-led study and without additional tools to quantitatively pinpoint the sources of air masses, these remain as hypotheses. An example of this would be on page 7187 line 21: "Moreover, the mean CH_4 seasonal cycle at HLE agrees well with the annual variation of convective precipitation over the Indian subcontinent (Fig. 5b), which is derived from ECMWF nudged Laboratoire de Météorologie Dynamique general circulation model (LMDz) (Hauglustaine et al., 2004). This agreement indicates that the summer maximum at HLE can be attributed to the enhanced biogenic CH_4 emissions from wetlands and rice paddies and deep convection that mixes surface emissions into the mid-to-upper troposphere." There is not enough information to say conclusively that biogenic emissions are responsible for the summer maximum without additional data (i.e. though models or isotopic data). So while the mechanism is proposed, it is stated too definitively. There are several statements like this throughout the text, which should be toned down and the authors should rephrase or remove statements such as this one.

[Response] Thanks a lot for your careful review and comments. In India, ruminant animals, natural wetlands and water-flooded rice paddies are the main sources of CH_4 emissions, accounting for ~40%, 15% and 16% of the total estimate. As we know, CH_4 emissions from ruminant animals do not show notable seasonality. By contrast, CH_4 emissions from natural wetlands and water-flooded rice paddies are greatly affected by climate conditions and subject to the seasonal variations of the Indian monsoon system. As illustrated in Fig. R1, emissions from wetlands and rice paddies show pronounced seasonality and have the maximum during July–September, exactly the same period when the SW monsoon prevails and the deep convection is most active. Therefore it is very likely that the summer maximum at HLE may be related to the enhanced biogenic CH_4 emissions from wetlands and rice paddies and deep convection that mixes surface emissions into the mid-to-upper troposphere. We agree that with the help of carbon isotopic measurements and/or chemical transport

model, we are able to further disentangle and quantify the contributions of meteorology and biogenic emissions to the CH_4 summer maximum at HLE. Following your suggestions, we added another panel to Fig. 5 and revised *Section 3.1.2* and *Conclusions* (Lines 471–482, 978) accordingly to clarify the statements.

4. Following up on the above statement, there are some sections, which are still quite speculative and not necessarily based on evidence and should be removed. These include: (a) Section 3.3 on elevated CH_4 and CO samples at PBL – There is not enough information to ascertain whether the samples at BKT are related to the samples at PBL. There would need to be a model simulation to show that the air mass at BKT on e.g., Sep 8 2009, arrived at PBL on Sep 16 2009. Otherwise it is too speculative and should be removed. (b) Discussion of bimodal H_2 on page 7196 line 17 – it is speculated the biomass burning from each hemisphere is the source of the double peaks. But there is no evidence to show that is the case.

[Response] Thanks a lot for your careful review and comments. (a) For *Section 3.3*, we agree that the mechanisms we proposed for the abnormal CH_4 and CO events and the possible linkage between PBL and BKT during the SW monsoon season are speculative, and need further verification with model experiments. Following your suggestion, we revised the manuscript and toned down the statements (Lines 938–945). (b) For discussion of the bimodal H_2 seasonal cycle at PBL, following your suggestion, we revised the manuscript and removed the sentences that are not accurate (Lines 769–771).

5. Many conclusions are drawn about Indian fluxes using HLE. However, from the text and looking at the trajectories, HLE mainly samples air from Africa and the Middle East. There are only a few trajectories that sample Indian air masses. It seems that the conclusions to the HLE data (with regards to Indian sources) should be changed to reflect this. Can HLE be used to discuss Indian sources?

[Response] Thanks a lot for your careful review and comments. In this study, we chose HLE as a reference station, and used the concentration gradients between PON, PBL and HLE to discuss the possible GHG sources in the Indian subcontinent. As we stated in *Section 2.1*, HLE (32.780 °N, 78.960 °E, 4517 m a.s.l.) is a high-altitude station situated in the western Himalayas. It dominantly samples mid-tropospheric air masses that pass over northern Africa and the Middle East throughout the year, and those coming from South and Southeast Asia during the SW monsoon season (also see the revised Fig. 1 colored by altitudes of back-trajectories). Therefore it is representative of free mid-troposphere background concentrations over northern mid-latitudes, rather than Indian air masses. That's why we chose this station as a background station, and used the concentration gradients between PON, PBL and HLE to infer whether or not there are substantial GHG emissions over South Asia (see details in *Section 3.1* for each species).

6. There appear to be some discrepancies in the text. The use of CARIBIC data and other remotely sensed data seems contradictory in places. In the discussion for SF_6, it states that the

CARIBIC samples are more representative of westerly jet transport rather than the SW monsoon. However, CARIBIC is used in the discussion for all other species in the context of Indian sources. It would also be useful to see trajectories for the comparison data to know whether they are sampling the same air masses.

[Response] Thanks a lot for your careful review and comments. In the discussion for SF_6, we compared the SF_6 seasonal cycle observed at HLE with that derived from CARIBIC flights. We cited Schuck et al. (2010), in which flask samples were taken during flights between Frankfurt and Chennai in 2008 over the domain 10–40°N, 50–80°E at flight altitudes 8–12.5km. As described in *Section 3* and *Section 5.3* in Schuck et al. (2010), the flask samples taken in summer were influenced by the monsoon anticyclone in the upper troposphere, as well as the westerly subtropical jet (see also Fig. R4). The summer maxima in CH_4 and N_2O by the CARIBIC flights were related to the monsoon anticyclone that can trap pollution uplifted by deep convection from the surface, and the back-trajectories analyses also show that samples taken over the monsoon region have ground contact (Fig. R4). The summer maximum in SF_6 was related to air samples collected north of 20°N along the flight routes, where air masses are more influenced by the westerly subtropical jet (and a smaller anticyclone located over the Arabian Peninsula embedded in it, see *Section 5.1* in Schuck et al. (2010) and Fig. 1 in Krishnamurti et al. (2008)) rather than the deep convection in the monsoon region.

As a high-altitude mountain station in the mid-troposphere (4517 m), HLE also samples polluted air masses uplifted by the deep convection in the monsoon region during summer as the CARIBIC flights do, but it is not influenced by the westerly subtropical jet located in the upper troposphere (also clearly seen by the colors of back-trajectories in Fig. R4). Therefore the summer enhancements of SF_6 observed by the CARIBIC flights are not detected by the flask measurements at HLE. Following your suggestion, we calculated and plotted back-trajectories for the CARIBIC flights investigated in Schuck et al. (2010) and added it to supplement (Fig. S8). We also revised the manuscript accordingly for clarification (Lines 629–634).

7. PON is located in a large urban area. While sampling is done between 1200-1800, the site would still be affected by local emissions. The analysis using PON for gradients between other sites could potentially be complicated by the fact that the site is impacted by local emissions. Therefore, PON may not be the best site to use for trend analysis. Can the authors comment on this? Could CO be used as a tracer for local emissions?

[Response] Thanks a lot for your careful review and comments. We agree that PON can be influenced by local emissions. Although the highway nearby has a low traffic flow, in-situ measurements at PON (not presented in this paper) do show that this site is heavily polluted by local emissions during nighttime. Therefore, we used two approaches to minimize the influences of local GHG sources/sinks. First, we took flask air samples at PON between 12:00 and 18:00 local time (actually 97% between 12:00 and 14:00 local time), when the sea

breeze moves towards land and the boundary layer air is well mixed (see *Section 2.1* for details). The recirculation of continental air mass during the sea breeze period should average regional influences, even though the footprint of PON is less than those of HLE and PBL. Second, when we performed the CCGVU curve-fitting, any data lying outside 3SD of the residuals were regarded as outliers and discarded from the time series, and this procedure was repeated until no outliers were identified (Harris et al., 2000; Zhang et al., 2007) (see *Section 2.3.1* for details). These outliers were likely a result of pollution by local emissions and not representative of regional background concentrations (denoted by crosses in each panel of Fig. 2, 4, 6, 8, 10 and 12). We believe that through the two approaches the local influences at PON should be sufficiently minimized.

Further, following your suggestion, we tried to use CO as a tracer for local emissions and filtered time series of other species by CO outliers. That means, for each species (other than CO), we removed the samples with abnormal CO values before the curve-fitting procedures. As shown in Table R1 and Fig. R2, filtering time series by CO outliers does not make significant difference to the trends, seasonal cycles and mean annual gradients (relative to HLE) for other species at this station. On the other hand, however, this filtering approach may substantially decrease the number of samples used to fit the smooth curve (e.g. ~38% for CH_4) and result in larger data gaps (Table R1, Fig. R2), probably compromising reliability of the analyses. Therefore finally we didn't use CO as a tracer of local emissions for additional filtering.

Specific comments:

Page 7173 line 15: change ‘dominant’ to ‘likely’ source of emissions

[Response] Following your suggestion, we revised it.

Page 7173 line 18-19: sentence needs restructuring. Suggest ‘to better constrain the GHG budget at regional and continental scales’

[Response] Following your suggestion, we revised it.

Introduction first paragraph: Text should state that the emissions from EDGAR, etc are using bottom-up methods, which generally have large uncertainties, and therefore top-down studies are needed as well.

[Response] Thanks for your suggestion. We agree that both bottom-up and top-down methods are important for estimation of GHG budgets. As we stated in the second paragraph of Introduction (please see the revised manuscript, Lines 65–75), current estimates of GHG budgets in India from both methods have larger uncertainties compared to Europe and North America.

Page 7174 line 11: what percent are natural emissions?

[Response] The natural CH_4 sources over land include emissions from wetlands, biomass burning and termites. Based on a combined dataset of (1) anthropogenic emissions from EDGARv4.2 FT2010 product, (2) wetland emissions from outputs of a global vegetation model (BIOME4-TG, Kaplan et al., 2006), (3) biomass burning emissions from Global Fire Emissions Database GFEDv3.0 product, and (4) termite emissions (Sanderson, 1996), we estimated that the natural emissions accounted for ~18% of the total CH_4 emissions over India.

The natural N_2O sources over land include emissions from uncultivated ecosystems, as well as biomass burning. Based on a combined dataset of (1) anthropogenic emissions from EDGARv4.2 FT2010 product, (2) fluxes from uncultivated ecosystems from the empirical of Bouwman et al. (2002), (3) biomass burning emissions from Global Fire Emissions Database GFEDv3.0 product, we estimated that the natural emissions accounted for ~53% of the total N_2O emissions over India. Note that both of them are rough estimates and subject to large uncertainties.

Page 7174 lines 15 – 17: Monitoring is not required by the UNFCCC.

[Response] Following your suggestion, we removed it.

Page 7175 lines 1-23: Following general comment above, a review of other surface measurements in India is needed in this paragraph. 'Besides a lack of observation sites' I agree that sites are sparse but they are not discussed.

[Response] Following your suggestions, we revised the second paragraph of the *Introduction* section and added a more detailed description of the surface atmospheric stations that have been recently established in India. We also rephrased a few sentences in the second and third paragraphs accordingly. Please see the revised manuscript Lines 83–101.

Page 7176 line 25: It is not possible to tell from the trajectories, what altitude these air masses originated from. HLE, for example, likely does not always sample surface emissions. It would be useful to see what altitude all of the sites are sampling. Also this would make comparison to aircraft observations easier to interpret.

[Response] Following your suggestion, we revised Fig. 1 and colored the back-trajectories by elevations of air masses instead of CO_2 levels. As we stated in *Section 2.1*, Fig. 1 shows that HLE dominantly samples mid-tropospheric air masses that pass over northern Africa and the Middle East throughout the year, and those coming from South and Southeast Asia during the SW monsoon season. Therefore it is representative of free mid-troposphere background concentrations over northern mid-latitudes.

Page 7177 line 17: manuscripts in preparation should not be cited

[Response] Following your suggestion, we removed it.

Page 7177 line 21: It looks like there are very few HLE trajectories coming from South Asia. Can the authors comment on the use of this site for regional work?

[Response] Thanks a lot for your careful review and comments. Please refer to our response to your general comment #5.

Page 7178 line 6: Do the sea breezes necessarily imply that they will be clean air masses? For example during the SW monsoon, the sea breeze will be a local effect on a dominant southwesterly flow. At PON, does this mean that air masses could still contain "local" emissions albeit the wind direction coming from the sea?

[Response] Thanks a lot for your careful review and comments. Please refer to our response to your general comment #7.

Page 7178 lines 5-7: Can CO be used as a tracer of local emissions for additional filtering for local emissions?

[Response] Thanks a lot for your careful review and comments. Please refer to our response to your general comment #7.

Page 7179 lines 19-23: Are flasks filled manually or automatically at a given time? Does an operator decide when conditions are correct for filling?

[Response] Flasks are flushed manually at a rate of 4–5 L min^{-1} for at least 10 minutes, corresponding to 40–50 L in total (i.e., flushing 40 times the volume of a flask). The operator decides how long flasks are flushed but the minimum required flushing time is 10 minutes.

Page 7180 line 19: Is there any impact of CO_2 on N_2O concentrations through this method? It is known that CO_2 can "dope" the signal for N_2O on an ECD.

[Response] Yes, the coelution of CO_2 is a concern in the gas chromatographic measurement of N_2O because CO_2 (with the same molecular weight as N_2O) reacts with intermediates of N_2O ionization in the ECD, thus enhancing the N_2O signal (Schmidt et al., 2001). We applied the procedures described in Lopez (2012) to solve the problem.

Page 7180: No description of the ECD or RDG setup (temps, flow rates) or information about carrier gases or calibration scales. Perhaps a table could provide all of the measurement info for each detector concisely.

[Response] Following your suggestion, we added in *Section 2.2.2* more details of the ECD and RGD setup as well as the carrier gases (Lines 259–272). We also added a table to list the configurations and parameters in the GC system (Table S1).

Page 7181 line 28: What are sampling uncertainties due to? local influence, human error?

[Response] The sampling uncertainties are mostly due to leakage of flask samplers or human errors (e.g., an operator who is not sufficiently trained yet and does not strictly follow the sampling or analysis protocol).

Page 7183 lines 2-3: Were the biases corrected?

[Response] No, the biases were not corrected as we don't know the true values.

Page 7184 line 12: 'additionally' should be 'additional'

[Response] Following your suggestion, we revised it.

Page 7185 line 12: HLE and CONTRAIL flights over New Delhi would likely be sampling different air masses, with HLE mostly seeming to sample air from the Middle East. Which altitude in the CONTRAIL profile represents the same air mass as HLE? Trajectories would be useful.

[Response] Following your suggestion, we computed and plotted five-day back-trajectories for all sampling hours of the in-situ CO_2 measurements over New Delhi by the CONTRAIL project (2006–2010). As shown in Fig. R3, the CONTRAIL flights at 3–6 km over New

Delhi sample the free-tropospheric air masses that pass over northern Africa and the Middle East throughout the year, and those coming from South Asia, Southeast Asia and the Arabian Sea during the SW monsoon season (Fig. R3a-c). They generally represents the same air mass as HLE (Fig. R3d), and do not show much difference across different altitude bands. We also added this figure in the Supplement (Fig. S7) and revised the main text accordingly (please see the revised manuscript Lines 396–397).

Page 7185 line 25: Again, it does not seem that HLE received many air masses from South Asia from the trajectories in Figure 1

[Response] Thanks a lot for your careful review and comment. Please refer to our response to your comment #5.

Page 7185 line 28: KZM and WLG, if they are more affected by northern air, then they would show a greater amplitude of the seasonal cycle. Can the authors comment?

[Response] Like HLE, KZM and WLG are high-altitude mountain stations, representative of the free-tropospheric background concentrations in northern mid-latitudes (Fig S4–5). As we know, the seasonal cycle of atmospheric CO_2 at surface observation stations in the Northern Hemisphere is driven primarily by net ecosystem production (NEP) fluxes from terrestrial ecosystem (Keeling et al., 1989; Manning, 1993; Erickson et al., 1996). In the far north, the amplitude of the CO_2 seasonal cycle ranges 15–20 ppm, and it diminishes southwards owing to the diminishing seasonality of plant activity towards the tropics (Keeling et al., 1996). As we mentioned in the manuscript, KZM and WLG are more influenced by northern air masses passing over Siberia with stronger seasonal CO_2 fluctuations, therefore CO_2 measurements at the two stations show larger amplitudes of seasonal cycles (as shown in Fig. 3b). The latitudinal gradients in the amplitude of the CO_2 seasonal cycle is also well illustrated in a 3D distribution of NOAA CO_2 Marine Boundary Layer (MBL) Reference (http://www.esrl.noaa.gov/gmd/ccgg/mbl/).

Page 7187 line 13: it seems that CARIBIC samples during the monsoon would not take one month to mix during this time of deep convection. Can the authors justify this statement? Also, why does vertical mixing lead to a larger seasonal cycle amplitude than HLE?

[Response] For the first question, we agree that during the SW monsoon, surface air masses with enhanced levels of trace gases are lifted by the strong deep convection over the Indian continent and rapidly mixed into the upper troposphere. Actually from Fig. 5a we can't tell a phase shift in CH_4 seasonal cycle by a lag of one month between the CARIBIC observations and HLE. For the CARIBC observations, the visible CH_4 seasonal maximum in September is not significant due to large errors of estimates in August and September (Fig. 5a). We removed this statement in the manuscript accordingly.

For the second question, during the SW monsoon period an anticyclone develops in the upper troposphere (Krishnamurti and Bhalme, 1976). Observations have shown persistent maxima

of many trace gases in the monsoon anticyclone during summer (Park et al., 2004; 2007), probably due to vertical transport of surface air masses by deep convection and subsequent accumulation and confinement of pollutants within the strong, closed circulation of the anticyclone (Li et al., 2005; Randel and Park, 2006). Randel and Park (2006) also showed that the monsoon anticyclone can trap air masses for up to several weeks depending on altitude, with more effective confinement occurring at higher altitudes. Since the CARIBIC flights sampled at altitudes 8–12.5km over this region (Schuck et al., 2010), we observe a larger amplitude of the CH_4 seasonal cycle than HLE.

Page 7187 line 16: Remove 'apparently'

[Response] Following your suggestion, we removed it.

Page 7187 lines 22-28: This discussion is too speculative and should be removed without further evidence (e.g., isotopic). There is not enough information to state that biogenic CH_4 emissions are responsible for the summer max at HLE. Furthermore, a model is needed to disentangle the meteorology from emissions.

[Response] Thanks a lot for your careful review and comments. Please refer to our response to your general comment #3.

Page 7187 line 29: be more specific - concentrations of trace gases would be enhanced at higher altitudes rather than the surface.

[Response] Following your suggestion, we revised it.

Page 7188 line 3: Earlier it is stated that KZM and WLG sample wetland emissions from the north. But here it is stated that their CH_4 increases are smaller because they are not influenced by deep convection. Does that necessarily imply that the increases will be smaller? There could be a large summer methane signal from wetlands.

[Response] The ground station measurements of CH_4 in the Northern Hemisphere usually show a summer minimum, predominantly due to oxidation of CH_4 by the OH radicals (Dlugokencky et al., 1994). The summer maxima observed at HLE, KZM and WLG likely result from transport of the air masses that are enriched in CH_4 and not yet consumed by OH before reaching the station. For KZM and WLG, the CH_4-enriched air masses are probably transported from Siberia with large wetland emissions in summer, and/or regional sources closer to the stations (Fang et al., 2013; also see back-trajectories in Fig. S4). Without deep convection during summer, at least the vertical transport of polluted air masses would be less efficient at the two stations, which could be one reason responsible for the smaller CH_4 enhancements compared to HLE. Indeed, further analyses (e.g. chemical transport model) are needed to resolve contribution of different sources and transport to the CH_4 enhancements at the three stations in summer. We revised the manuscript accordingly to make it clearer and precise (Lines 483–485).

Page 7188 line 10: Why does PON not sample surface emissions? The trajectories during July look like they pass over southern India.

[Response] Thanks a lot for your careful review and comments. We agree that this statement is not consistent with the back-trajectories at PON and removed it from the manuscript accordingly.

Page 7189 line 18: Why would it be argued that N_2O is 'more noisy than CO_2 and CH_4 due to regional sources synoptic variability'? Also, N_2O measurement has lower signal to noise (i.e. precision is lower than CO_2 and CH_4).

[Response] Thanks a lot for your careful review and comments. As you mentioned, the N_2O measurement has a lower signal-to-noise ratio. When we argue that the seasonal cycle of N_2O is noisier compared to CO_2 and CH_4 in the manuscript, it means the N_2O seasonal cycle has a larger uncertainty (i.e. lower precision, also indicated by the wide shaded area in Fig. 7). Given that the N_2O seasonal cycle is very small, synoptic events are more likely to mask the seasonal signal. As shown in Table 1, if we take the ratio of the seasonal cycle amplitude to the residual standard deviation (RSD, an indicator of synoptic variability) as a surrogate of the signal-to-noise ratio, we find that this ratio is significantly lower for N_2O (2.0, 1.5 and 2.0 for HLE, PON and PBL) than CO_2 (11.1, 1.9 and 7.1 for HLE, PON and PBL) and CH_4 (3.2, 3.6, 6.3 for HLE, PON and PBL). Following your suggestion, we revised the statement in the manuscript for clarification (Lines 541–542).

Page 7190 line 7: CARIBIC enrichment only during monsoon – why April-December 2008?

[Response] Following your suggestion, we revised the sentence to "Like CH_4, the N_2O enhancement at HLE during the summer monsoon period (June-September) is consistent with the aircraft flask measurements at flight altitudes 8–12.5 km from the CARIBIC project in 2008 (Schuck et al., 2010)" (Lines 557–560).

Page 7191 line 24: Even if there were no SF_6 emissions (rather than weak SF_6 emissions), this would imply that sites should follow the background. This still doesn't explain why there is a negative gradient.

[Response] The negative gradient between PON and HLE is likely due to the fact that HLE dominantly samples air masses passing over North Africa and the Middle East, where SF_6 emissions are substantial (Fig. R5). By contrast, PON receives air masses from the South India (during the boreal summer) and the northeast parts of the Indian subcontinent (during the boreal winter), which are much less polluted by SF_6. As PBL samples air masses from Southeast Asia and Southwest China (during the boreal winter) with notable SF_6 emissions (Fig. R5), the gradient between PBL and HLE is statistically insignificant. We revised the manuscript accordingly for clarification (Lines 600–602).

Page 7192 lines 14-18: It is mentioned here that CARIBIC samples different air masses to HLE. It is unclear therefore why the CARIBIC comparison is made for CH_4 and N_2O. This seems like a contradiction and so perhaps CARIBIC comparison should be removed for CH_4 and N_2O as well for HLE.

[Response] Thanks a lot for your careful review and comment. Please refer to our response to your general comment #6.

Page 7193 line 23: It is difficult to see a one month lag in Fig 11.

[Response] Please also refer to Table 1. The lag in the CO seasonal minimum between WLG and HLE is about 30 days. We added this information to the manuscript (Line 680).

Page 7193 line 16: Could the larger variability also be due to local sources?

[Response] Thanks a lot for your careful review and comment. Please refer to our response to your general comment #7.

Page 7196 lines 19-25: This discussion about bimodal H_2 seasonal cycle being due to biomass burning is very speculative and should be removed. There is not enough information or model runs to demonstrate that this is the case.

[Response] Following your suggestion, we revised the manuscript and removed the sentences that are not accurate (Lines 769–771).

Page 7197 line 21: Describe why anthropogenic CO emissions are lower in summer than winter?

[Response] The anthropogenic CO emissions in India are mainly contributed by residential energy use (57%) and agricultural waste burning (19%) (EDGAR v4.2). The anthropogenic CO emissions are lower in summer than in winter, mainly due to the less residential fuel use for heating (Streets et al., 2003). We added this information to the manuscript accordingly (Line 796).

Page 7198 line 3: Why would uplift contribute to maximum CH_4/CO ratio, as both species are uplifted together?

[Response] As we know, HLE is a high-altitude mountain station (4517m a.s.l.) and the CARIBIC measurements used for comparison in this study were taken at flight altitudes 8 – 12.5km (Schuck et al., 2010). Without the convective uplift that mixes the surface polluted air masses to the mid-to-upper troposphere during the SW monsoon, the summer maximum $\Delta CH_4/\Delta CO$ ratio would not be observed by HLE or the CARIBIC flights.

Section 3.3: This section is too speculative, as the appropriate model simulations have not been performed to assess whether the elevated events are related to elevations at BKT. With

the model simulation, linking the time and position of the elevated event at BKT with the time and position of the elevated event at PBL, this section should be removed.

[Response] We agree that the mechanism we proposed for the abnormal CH_4 and CO events and the possible linkage between PBL and BKT during the SW monsoon season are speculative, and need further verification with model experiments. Following your suggestion, we revised the manuscript and toned down the statements (Lines 938–945).

Conclusions page 7204 line 8 – The summertime maximum being attributed definitively to biogenic emissions is too speculative without other information. The authors should tone down the statement.

[Response] Following your suggestion, we revised the manuscript and tone down the statement accordingly (Lines 977–981, 986–991). Please refer to the response to general comment #3 for a more detailed discussion of the statement.

Figures 3, 5, 7 etc should show uncertainties, from measurement uncertainty, sampling uncertainty and if averaged into seasonal cycle, the variability in the seasonal cycle. This would provide an indication for the significance of the seasonal cycle. Some panels in figures contain uncertainties, some do not.

[Response] All the plots of seasonal cycles show uncertainties, including those in the supplementary document. For a few stations (e.g., HLE), the seasonal cycle of a species may be too small (relative to the scale of the plot) too be visible. We tried to improve the quality of these figures for better display.

Supplement - Back trajectories for comparison data (KZM, WLG) should also include trajectories for CARIBIC, etc.

[Response] Following your suggestion, we calculated and plotted back-trajectories for the CONTRAIL and CARIBIC measurements we used for comparison in this study (Fig. R3-4, also see Fig. S7–8 in the supplement).

Supplement - A description of KZM and WLG is needed. Are they mountain sites, etc?

[Response] Yes, they are high-altitude mountain stations. The geographic locations (latitude, longitude and altitude) of the two stations were given in the manuscript in *Section 3.1.1* (Lines 370–372).

Short title - Change to ’Five years (plural) of flask measurements’

[Response] We will revise it when resubmitting the paper.

References

Bouwman, A.F., Boumans, L.J.M., Batjes, N.H., 2002. Modeling global annual N_2O and NO emissions from fertilized fields. Global Biogeochem. Cycles 16, 1080. doi:10.1029/2001GB001812

Dlugokencky, E. J., Steele, L. P., Lang, P. M. and Masarie, K. A.: The growth rate and distribution of atmospheric methane, J. Geophys. Res.-Atmos., 99(D8), 17021–17043, doi:10.1029/94JD01245, 1994.

Erickson, D. J., Rasch, P. J., Tans, P. P., Friedlingstein, P., Ciais, P., Maier-Reimer, E., Six, K., Fischer, C. A. and Walters, S.: The seasonal cycle of atmospheric CO_2: A study based on the NCAR Community Climate Model (CCM2), J. Geophys. Res. Atmos., 101(D10), 15079–15097, doi:10.1029/95JD03680, 1996.

Fang, S.-X., Zhou, L.-X., Masarie, K. A., Xu, L. and Rella, C. W.: Study of atmospheric CH_4 mole fractions at three WMO/GAW stations in China, J. Geophys. Res.-Atmos., 118(10), 4874–4886, doi:10.1002/jgrd.50284, 2013.

Ganesan, A. L., Chatterjee, A., Prinn, R. G., Harth, C. M., Salameh, P. K., Manning, A. J., Hall, B. D., Mühle, J., Meredith, L. K., Weiss, R. F., O'Doherty, S., and Young, D.: The variability of methane, nitrous oxide and sulfur hexafluoride in Northeast India, Atmos. Chem. Phys., 13, 10633-10644, 10.5194/acp-13-10633-2013, 2013.

Kaplan, J. O., Folberth, G. and Hauglustaine, D. A.: Role of methane and biogenic volatile organic compound sources in late glacial and Holocene fluctuations of atmospheric methane concentrations, Global Biogeochem. Cycles, 20(2), GB2016, doi:10.1029/2005GB002590, 2006.

Keeling, C. D., Bacastow, R. B., Carter, A. F., Piper, S. C., Whorf, T. P., Heimann, M., Mook, W. G. and Roeloffzen, H.: A three-dimensional model of atmospheric CO_2 transport based on observed winds: 1. Analysis of observational data, in Aspects of Climate Variability in the Pacific and the Western Americas, pp. 165–236, American Geophysical Union., 1989.

Keeling, C. D., Chin, J. F. S. and Whorf, T. P.: Increased activity of northern vegetation inferred from atmospheric CO_2 measurements, Nature, 382(6587), 146–149 [online] Available from: http://dx.doi.org/10.1038/382146a0, 1996.

Krishnamurti, T. N. and Bhalme, H. N.: Oscillations of a Monsoon System. Part I. Observational Aspects, J. Atmos. Sci., 33(10), 1937–1954, doi:10.1175/1520-0469(1976)033, 1976.

Krishnamurti, T.N., Biswas, M.K., Rao, D.V.B., 2008. Vertical extension of the Tibetan high of the Asian summer monsoon. Tellus A 60, 1038–1052. doi:10.1111/j.1600-0870.2008.00359.x

Lal, S., Chandra, N., Venkataramani, S.: A study of CO_2 and related trace gases using a laser based technique at an urban site in western India. Submitted to Curr. Sci., 2015.

Li, Q., Jiang, J. H., Wu, D. L., Read, W. G., Livesey, N. J., Waters, J. W., Zhang, Y., Wang, B., Filipiak, M. J., Davis, C. P., Turquety, S., Wu, S., Park, R. J., Yantosca, R. M. and Jacob, D. J.: Convective outflow of South Asian pollution: A global CTM simulation compared with EOS MLS observations, Geophys. Res. Lett., 32(14), L14826, doi:10.1029/2005GL022762, 2005.

Lopez, M.: Estimation des émissions de gaz à effet de serre à différentes échelles en France à l'aide d'observations de haute précision, Ph.D, Université Paris-Sud, 2012.

Manning, M.: Seasonal Cycles in Atmospheric CO_2 Concentrations, in The Global Carbon Cycle SE - 3, vol. 15, edited by M. Heimann, pp. 65–94, Springer Berlin Heidelberg., 1993.

Matthews, E., Fung, I. and Lerner, J.: Methane emission from rice cultivation: Geographic and seasonal distribution of cultivated areas and emissions, Global Biogeochem. Cycles, 5(1), 3–24, doi:10.1029/90GB02311, 1991.

Park, M., Randel, W. J., Gettelman, A., Massie, S. T. and Jiang, J. H.: Transport above the Asian summer monsoon anticyclone inferred from Aura Microwave Limb Sounder tracers, J. Geophys. Res.-Atmos., 112(D16), D16309, doi:10.1029/2006JD008294, 2007.

Park, M., Randel, W. J., Kinnison, D. E., Garcia, R. R. and Choi, W.: Seasonal variation of methane, water vapor, and nitrogen oxides near the tropopause: Satellite observations and model simulations, J. Geophys. Res.-Atmos., 109(D3), D03302, doi:10.1029/2003JD003706, 2004.

Randel, W. J. and Park, M.: Deep convective influence on the Asian summer monsoon anticyclone and associated tracer variability observed with Atmospheric Infrared Sounder (AIRS), J. Geophys. Res.-Atmos., 111(D12), D12314, doi:10.1029/2005JD006490, 2006.

Sanderson, M. G.: Biomass of termites and their emissions of methane and carbon dioxide: A global database, Global Biogeochem. Cycles, 10(4), 543–557, doi:10.1029/96GB01893, 1996.

Schmidt, M., Glatzel-Mattheier, H., Sartorius, H., Worthy, D. E. and Levin, I.: Western European N_2O emissions: A top-down approach based on atmospheric observations, J. Geophys. Res.-Atmos., 106(D6), 5507–5516, doi:10.1029/2000JD900701, 2001.

Schuck, T. J., Brenninkmeijer, C. A. M., Baker, A. K., Slemr, F., von Velthoven, P. F. J. and Zahn, A.: Greenhouse gas relationships in the Indian summer monsoon plume measured by the CARIBIC passenger aircraft, Atmos. Chem. Phys., 10(8), 3965–3984, doi:10.5194/acp-10-3965-2010, 2010.

Streets, D. G., Bond, T. C., Carmichael, G. R., Fernandes, S. D., Fu, Q., He, D., Klimont, Z., Nelson, S. M., Tsai, N. Y., Wang, M. Q., Woo, J. H., and Yarber, K. F.: An inventory of gaseous and primary aerosol emissions in Asia in the year 2000, J. Geophys. Res.-Atmos., 108, 8809, 10.1029/2002jd003093, 2003.

Tiwari, Y. K., Vellore, R. K., Ravi Kumar, K., van der Schoot, M., and Cho, C.-H.: Influence of monsoons on atmospheric CO_2 spatial variability and ground-based monitoring over India, Sci. Total Environ., 490, 570-578, http://dx.doi.org/10.1016/j.scitotenv.2014.05.045, 2014.

Tables

Table R1 Features of the smoothed fitting curves for flask measurements at PON (2007–2011). For each species, the smoothed curves are fitted to the data not filtered by CO outliers and the data filtered by CO outliers. The annual mean values and average peak-to-peak amplitude are calculated from the smoothed curve and mean season cycle, respectively. Uncertainty of each estimate is calculated from 1 s.d. of 1000 bootstrap replicates.

	Not CO filtered	CO filtered
CO_2 (ppm)		
N_{fit}	121	105
Annual mean 2007	386.6±0.9	386.5±1.1
Annual mean 2008	388.1±0.9	388.0±0.9
Annual mean 2009	389.0±0.6	388.4±0.8
Annual mean 2010	391.3±1.5	391.2±1.5
Annual gradient relative to HLE	2.9±1.2	2.6±1.4
Trend	1.7±0.1	1.7±0.1
RSD	4.0	4.1
Amplitude	7.6±1.4	7.8±1.6
D_{max}	111.0±13.4	116.0±14.1
D_{min}	327.0±54.3	327.0±55.8
CH_4 (ppb)		
N_{fit}	164	101
Annual mean 2007	1859.2±6.7	1854.2±5.9
Annual mean 2008	1856.1±10.4	1857.3±6.8
Annual mean 2009	1865.7±5.1	1855.5±6.2
Annual mean 2010	1876.9±9.1	1877.3±7.3
Annual gradient relative to HLE	37.4±10.7	34.0±11.0
Trend	9.4±0.1	9.0±0.1
RSD	34.4	19.8
Amplitude	124.1±10.2	127.8±11.4
D_{max}	337.0±6.1	331.0±5.4
D_{min}	189.0±10.7	192.0±9.8
N_2O (ppb)		
N_{fit}	137	110
Annual mean 2007	324.8±0.3	324.9±0.4
Annual mean 2008	326.3±0.3	326.3±0.3
Annual mean 2009	326.7±0.3	326.4±0.3
Annual mean 2010	327.1±0.5	327.0±0.5
Annual gradient relative to HLE	3.1±0.3	3.0±0.3
Trend	0.8±0.1	0.7±0.1
RSD	1.4	1.4
Amplitude	1.2±0.5	1.1±0.5

D_{max}	262.0±83.2	262.0±46.1
D_{min}	141.0±48.2	97.0±65.8
SF_6 (ppt)		
N_{fit}	174	139
Annual mean 2007	6.19±0.01	6.19±0.02
Annual mean 2008	6.49±0.02	6.49±0.02
Annual mean 2009	6.77±0.01	6.77±0.02
Annual mean 2010	7.08±0.02	7.08±0.02
Annual gradient relative to HLE	-0.06±0.03	-0.06±0.03
Trend	0.31±0.05	0.31±0.06
RSD	0.05	0.05
Amplitude	0.24±0.02	0.24±0.03
D_{max}	327.0±12.1	327.0±21.7
D_{min}	204.0±3.3	205.0±3.4
CO (ppb)		
N_{fit}	139	139
Annual mean 2007	200.5±7.8	200.5±7.8
Annual mean 2008	175.3±13.1	175.3±13.1
Annual mean 2009	174.3±4.8	174.3±4.8
Annual mean 2010	185.1±8.7	185.1±8.7
Annual gradient relative to HLE	82.4±10.7	82.4±10.7
Trend	0.4±0.1	0.4±0.1
RSD	32.0	32.0
Amplitude	78.2±11.6	78.2±11.6
D_{max}	4.0±160.2	4.0±160.2
D_{min}	238.0±46.1	238.0±46.1
H_2 (ppb)		
N_{fit}	140	120
Annual mean 2007	574.5±2.4	573.7±3.2
Annual mean 2008	558.2±5.3	558.3±5.1
Annual mean 2009	562.4±1.6	561.9±1.6
Annual mean 2010	563.9±2.3	563.0±2.5
Annual gradient relative to HLE	29.8±4.1	29.3±3.7
Trend	-1.3±0.1	-1.3±0.1
RSD	8.4	8.3
Amplitude	21.6±3.4	21.1±3.8
D_{max}	96.0±9.6	97.0±9.8
D_{min}	219.0±10.3	215.0±11.9

Figures

Figure R1 The mean CH_4 seasonal cycles observed at HLE and seasonal variations of CH_4 emissions from rice paddies and wetlands over the Indian subcontinent. The CH_4 emissions from rice paddies are extracted from a global emission map for the year 2010 (EDGAR v4.2), imposed by the seasonal variation on the basis of Matthews et al. (1991). The CH_4 emissions from wetlands are extracted from outputs of a global vegetation model (BIOME4-TG, Kaplan et al., 2006). The seasonal variation of deep convection over the Indian subcontinent is also presented, indicated by convective precipitation obtained from an LMDz simulation nudged with ECMWF reanalysis. The CH_4 emissions and convective precipitation are averaged over the domain of 10–35 °N, 70°–90°E to give a regional mean estimate.

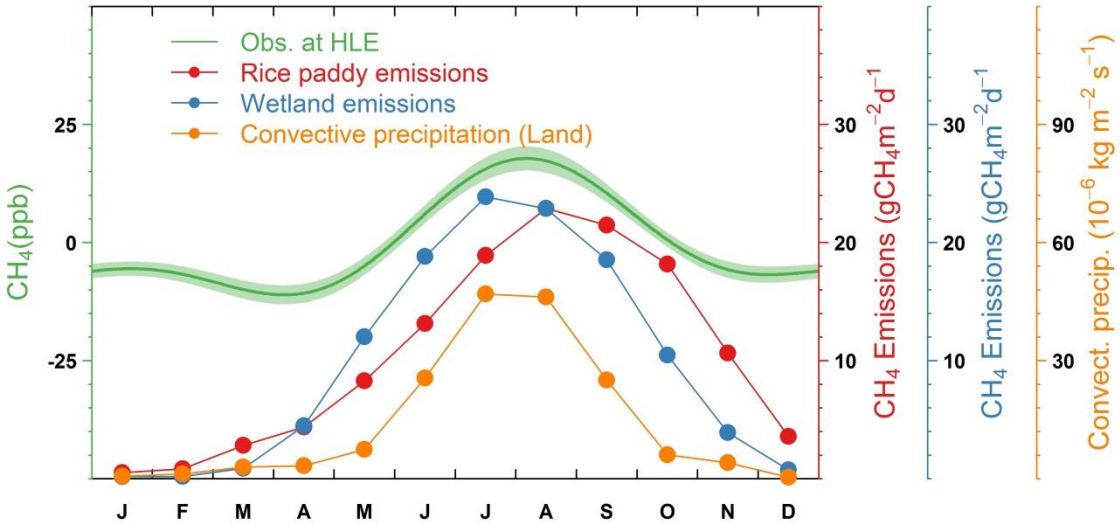

Figure R2 Time series of flask measurements at PON (2007–2011) with smoothed fitting curves for **(a)** CO_2, **(b)** CH_4, **(c)** N_2O, **(d)** SF_6 and **(e)** H_2. The open circles denote flask data used to fit the solid smoothed curves, while the crosses denote discarded flask data lying outside 3 times the residual standard deviations from the smoothed curve fits as well as those filtered by CO outliers. For PON, the solid (dotted) red line indicates the smoothed curve fitted to the data (not) filtered by CO outliers. The flask measurements at HLE and the corresponding smoothed fitting curve are also presented for comparison.

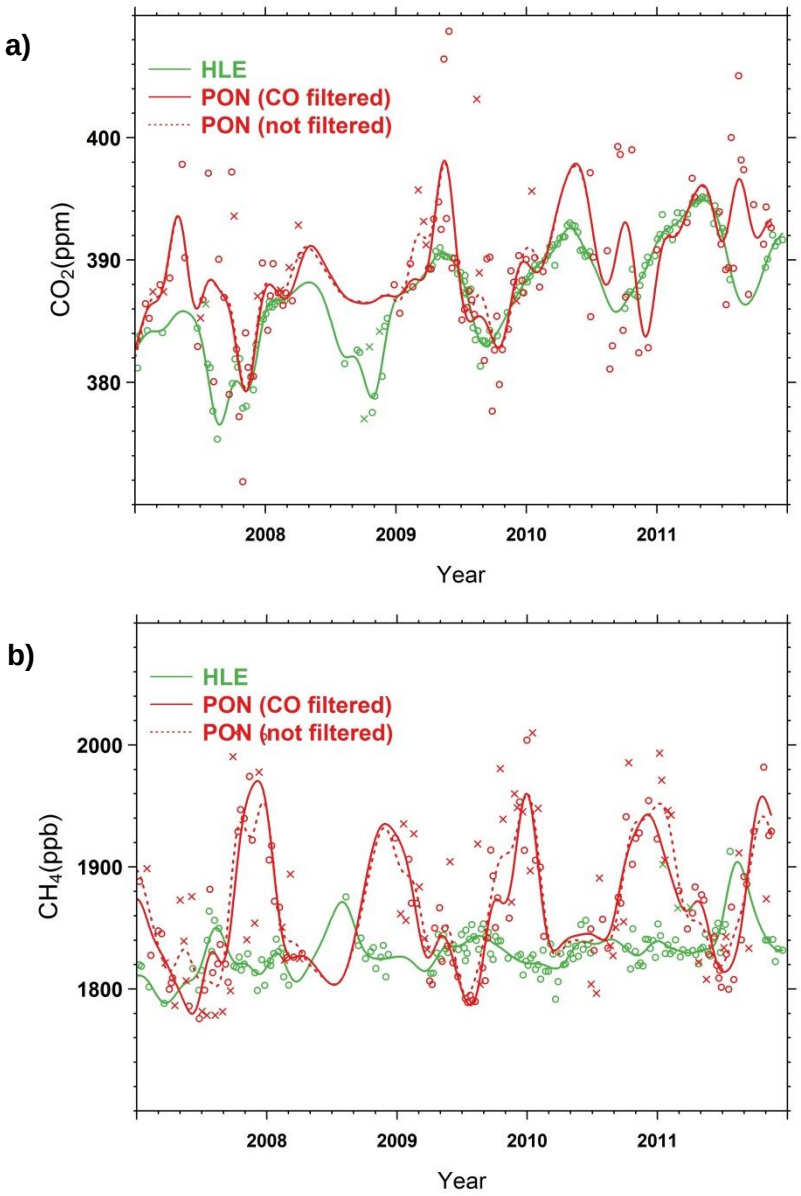

c)

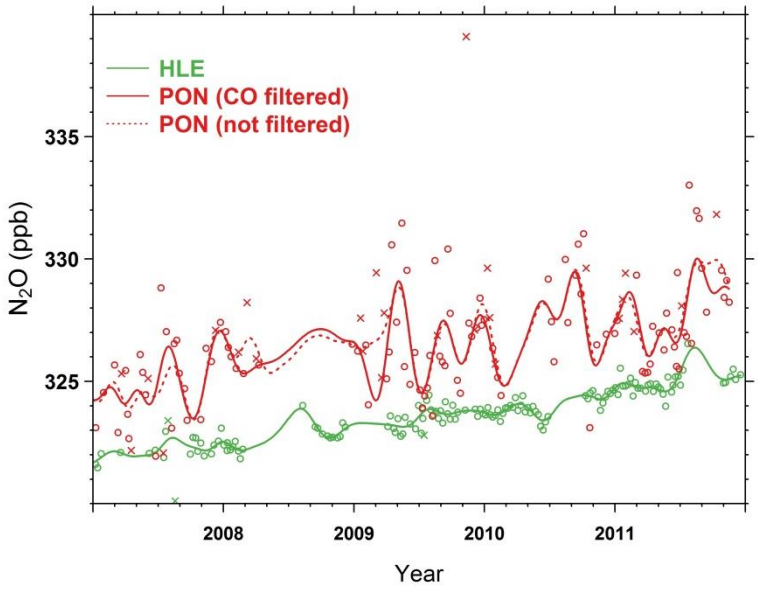
HLE
PON (CO filtered)
PON (not filtered)
335
330
325
N2O (ppb)
2008
2009
2010
2011
Year

d)

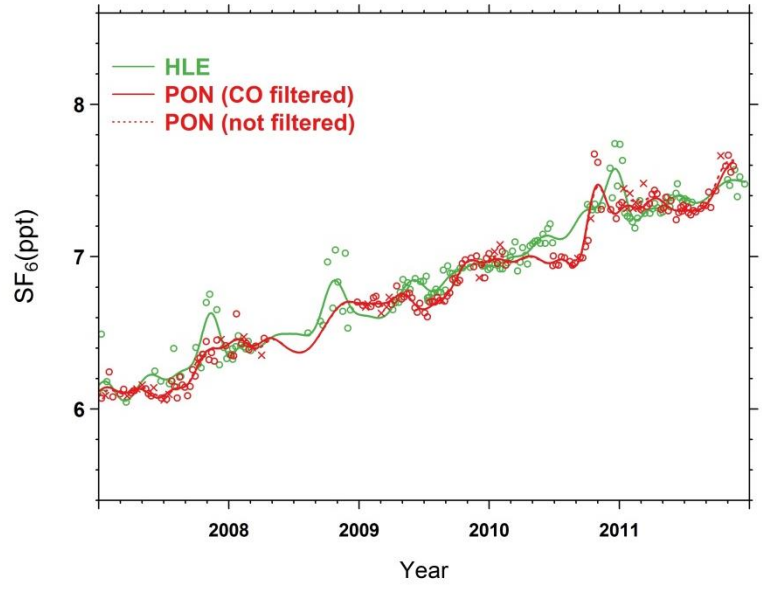
HLE
PON (CO filtered)
PON (not filtered)
8
7
6
SF6(ppt)
2008
2009
2010
2011
Year

e)

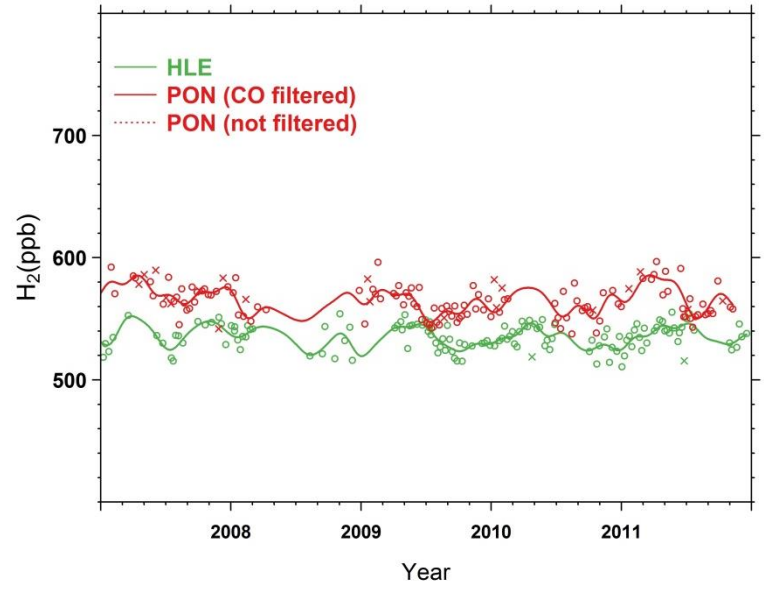
HLE
PON (CO filtered)
PON (not filtered)
700
600
500
H2(ppb)
2008
2009
2010
2011
Year

Figure R3 Five-day back-trajectories calculated for all sampling hours of the in-situ CO_2 measurements over New Delhi by the CONTRAIL project (2006–2010). Back-trajectories are computed and plotted at different altitude bands: **(a)** 3–4 km, **(b)** 4–5 km, and **(c)** 5–6 km. For comparison, back-trajectories for all sampling dates of the flask measurements at HLE (2007–2011) are also presented in **(d)**. All back-trajectories are colored by the elevation of air masses at hourly time step.

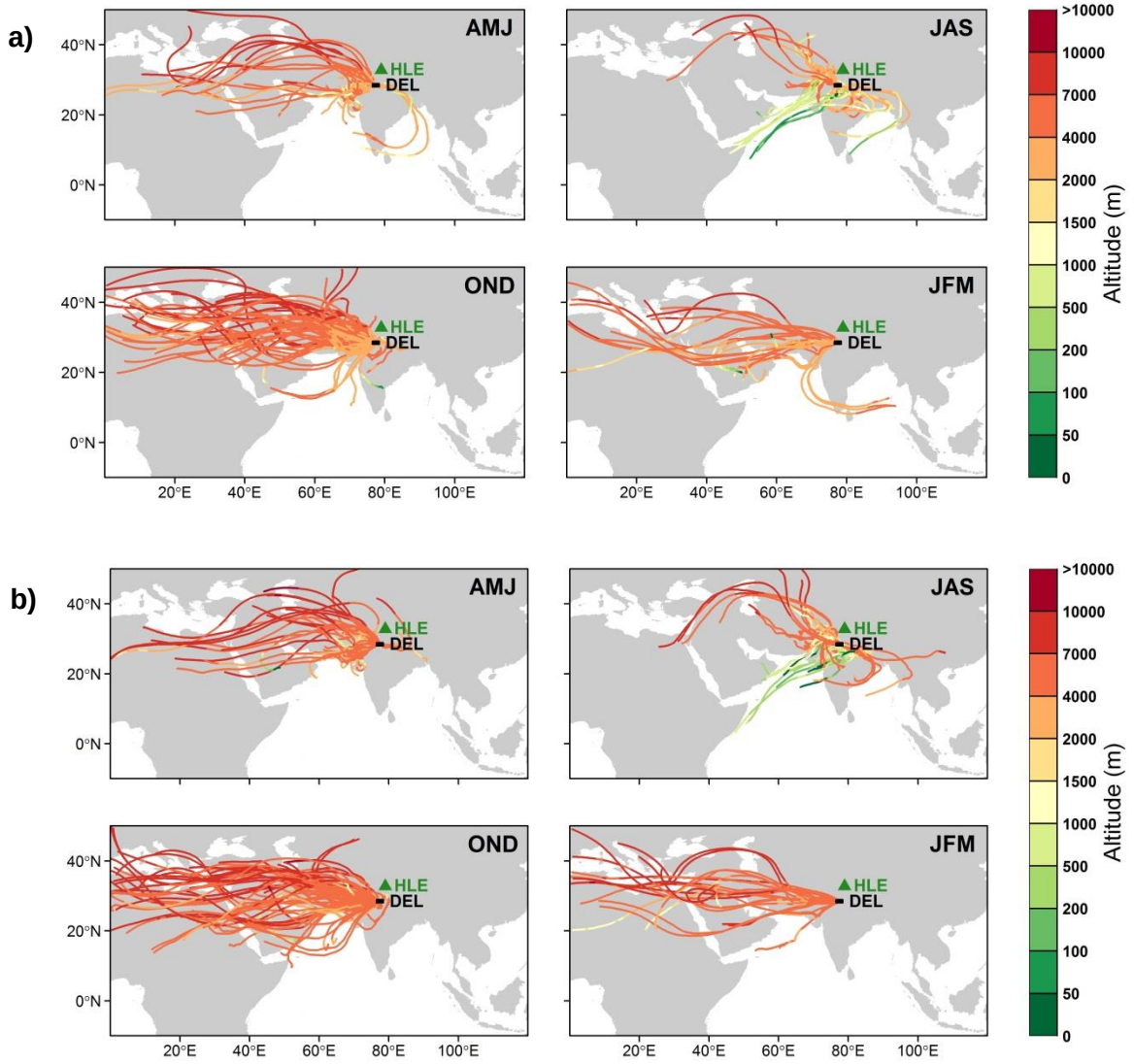

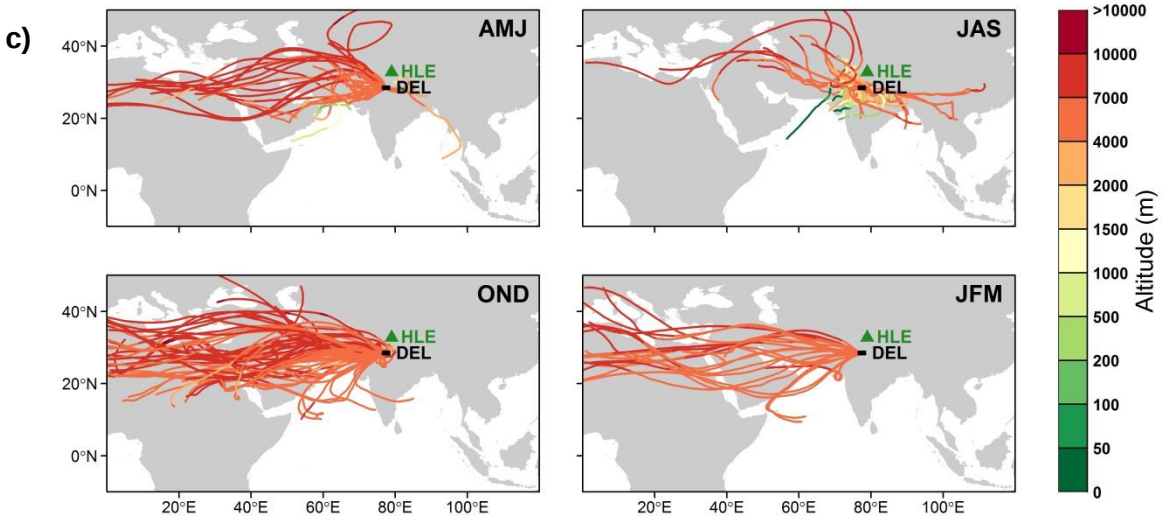
c)
AMJ
JAS
OND
JFM
HLE
DEL
40°N
20°N
0°N
20°E
40°E
60°E
80°E
100°E
>10000
10000
7000
4000
2000
1500
1000
500
200
100
50
0
Altitude (m)

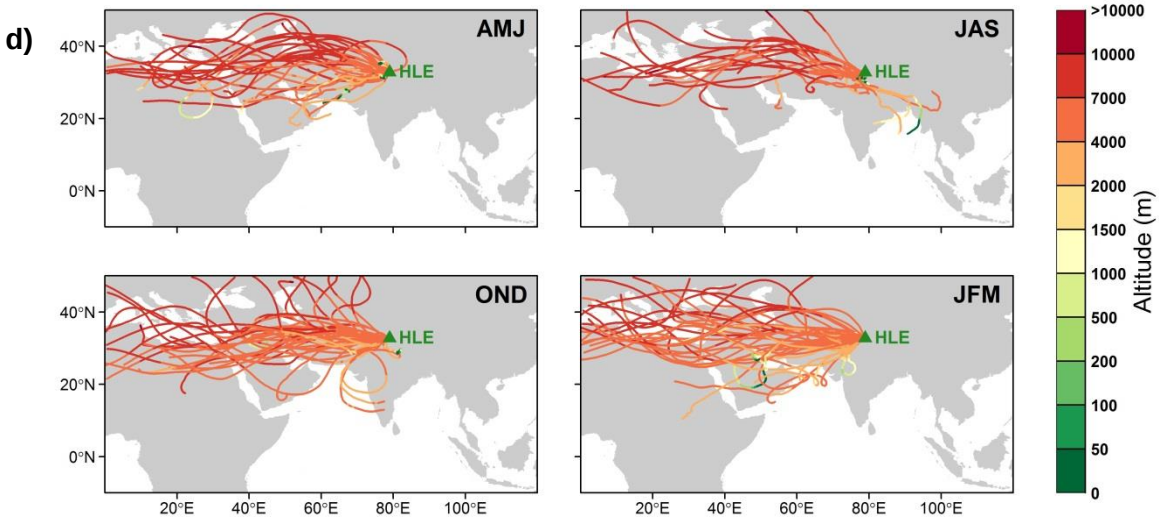
d)
AMJ
JAS
OND
JFM
HLE
40°N
20°N
0°N
20°E
40°E
60°E
80°E
100°E
>10000
10000
7000
4000
2000
1500
1000
500
200
100
50
0
Altitude (m)

Figure R4 (a) Five-day back-trajectories calculated for all sampling hours of the flask measurements by the CARIBIC flight between Frankfurt and Chennai at flight altitudes 8–12.5 km for the year 2008. The box indicates the domain of 10–40°N, 50–80°E, where flask samples within it were investigated in Schuck et al. (2010). **(b)** Five-day back-trajectories calculated for all sampling dates over the period 2007–2011 at HLE. All back-trajectories are colored by the elevation of air masses at hourly time step.

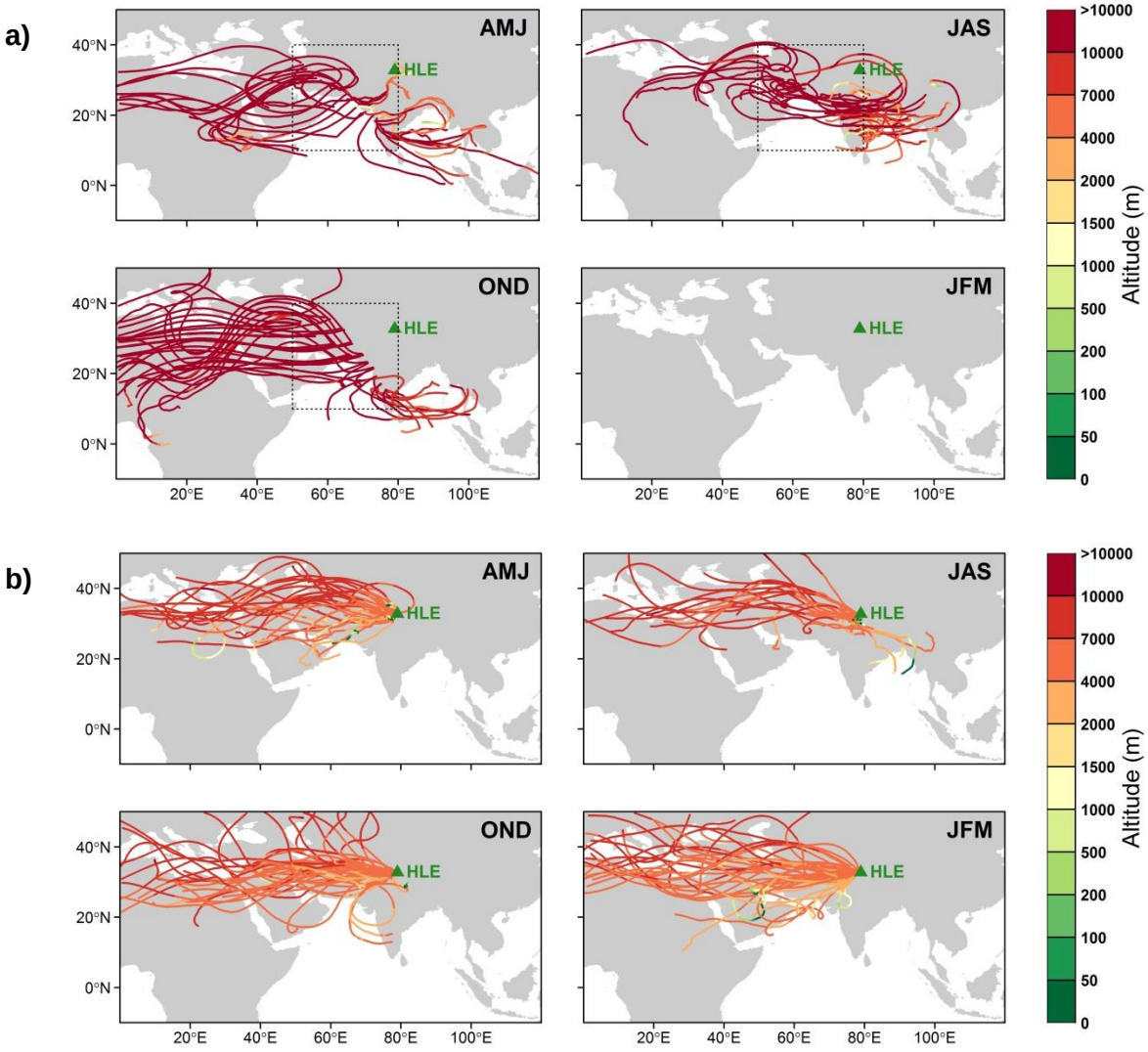

Figure R5 The map of SF_6 emissions for the year 2010 based on the EDGARv4.2 FT2010 dataset. This map is produced by EDGAR and can be downloaded from the website (http://edgar.jrc.ec.europa.eu/).

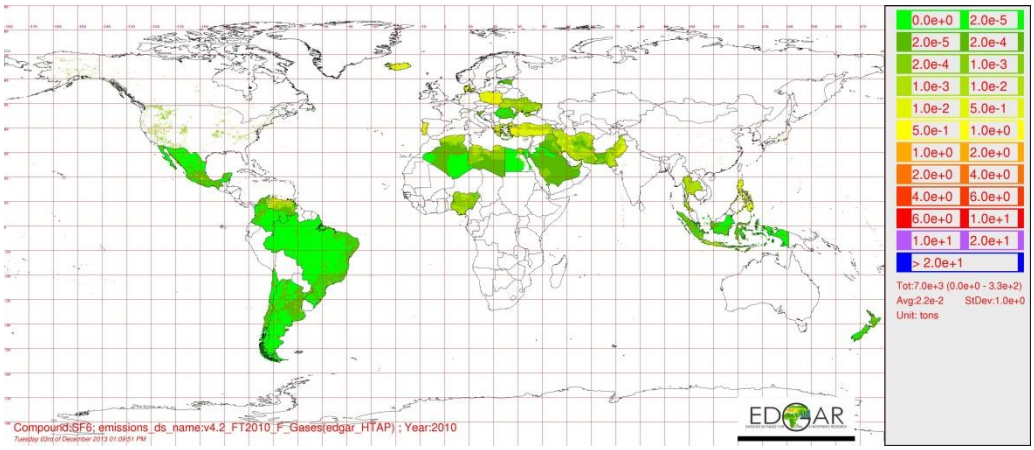

List of changes

Changes to the main text

Page 7173, Line 2: change “With the rapid growth” to “With a rapid growth”.

Page 7173, Line 6: add “an” after “As a result of”.

Page 7173, Line 10: add “the” before “five-year measurements (2007–2011)”.

Page 7173, Line 15: change “dominant” to “likely”.

Page 7173, Lines 18–19: change “allow a better understanding of, and constraints on the GHG budgets at regional and continental scales” to “better constrain the GHG budgets at regional and continental scales”.

Page 7173, Line 24: change “during the recent decades” to “during recent decades”.

Page 7174, Line 2: add “, much faster than rates of most developed countries and economies like the USA (9%) and EU (-14%) over the same period” after “from 1.4 to 2.8 $GtCO_2eq$”.

Page 7174, Lines 5–7: change “… the more developed countries (in 2010, the per capita GHG emission rates were 2.2, 10.9, 17.6, and 21.6 $tonCO_2eq$/capita for India, the UK, Russia, and the USA, respectively; EDGAR v4.2)” to “… the more developed countries. For comparison, in 2010, the per capita GHG emission rates were 2.2, 10.9, 17.6, and 21.6 $tonCO_2eq$/capita for India, the UK, Russia, and the USA, respectively (EDGAR v4.2)”.

Page 7174, Line 8: change “agriculture-related” to “agricultural”.

Page 7174, Lines 12–14: change “Reducing these two non-CO_2 GHG emissions possibly offers a cost-effective way to mitigate future climate change (Montzka et al., 2011)” to “Reducing emissions of these two non-CO_2 GHGs may offer a more cost-effective way to mitigate future climate change than by attempting to directly reduce CO_2 emissions (Montzka et al., 2011)”.

Page 7174, Line 15: remove “monitoring and”.

Page 7174, Line 18: change “the top-down approach or bottom-up approach” to “the top-down approaches (based on atmospheric inversions) or bottom-up approaches (based on emission inventories or biospheric models)”.

Page 7174, Line 24: add “, much larger compared to those of Europe (~30%, see Luyssaert et al., 2012) and North America (~60%, see King et al., 2015), where observational networks are denser and emission inventories are more accurate” after “as high as 100–150%”.

Page 7175, Line 1: add “– 15.08°N, 73.83°E, 60m a.s.l.” after “CRI”.

Page 7175, Lines 3–8: change “Although recent aircraft and satellite observations …, a denser atmospheric observational network …, … sources and sinks of GHGs” to “Recently a few other ground stations have been established in Western India and the Himalayas to monitor GHGs and atmospheric pollutants, which are located in Sinhagad (SNG – 18.35°N, 73.75°E, 1600m a.s.l.; Tiwari and Kumar, 2012; Tiwari et al., 2014), Mount Abu (24.60°N, 72.70°E, 1700m a.s.l.; S. Lal, personal communication), Ahmedabad (23.00°N, 72.50°E, 55m a.s.l.; Lal et al., 2015), Nainital (29.37°N, 79.45°E, 1958m a.s.l.; Kumar et al., 2010) and Darjeeling (27.03°N, 88.15°E, 2194m a.s.l.; Ganesan et al., 2013). Most of these stations started to measure atmospheric GHG concentrations very recently (e.g. Sinhagad – since 2009; Ahmedabad – since 2013; Mount Abu – since 2013; Nainital – since 2006; Darjeeling – since 2011), and datasets are not always available. In addition, aircraft and satellite observations have also been carried out and provided useful constraints on estimates of GHG fluxes in this region (Park et al., 2007; Xiong et al., 2009; Schuck et al., 2010; Patra et al., 2011b; Niwa et al., 2012; Zhang et al., 2014). Although inclusion of measurements from South Asia significantly reduces uncertainties in top-down estimates of regional GHG emissions (e.g., Huang et al., 2008; Niwa et al., 2012; Zhang et al., 2014), a denser atmospheric observational network with sustained measurements is still needed over this vast and fast-growing region for an improved, more detailed, and necessary understanding of GHG budgets”

Page 7175, Line 9: change “Besides a lack of observation sites” to “Besides the lack of a comprehensive observational network”.

Page 7175, Line 17: add “On the contrary, little deep convection occurs over South Asia during the winter monsoon period, which carries less moisture (Lawrence and Lelieveld, 2010).” after “… lower stratosphere (Schuck et al., 2010; Lawrence and Lelieveld, 2010).”.

Page 7175, Line 21: change “to retrieve accurate inversion” to “for retrieving reliable inversion”.

Page 7175, Line 22: change “is valuable” to “would be valuable”.

Page 7175, Line 25: add “the” before “Indo-French collaboration”.

Page 7175, Line 25: change “aiming to monitor GHGs” to “with the objective of monitoring the atmospheric concentrations of GHGs”.

Page 7176, Line 1: change “describe main aspects of the stations” to “describe the main features of these stations”.

Page 7176, Line 5: change “are measured” to “were measured”.

Page 7176, Lines 8–10: change “We also analyze covariances between species (using deviations from their smoothed fitting curves) for synoptic variations (Sect. 3.2)” to “We

examine synoptic variations of CO_2, CH_4 and CO by analyzing the co-variances between species, using deviations from their smoothed fitting curves (Sect. 3.2)"

Page 7176, Lines 11–12: change "We summarize the paper and draw conclusion in Sect. 4" to "A summary of the paper as well as conclusions drawn from these results are given in Sect. 4".

Page 7176, Line 20: add "the" before "India Meteorological Department".

Page 7176, Line 22: add "the" before "winter season".

Page 7177, Line 4: change "The Hanle (HLE) station (32.78 °N, 78.96 °E, 4517 m a.s.l.)" to "The Hanle (HLE) station (32.780 °N, 78.960 °E, 4517 m a.s.l.)".

Page 7177, Lines 7–8: change "with the Indian Institute of Astrophysics" to "between the Indian Institute of Astrophysics and LSCE, France".

Page 7177, Line 8: Add "The flask sampling inlet is installed on the top of a 3 m mast fixed on the roof of a 2m high building, and the ambient air is pumped through a Dekabon tubing with a diameter of 1/4"." before "The area around the station …".

Page 7177, Line 12: remove ", industrialized" before "city of Leh".

Page 7177, Line 15: add "the" before "background free tropospheric air masses"

Page 7177, Line 15: change "the mid-latitude of Northern Hemisphere" to "the northern mid-latitudes".

Page 7177, Line 16: add "at this station" after "Regular flask air sampling".

Page 7177, Line 16: add "continuous" before "in-situ CO_2".

Page 7177, Line 19: change "HLE dominantly sampled" to "HLE dominantly samples".

Page 7177, Line 21: change "Fig. 1" to "Fig. 1a"

Page 7177, Line 23: change "The Pondicherry (PON) station (12.01 °N, 79.86 °E, 20 m a.s.l)" to "The Pondicherry (PON) station (12.010 °N, 79.860 °E, 20 m a.s.l)".

Page 7177, Lines 26–28: change "The flask sampling inlet was initially located on a 10 m mast fixed on the roof of the University Guest House, later moved to a 30 m high tower in June, 2011." to "The flask sampling inlet, initially located on a 10 m mast fixed on the roof of the University Guest House, was later moved to a 30 m high tower in June, 2011".

Page 7177, Line 28: add "The ambient air is pumped from the top of the tower through a Dekabon tubing with a diameter of 1/4"." before "The surrounding village Kalapet".

Page 7177, Line 29: add “with a low traffic flow especially during the nighttime” after “to the west of the station”.

Page 7178, Line 2: change “with populations of over 4 million” to “with populations of over 6”.

Page 7178, Line 3: change “120 km” to “143 km”

Page 7178, Line 3: change “260 km” to “330 km”

Page 7178, Lines 7–8: change “Flask sampling began in September, 2006. Over the period 2007–2011, a total of 185 flask sample pairs were collected at PON” to “Flask sampling at PON began in September, 2006 and over the period 2007–2011, a total of 185 flask sample pairs were collected at the site”.

Page 7178, Line 8: change “Fig. 1” to “Fig. 1a”.

Page 7178, Line 15: change “The Port Blair (PBL) station (11.65 °N, 92.76 °E, 20 m a.s.l.)” to “The Port Blair (PBL) station (11.650 °N, 92.760 °E, 20 m a.s.l.)”.

Page 7178, Line 20: add “The flask sampling inlet is located on the top of a 30 m high tower, and the ambient air is pumped through a Dekabon tubing with a diameter of 1/4”.” before “The main city on the Andaman Islands”.

Page 7178, Line 27: change “Fig. 1” to “Fig. 1a”.

Page 7179, Lines 9–10: change “with KEL-F (PTCFE) valves (Glass Expansion, Australia or Normag, Germany) fitted at both ends” to “with valves sealed by caps made from KEL-F (PTCFE) fitted at both ends”.

Page 7179, Lines 10–14: change “Besides, flask equipped with the original Teflon PFA O-ring valves …, and a storage correction for the loss … is applied after analyses of the samples.” to “Besides, a few flasks are equipped with valves sealed by the original Teflon PFA O-ring (Glass Expansion, Australia), accounting for ~5.0, 1.2 and 1.1% of air samples respectively for HLE, PON and PBL during the study period. For the air samples stored in flasks sealed with the original Teflon PFA O-ring, corrections are made for the loss of CO_2 (+0.0027 ppm/day) and of N_2O (+0.0035 ppb/day) after analyses of the samples.”.

Page 7179, Line 21: add “the” before “ambient pressure”.

Page 7180, Line 4: change “(HP86890, Agilent)” to “(HP6890, Agilent)”.

Page 7180, Line 9: remove “(Lopez et al., 2012; Yver et al., 2009)”.

Page 7180, Line 9: add “In the following paragraph we summarize the major configurations and parameters of the GC systems (also see Table S1). Further details on the analyzer

configuration are described in Lopez (2012) and Yver et al. (2009).” after “… UV absorption.”.

Page 7180, Line 14: add “with flask overpressure” after “The air samples are flushed”.

Page 7180, Line 15: change “a 10 mL sample loop for N_2O and SF_6 analyses ” to “ a 15 mL sample loop for N_2O and SF_6 analyses ”.

Page 7180, Line 17: change “the sampled air” to “the air sample”.

Page 7180, Lines 17–25: change “For the CO_2 and CH_4 separation ... For N_2O and SF_6 separation … Detection of CH_4 and CO_2 … Detection of N_2O and SF_6 is performed in the ECD.” to “The CO_2 and CH_4 separation is performed using a Hayesep-Q (12’ × 3/16”OD, mesh 80/100) analytical column placed in an oven at 80°C, with a N_2 5.0 carrier gas at a flow rate of 50 ml min^{-1}. Detection of CH_4 and CO_2 (after conversion to CH_4 using a Ni catalyst and H_2 gas) is performed in the FID kept at 250°C. The flame is fed with H_2 (provided by a NM-H_2 generator from F-DBS) at a flow rate of 100 ml min^{-1} and zero air (provided by a 75-82 zero air generator from Parker-Balston) at a flow rate of 300 ml min^{-1}. For N_2O and SF_6 separation, a Hayesep-Q (4’ × 3/16” OD, mesh 80/100) pre-column and a Hayesep-Q (6’ × 3/16” OD, mesh 80/100) analytical column, both placed in an oven at 80°C, are used together with an Ar/CH_4 carrier gas at a flow rate of 40 ml min^{-1}. Detection of N_2O and SF_6 is performed in the ECD heated at 395°C.”.

Page 7180, Lines 26–27: change “a pre-column (Unibeads 1S mesh 60/80; 1/8 inches OD × 16.5 inches)” to “a Unibeads 1S pre-column (16.5” × 1/8” OD; mesh 60/80)”.

Page 7180, Lines 27–28: change “an analytical column (Molecular Sieve 5°A mesh 60/80; 1/8 inches CD × 80 inches)” to “a Molecular Sieve 5Å analytical column (80” × 1/8” OD; mesh 60/80)”.

Page 7181, Line 1: change “H_2 from CO, both of which are analyzed in the RGD detector.” to “H_2 from CO. Both columns are placed in an oven kept at 105°C. CO and H_2 are analyzed in the RGD detector heated to 265°C.”.

Page 7181, Line 4: add “The calibration and quality control cylinders are filled and spiked in a matrix of synthetic air containing N_2, O_2 and Ar prepared by Deuste Steininger (Germany).” before “The concentration of the sample”.

Page 7181, Lines 10–11: change “(Dlugokencky et al., 2005; Zhao and Tans, 2006; Jordan and Steinberg, 2011; Hall et al., 2007)” to “(CO_2: WMOX2007; CH_4: NOAA2004; N_2O: NOAA2005A; SF_6: NOAA2005; CO: WMOX2004; H_2: WMOX2009; Hall et al., 2007; Dlugokencky et al., 2005; Jordan and Steinberg, 2011; Zhao and Tans, 2006)”.

Page 7181, Line 16: add “the” before “values of a flask target”.

Page 7181, Lines 21–22: remove “More detailed descriptions of flask analysis are available in Yver et al. (2009) and Lopez et al. (2014).”.

Page 7181, Line 24: change “stem” to “stemmed”.

Page 7182, Lines 2–3: change “The percentages of retained flask pairs after flagging amount to” to “The percentages of flask pairs retained for analyses are”.

Page 7182, Lines 12–17: remove “Finally, all results are linked to the international scales defined for each species … against the primary scale maintained at LSCE (Hall et al., 2007; Dlugokencky et al., 2005; Jordan and Steinberg, 2011; Zhao and Tans, 2006).”.

Page 7183, Line 1: change “within the noise” to “within the noise level”.

Page 7183, Line 16: change “until no outliers were identified” to “until no outliers remained”.

Page 7183, Line 17: add “These outliers were likely a result of pollution by local emissions and not representative of regional background concentrations.” before “The data discarded”.

Page 7183, Lines 25–26: change “belong to other networks (e.g., NOAA/ESRL and Integrated Carbon Observation System (ICOS))” to “belong to networks of NOAA/ESRL (http://www.esrl.noaa.gov/gmd/) and Integrated Carbon Observation System (ICOS, https://www.icos-cp.eu/)”.

Page 7183, Line 27: change “Table S1” to “Table S5”.

Page 7184, Lines 4–5: change “As in previous studies, we used slopes calculated from the orthogonal distance regression as ratios between species” to “To determine the ratio between each species pair, as in previous studies, we used the slope calculated from the orthogonal distance regression (Press et al., 2007)”.

Page 7184, Line 6: add “We also bootstrapped the orthogonal distance regression procedure 1000 times and estimated the 1-σ uncertainty for each ratio. The analyses were performed with R3.1.0 (R Core Team, 2014) following the recipes described in Teetor (2011).” at the end of this paragraph.

Page 7184, Line 12: change “additionally” to “additional”.

Page 7184, Line 21: change “Fig. 1” to “Fig. 1a”.

Page 7184, Line 22: change “are influenced by local and synoptic events” to “are more influenced by synoptic events”.

Page 7185, Line 3: change “Figs. 1 and 2b” to “Figs. 1a and 2b”.

Page 7185, Lines 14–15: change “by Airliner (CONTRAIL)” to “by Airliner (CONTRAIL, http://www.cger.nies.go.jp/contrail/)”.

Page 7185, Line 14: add “R=0.98–0.99, p<0.001,” before “Fig. 3a”.

Page 7185, Line 14: add “and back-trajectories show that they represent air masses with similar origins as HLE (Fig. S7),” before “confirming that HLE”.

Page 7185, Line 15: add “the” before “regional free mid-troposphere background”.

Page 7185, Line 22: add “the” before “air mass origins”.

Page 7185, Line 25: change “Fig. 1” to “Fig. 1a”.

Page 7186, Line 7: add “the peak-to-peak amplitudes of the CO_2 mean seasonal cycles were 7.6±1.4 and 11.1±1.3 ppm, with their maxima observed in April.” after “At PON and PBL,”.

Page 7186, Line 7: change “the CO_2 mean seasonal cycle” to “The CO_2 mean seasonal cycle”.

Page 7186, Line 15: change “Fig. 1” to “Fig. 1a”.

Page 7186, Line 17: add “The CO_2 mean seasonal cycle at PON is also similar to that observed at CRI (15.08°N, 73.83°E, 60m a.s.l.), another station on the southwest coast of India, yet the seasonal maximum at CRI is reached slightly earlier than at PON in March (Bhattacharya et al., 2009; Tiwari et al., 2011, 2014). The SNG station (18.35°N, 73.75°E, 1600m a.s.l.), located over the Western Ghats, observes a larger CO_2 seasonal cycle with a peak-to-peak amplitude of ~20 ppm (Tiwari et al., 2014).” at the end of this paragraph.

Page 7186, Line 19: add “the” before “time series of CH_4”.

Page 7186, Line 21: change “annual mean CH_4” to “the annual mean CH_4 concentration”.

Page 7186, Line 26: add “, as well as those from regional sources closer to the stations” after “wetland CH_4 emissions in summer”.

Page 7186, Line 26: add “Fang et al., 2013;” before “Fig. S4”.

Page 7186, Line 26: add “may” before “further contribute”.

Page 7186, Line 27: change “the two stations” to “these two stations”.

Page 7186, Line 28: change “were higher than at HLE” to “were higher than those at HLE”.

Page 7187, Line 5: change “intense” to “high”.

Page 7187, Line 5: add “The in-situ measurements at Darjeeling, India (27.03°N, 88.25°E, 2194 m a.s.l.), another station located in the eastern Himalayas, also showed large variability

and frequent pollution events in CH_4 mole fractions, which largely result from the transport of CH_4-polluted air masses from the densely populated Indo-Gangetic Plains to the station (Ganesan et al., 2013).” at the end of this paragraph.

Page 7187, Line 12: change “(CARIBIC)” to “(CARIBIC, http://www.caribic-atmospheric.com/)”.

Page 7187, Lines 13–14: change “although an apparent phase shift (lag by one month) and a larger seasonal cycle amplitude are found” to “although a larger seasonal cycle amplitude is found”.

Page 7187, Line 16: remove “Apparently,”.

Page 7187, Line 18: change “enhancement of CH_4” to “enhancements of CH_4”.

Page 7187, Lines 21–25: change “Moreover, the mean CH_4 seasonal cycle at HLE agrees well with the annual variation of convective precipitation over the Indian subcontinent (Fig. 5b), which is derived from ECMWF nudged Laboratoire de Météorologie Dynamique general circulation model (LMDz) (Hauglustaine et al., 2004). This agreement indicates that the summer maximum at HLE can be attributed to …” to “Moreover, the mean CH_4 seasonal cycle at HLE agrees well with the seasonal variations of CH_4 emissions from wetlands and rice paddies and convective precipitation over the Indian subcontinent (Fig. 5b), suggesting that the summer maximum at HLE are likely related to …”.

Page 7187, Line 29: change “thereby enhancing concentrations trace gases” to “therefore concentrations of trace gases would be enhanced at higher altitudes rather than at the surface”.

Page 7188, Line 1: add “Further analyses of carbon isotopic measurements and/or chemical transport model are needed to disentangle and quantify the contributions of meteorology and biogenic emissions to the CH_4 summer maximum at HLE.” before “As stated above”.

Page 7188, Line 3: change “since” to “possibly because”.

Page 7188, Line 5: change “At PON and PBL, in contrast to HLE, the CH_4 mean seasonal cycles have” to “In contrast to HLE, the CH_4 mean seasonal cycles at PON and PBL have”.

Page 7188, Line 6: change “Fig. 5b” to “Fig. 5c”.

Page 7188, Line 7: change “This not only reflect” to “These not only reflect”.

Page 7188, Line 8: change “at low altitude from the Southwest” to “at low altitudes from the southwest”.

Page 7188, Lines 9–10: remove “Since these air masses do not collect additional CH_4 from the various surface sources, they remain depleted in CH_4.”.

Page 7188, Line 11: change “In winter” to “In boreal winter”.

Page 7188, Line 13: add “As PON and PBL, the flask measurements at CRI also showed the seasonal maximum CH_4 values during the NE monsoon season, reflecting influences of air masses with elevated CH_4 from the Indian subcontinent (Bhattacharya et al., 2009; Tiwari et al., 2013).” at the end of this paragraph.

Page 7188, Line 15: add a new paragraph after the section title: “Nitrous oxide (N_2O) is a potent greenhouse gas that has the third largest contribution to anthropogenic radiative forcing after CO_2 and CH_4 (IPCC, 2013). It also becomes the dominant ozone depleting substance (ODS) emitted in the 21st century with the decline of chlorofluorocarbons (CFCs) under the Montreal Protocol (Ravishankara et al., 2009). Since the pre-industrial era, the atmospheric N_2O increased rapidly from ~270 ppb to ~325 ppb in 2011 (IPCC, 2013), largely as the result of human activities. Of the several known N_2O sources, agricultural activities (mainly through nitrogen fertilizer use) contribute to ~58% of the global anthropogenic N_2O emissions, with a higher share in a predominantly agrarian country like India (~75%; Garg et al., 2012).”.

Page 7188, Line 15: change “Time series” to “The time series”.

Page 7188, Line 16: change “the annual mean N_2O” to “the annual mean N_2O concentration”.

Page 7188, Line 18: add “, smaller than that at MLO (1.0±0.0 ppb/yr, Table 1)” after “(r^2 = 0.97, p = 0.001)”.

Page 7188, Lines 24–25: remove “at Mauna Loa (MLO) and”.

Page 7188, Line 25: remove “1.6 and”.

Page 7188, Line 25: remove “, respectively”.

Page 7188, Line 25: change “analyze” to “analyzed”.

Page 7188, Line 27: change “Table S1” to “Table S5”.

Page 7189, Line 1: change “(Fig. S7, Table S5)” to “(Fig. S9, Table S6)”.

Page 7189, Lines 6–7: change “(Fig. S7, Table S5)” to “(Fig. S9, Table S6)”.

Page 7189, Line 9: change “Table S5” to “Table S6”.

Page 7189, Line 12: change “during the observation period,” to “during the observation period.”.

Page 7189, Line 12: add “The in-situ measurements at Darjeeling also exhibited N_2O enhancements to be above the background level, suggesting significant N_2O sources in this region (Ganesan et al., 2013).” after “during the observation period”.

Page 7189, Line 12: add “These sources may be” before “related to emissions from”.

Page 7189, Line 13: change “as well as emissions in” to “as well as emissions from”.

Page 7189, Lines 17–18: change “more noisy due to regional sources and synoptic variability” to “has a larger uncertainty probably because synoptic events are more likely to mask the seasonal signal”.

Page 7189, Line 22: change “Table S6” to “Table S7”.

Page 7189, Line 24: change “Fig. S8, Table S5” to “Fig. S10, Table S6”.

Page 7189, Line 25: change “attributed to” to “likely due to”.

Page 7189, Line 29: change “is influenced by” to “may probably be influenced by”.

Page 7190, Line 2: change “intensive nitrogen fertilizer use” to “the intensive use of nitrogen fertilizers”.

Page 7190, Line 7: change “during April–December 2008” to “in 2008”.

Page 7190, Lines 11–13: change “the air masses transported by the SW monsoon do not collect substantial amounts of CH_4, but N_2O” to “the air masses arriving at the site during the southwest monsoon period is relatively enriched in N_2O compared to CH_4, reflecting differences in their relative emissions along the air mass route”.

Page 7190, Line 29: change “Table S6” to “Table S7”.

Page 7191, Line 5: add a new paragraph after the section title: “Sulfur hexafluoride (SF_6) is an extremely stable greenhouse gas, with an atmospheric lifetime as long as 800–3200 year and a global warming potential (GWP) of ~23,900 over a 100-year time horizon (Ravishankara et al., 1993; Morris et al., 1995; IPCC, 2013). The main sources of atmospheric SF_6 emissions are electricity distribution systems, magnesium production, and semi-conductor manufacturing (Olivier et al., 2005), while its natural sources are negligible (Busenberg and Plummer, 2000). As its sources are almost purely anthropogenic (Maiss et al., 1996), SF_6 is widely considered as a good tracer for population density, energy consumption and anthropogenic GHG emissions (Haszpra et al., 2008).”.

Page 7191, Line 5: change “time series” to “the time series”.

Page 7191, Line 9: change “Figs. 8 and S9a” to “Figs. 8 and S11a”.

Page 7191, Line 10: change “Table S7” to “Table S8”.

Page 7191, Lines 10–11: change “The annual mean SF_6 mole fractions at PON and PBL were lower than at HLE by -0.060±0.030 and -0.002±0.097 ppt, respectively.” to “The annual mean SF_6 gradient between PON and HLE is -0.060±0.030 ppt, whereas the gradient between PBL and HLE is statistically insignificant (-0.002±0.097 ppt).”.

Page 7191, Line 12: remove “, PBL”.

Page 7191, Line 15: remove “MLO and”.

Page 7191, Line 15: remove “0.33 and”.

Page 7191, Line 15: remove “,respectively”.

Page 7191, Line 20: change “Table S7” to “Table S8”.

Page 7191, Lines 20–21: change “Given that the atmospheric lifetime of SF_6 is 800–3200 years (Ravishankara et al., 1993; Morris et al., 1995),” to “Given the long atmospheric lifetime of SF_6,”.

Page 7191, Line 22: change “offsets” to “gradients”.

Page 7191, Line 24: change “the slight negative offsets between PON, PBL and HLE imply” to “the slight negative gradient between PON and HLE implies”.

Page 7191, Line 26: add “SF_6” before “measurements at Darjeeling”.

Page 7191, Lines 26–27: remove “, India (27.03° N, 88.25° E, 2194 m a.s.l.), another station located in the eastern Himalayas (Ganesan et al., 2013)”.

Page 7192, Lines 1–2: change “the Middle East and South/southeast Asia, respectively” to “the Middle East, South/Southeast Asia and China”.

Page 7192, Line 2: change “Figs. 8b and S6c” to “Figs. 8b and S6d”.

Page 7192, Line 8: change “Table S8” to “Table S9”.

Page 7192, Line 14: change “demonstrate” to “demonstrated”.

Page 7192, Line 15: change “an SF_6 enhancement” to “SF_6 enhancements”.

Page 7192, Lines 16–17: change “collected samples identified the influences of westerly jet transport” to “showed that the summer enhancements in SF_6 were more related to the influences of westerly jet transport in the upper troposphere”.

Page 7192, Line 18: add “that contributed to the summer maxima in CH_4 and N_2O” after “sources from India”.

Page 7192, Line 18: add “, Fig. S8” after “Schuck et al., 2010”.

Page 7192, Line 20: change “Figs. 9b and S6c” to “Figs. 9b and S6d”.

Page 7192, Line 21: change “Table S8” to “Table S9”.

Page 7192, Line 22: remove “southwesterly”.

Page 7192, Line 23: add “and China” after “Asia”.

Page 7192, Line 23: change “Fig. S6c” to “Fig. S6d”.

Page 7192, Line 25: add a new paragraph after the section title “Carbon monoxide (CO) plays important roles in atmospheric chemistry, as the dominant sink for the hydroxyl radical (OH, the main tropospheric oxidant) and a precursor of tropospheric ozone under high NO_x ($NO+NO_2$) concentrations (Logan et al., 1981; Novelli et al., 1998; Seinfeld and Pandis, 2006). Although CO does not act as a greenhouse gas, it modulates the atmospheric concentrations of CH_4 (the second anthropogenic greenhouse gas after CO_2) through competition for the OH radicals. At the global scale, it contributes to an indirect positive radiative forcing of $0.23\pm0.07 Wm^{-2}$ (IPCC, 2013). Besides, CO is an excellent tracer for combustion processes, with emission sources mainly contributed by incomplete combustion of fossil fuel and biofuels, and by biomass burning (Granier et al., 2011). In India, biofuel and agricultural waste burning account for 70–80% of the total anthropogenic CO emissions (EDGAR v4.2; Streets et al., 2003b; Yevich and Logan, 2003).”.

Page 7192, Line 28: change “CO at HLE is lower than at the two stations” to “The CO mole fractions at HLE are lower than those at”.

Page 7193, Line 1: remove “further north in Asia,”.

Page 7193, Line 16: change “CO time series” to “the CO time series”.

Page 7193, Line 24: add “Table 1,” before “Fig. 11c and d”.

Page 7194, Line 1: add “probably” to “due to”.

Page 7194, Line 11: change “CO enhancement” to “the CO enhancement”.

Page 7194, Line 25: change “surface CO at PON and PBL is low” to “the surface CO concentrations at PON and PBL are low”.

Page 7194, Lines 27–28: change “from Northeast India and Southeast Asia” to “from Northeast India, Southeast Asia and China”.

Page 7194, Line 28: change “Fig. S6d” to “Fig. S6e”.

Page 7194, Line 28: add “probably” before “influenced by”.

Page 7195, Line 2: add a new paragraph after the section title: “Hydrogen (H_2) is the second most abundant reduced trace gas in the troposphere after CH_4, with an average mole fraction of ~530 ppb (Novelli et al., 1999). It plays important roles in tropospheric and stratospheric chemistry and indirectly impacts budgets of CH_4, CO and non-methane hydrocarbons (NMHCs) through reaction with the OH radicals (Novelli et al., 1999; Ehhalt and Rohrer, 2009). Like CO, H_2 is also a good tracer for incomplete combustion emissions from fossil fuel and biomass/biofuel burning, which is quite extensive in India (Streets et al., 2003b; Yevich and Logan, 2003).”.

Page 7195, Line 16: change “Fig. S10c and d” to “Fig. S12c and d”.

Page 7195, Line 17: change “Table S9” to “Table S10”.

Page 7195, Line 20: change “Fig. S6e” to “Fig. S6f”.

Page 7195, Line 26: change “Fig. S6e” to “Fig. S6f”.

Page 7195, Line 27: change “The mean H_2 seasonal cycle” to “The mean H_2 seasonal cycles”.

Page 7196, Line 2: change “Figs. 13d and S11a” to “Figs. 13d and S13a”.

Page 7196, Line 3: change “Tables 1 and S9” to “Tables 1 and S10”.

Page 7196, Line 11: change “can be explained mainly by” to “may be attributed to”.

Page 7196, Line 15: change “Tables 1, Table S9” to “Tables 1 and S10”.

Page 7196, Line 15: change “Figs. 13a and b and S11b” to “Figs. 13a and b and S13b”.

Page 7196, Lines 21–22: change “can be driven by” to “could be related to”.

Page 7196, Lines 22–25: remove “The April, and larger peak is likely due to H_2 emitted from biomass burning in South and Southeast Asia and transported by the NE monsoon, while the October peak is possibly a result of the long-range transport of H_2-polluted air from biomass burning in tropical Africa (Fig. S6e).”.

Page 7197, Line 22: add “due to less residential fuel use for heating, see” before “Streets et al., 2003a”.

Page 7198, Line 2: change “is the result of” to “may be the result of”.

Page 7198, Line 10: change “1.5 to 4 times of” to “1.5 to 4 times that of”.

Page 7198, Line 12: change “Table S10” to “Table S11”.

Page 7198, Line 15: add “the” before “$\Delta CH_4/\Delta CO$ values”.

Page 7198, Line 16: change “Table S10” to “Table S11”.

Page 7198, Line 29: change “Table S10” to “Table S11”.

Page 7199, Line 5: change “primary energy source” to “primary energy sources”.

Page 7199, Line 22: change “the mid-Northern latitudes” to “the northern mid-latitudes”.

Page 7200, Line 2: change “Fig. 1” to “Fig. 1a”.

Page 7200, Line 10: remove “local” before “urban and industrial sources”.

Page 7200, Line 11: change “Fig. 1” to “Fig. 1a”.

Page 7200, Line 17: change “Fig. S12a” to “Fig. S14a”.

Page 7200, Line 23: change “Fig. S12b” to “Fig. S14b”.

Page 7202, Lines 18–19: remove “To investigate the sources and origins that may have contributed to the two events,”

Page 7202, Line 19: change “we analyzed” to “We further analyzed”.

Page 7202, Line 27: change “points to” to “possibly suggests”.

Page 7203, Line 1: change “may be related to” to “could be related to”.

Page 7203, Lines 26–27: change “Fig. S13” to “Fig. S15”.

Page 7203, Lines 3–5: change “A detailed analysis is needed in the future to further explore the linkage between atmospheric observations at the two stations during the SW monsoon season and the dominant sources of abnormal pollution events.” to “Note that the mechanisms we propose for the abnormal CH_4 and CO events and the possible linkage between PBL and BKT during the SW monsoon season are still speculative. Model experiments are needed to further confirm these hypotheses.”.

Page 7203, Line 7: change “five-year (2007–2011)” to “the results of”.

Page 7203, Line 9: add “, over the period of 2007–2011” after “Blair (PBL)”.

Page 7203, Line 9: change “the three stations” to “these three stations”.

Page 7203, Line 9: change “at high altitude” to “at a high altitude”.

Page 7203, Line 10: add “the” before “Northern Hemisphere”.

Page 7203, Line 12: add “the” before “Andaman Islands”.

Page 7203, Line 13: change “flask pairs sampled in India respectively at HLE, PON and PBL” to “flask pair samples collected respectively from HLE, PON and PBL”.

Page 7203, Lines 13–14: add “(for PBL between 2009 and 2011)” after “between 2007 and 2011”.

Page 7203, Line 20: change “offsets” to “annual gradients”.

Page 7203, Line 20: change “using HLE” to “with respect to HLE”.

Page 7203, Line 22: change “footprint” to “footprints”.

Page 7203, Line 22–23: change “Particularly” to “In particular”.

Page 7203, Line 24: add “the” before “typical N_2O gradients”.

Page 7204, Line 6: change “The strong influence of monsoon circulations” to “Strong influences of the monsoon circulations”.

Page 7204, Line 8: change “can be attributed to” to “is likely related to”.

Page 7204, Line 10: change “deep convection that is associated with the SW monsoon and mixes surface emissions” to “deep convection associated with the SW monsoon that mixes surface emissions”.

Page 7204, Line 13: change “at low altitude” to “at low altitudes”.

Page 7204, Line 16: add two sentences at the end of this paragraph “Besides, measurements of $\delta^{13}C$-CO_2 have been recently started for HLE, and the 4-D distributions of CO_2 and CH_4 have been realistically simulated using a chemical transport model (LMDz-OR-INCA, Hauglustaine et al., 2004; Folberth et al., 2006) with zoom over South and East Asia (manuscript in preparation). Both of them may serve as valuable tools to disentangle and quantify contributions of different sources and meteorology to trace gas signals.”.

Page 7204, Line 17: add a sentence at the beginning of this paragraph “Apart from the flask measurements of trace gases presented in this study for the three stations, in-situ continuous measurements of CO_2 and CH_4 have also been deployed at HLE, PON and PBL in parallel, which would considerably contribute to the value of the stations through high-frequency air sampling.”.

Page 7204, Lines 19–20: change “reduction in the uncertainty by the inclusion of HLE in the CO_2 inversion over temperate Eurasia” to “reduction in the uncertainty of inverted CO_2 fluxes over temperate Eurasia by the inclusion of measurements at HLE”.

Page 7204, Line 20: change “will require” to “requires”.

Page 7204, Line 22: add “atmospheric” before “ground stations”.

Page 7204, Lines 22–23: change “to monitor GHGs and atmospheric pollutants along the western coast of India” to “in western India”.

Page 7204, Line 24: change “and in the Himalayas” to “and the Himalayas”.

Page 7204, Lines 24–25: add “, with their concentration footprints covering Central India (e.g., the Sinhagad station; Tiwari et al., 2014; Tiwari and Kumar, 2012), the Indo-Gangetic Plains and a large extent of the Himalayas (e.g., the Dajeeling station; Ganesan et al., 2013)” after “(Kumar et al., 2010; Ganesan et al., 2013)”.

Changes to the references

Page 7206, Line 17: add a reference: "Busenberg, E. and Plummer, L. N.: Dating young groundwater with sulfur hexafluoride: Natural and anthropogenic sources of sulfur hexafluoride, Water Resour. Res., 36(10), 3011–3030, doi:10.1029/2000WR900151, 2000."

Page 7207, Line 13: add a reference: "Fang, S.-X., Zhou, L.-X., Masarie, K. A., Xu, L. and Rella, C. W.: Study of atmospheric CH_4 mole fractions at three WMO/GAW stations in China, J. Geophys. Res.-Atmos., 118(10), 4874–4886, doi:10.1002/jgrd.50284, 2013."

Page 7207, Line 16: add a reference: "Folberth, G. A., Hauglustaine, D. A., Lathière, J. and Brocheton, F.: Interactive chemistry in the Laboratoire de Météorologie Dynamique general circulation model: model description and impact analysis of biogenic hydrocarbons on tropospheric chemistry, Atmos. Chem. Phys., 6(8), 2273–2319, doi:10.5194/acp-6-2273-2006, 2006."

Page 7208, Line 1: add a reference: "Granier, C., Bessagnet, B., Bond, T., D'Angiola, A., Denier van der Gon, H., Frost, G., Heil, A., Kaiser, J., Kinne, S., Klimont, Z., Kloster, S., Lamarque, J.-F., Liousse, C., Masui, T., Meleux, F., Mieville, A., Ohara, T., Raut, J.-C., Riahi, K., Schultz, M., Smith, S., Thompson, A., van Aardenne, J., van der Werf, G. and van Vuuren, D.: Evolution of anthropogenic and biomass burning emissions of air pollutants at global and regional scales during the 1980–2010 period, Clim. Change, 109(1-2), 163–190, doi:10.1007/s10584-011-0154-1, 2011. "

Page 7208, Line 23: add a reference: "Huang, J., Golombek, A., Prinn, R., Weiss, R., Fraser, P., Simmonds, P., Dlugokencky, E. J., Hall, B., Elkins, J., Steele, P., Langenfelds, R., Krummel, P., Dutton, G. and Porter, L.: Estimation of regional emissions of nitrous oxide from 1997 to 2005 using multinetwork measurements, a chemical transport model, and an inverse method, J. Geophys. Res.-Atmos., 113(D17), D17313, doi:10.1029/2007JD009381, 2008."

Page 7209, Line 18: add a reference: "Kaplan, J. O., Folberth, G. and Hauglustaine, D. A.: Role of methane and biogenic volatile organic compound sources in late glacial and Holocene fluctuations of atmospheric methane concentrations, Global Biogeochem. Cycles, 20(2), GB2016, doi:10.1029/2005GB002590, 2006."

Page 7209, Line 22: add a reference: "King, A. W., Andres, R. J., Davis, K. J., Hafer, M., Hayes, D. J., Huntzinger, D. N., de Jong, B., Kurz, W. A., McGuire, A. D., Vargas, R., Wei, Y., West, T. O. and Woodall, C. W.: North America's net terrestrial CO_2 exchange with the atmosphere 1990–2009, Biogeosciences, 12(2), 399–414, doi:10.5194/bg-12-399-2015, 2015."

Page 7210, Line 1: add a reference: "Lal, S., Chandra, N., Venkataramani, S.: A study of CO_2 and related trace gases using a laser based technique at an urban site in western India. Submitted to Curr. Sci., 2015."

Page 7211, Line 12: change the reference to: "Lopez, M., Schmidt, M., Ramonet, M., Bonne, J.-L., Colomb, A., Kazan, V., Laj, P., and Pichon, J.-M.: A gas chromatograph system for semi-continuous greenhouse gas measurements at Puy de Dôme station, Centeral France, Atmos. Meas. Tech. Discuss., 8(3), 3121–3170, doi:10.5194/amtd-8-3121-2015, 2015."

Page 7211, Line 15: add a reference: “Luyssaert, S., Abril, G., Andres, R., Bastviken, D., Bellassen, V., Bergamaschi, P., Bousquet, P., Chevallier, F., Ciais, P., Corazza, M., Dechow, R., Erb, K.-H., Etiope, G., Fortems-Cheiney, A., Grassi, G., Hartmann, J., Jung, M., Lathière, J., Lohila, A., Mayorga, E., Moosdorf, N., Njakou, D. S., Otto, J., Papale, D., Peters, W., Peylin, P., Raymond, P., Rödenbeck, C., Saarnio, S., Schulze, E.-D., Szopa, S., Thompson, R., Verkerk, P. J., Vuichard, N., Wang, R., Wattenbach, M. and Zaehle, S.: The European land and inland water CO_2, CO, CH_4 and N_2O balance between 2001 and 2005, Biogeosciences, 9(8), 3357–3380, doi:10.5194/bg-9-3357-2012, 2012.”

Page 7211, Line 19: add a reference: “Matthews, E., Fung, I. and Lerner, J.: Methane emission from rice cultivation: Geographic and seasonal distribution of cultivated areas and emissions, Global Biogeochem. Cycles, 5(1), 3–24, doi:10.1029/90GB02311, 1991.”

Page 7213, Line 9: add a reference: “Olivier, J. G. J., Van Aardenne, J. A., Dentener, F., Ganzeveld, L. and Peters, J. A. H. W.: Recent trends in global greenhouse gas emissions: regional trends and spatial distribution of key sources, in Non-CO_2 Greenhouse Gases (NCGG-4), edited by A. Van Amstel, pp. 325–330, Millpress, Rotterdam, The Netherlands., 2005.”

Page 7214, Line 17: add a reference: “Press, W.H., Teukolsky, S.A., Vetterling, W.T., Flannery, B.P., 2007. Straight-Line Data with Errors in Both Coordinates, in: Numerical Recipes: The Art of Scientific Computing. Cambridge University Press, New York, pp. 785–788.”

Page 7214, Line 21: add a reference: “R Core Team: R: A language and environment for statistical computing. R Foundation for Statistical computing, Vienna, Austria. Available from: http://www.r-project.org/, 2014.”

Page 7214, Line 26: remove the reference: “Ramonet, M., Indira, N. K., Bhatt, B. C., Delmotte, M., Schmidt, M., Wastine, B., Vuillemin, C., Gal, B., Lin, X., Paris, J. D., Cloué, O., Stohl, A., Conway, T. J., Ciais, P., Swathi, P. S., and Gaur, V. K.: Atmospheric CO_2 monitoring at Hanle, India, in preparation.”.

Page 7214, Line 26: add a reference: “Ravishankara, A. R., Daniel, J. S. and Portmann, R. W.: Nitrous oxide (N_2O): The dominant ozone-depleting substance emitted in the 21st century, Science, 326(5949), 123–125, doi:10.1126/science.1176985, 2009.”

Page 7215, Line 24: add a reference: “Seinfeld, J. H. and Pandis, S. N.: Atmospheric Chemistry and Physics: From Air Pollution to Climate Change, John Wiley and Sons, Hoboken, New Jersey, USA., 2006.”

Page 7216, Line 13: add a reference: “Teetor, P., 2011. Performing Simple Orthogonal Regression, in: Loukides, M. (Ed.), R Cookbook. O’Reilly Media, Sebastopol, pp. 340–341.”

Changes to the table

Page 7220, change Table 1 as follows:

Table 1 Annual mean values, trend, and average peak-to-peak amplitudes of trace gases at HLE, PON, PBL and the two additional NOAA/ESRL stations – KZM and WLG. For each species at each station, the annual mean values and average peak-to-peak amplitude are calculated from the smoothed curve and mean seasonal cycle, respectively. The residual standard deviation (RSD) around the smoothed curve and the Julian days corresponding to the maximum (D_{max}) and minimum (D_{min}) of the mean seasonal cycle are given as well. Uncertainty of each estimate is calculated from 1 s.d. of 1000 bootstrap replicates.

	HLE	PON	PBL	KZM	WLG
CO_2 (ppm)					
Annual mean 2007	382.3±0.3	386.6±0.9	–	382.7±0.2	384.2±0.2
Annual mean 2008	384.6±0.5	388.1±0.9	–	385.7±0.2	386.0±0.2
Annual mean 2009	387.2±0.2	389.0±0.6	–	–	387.4±0.2
Annual mean 2010	389.4±0.1	391.3±1.5	387.6±0.7	–	390.1±0.2
Annual mean 2011	391.4±0.3	–	390.2±0.6	–	392.2±0.2
Trend (yr^{-1})	2.1±0.0	1.7±0.1	–	–	2.0±0.0
(Trend at MLO: 2.0±0.0)					
RSD	0.7	4.0	1.5	1.5	1.4
Amplitude	8.2±0.4	7.6±1.4	11.1±1.3	13.8±0.5	11.1±0.4
D_{max}	122.0±2.9	111.0±13.4	97.0±26.0	75.0±2.6	100.0±1.5
D_{min}	261.0±3.0	327.0±54.3	242.0±7.7	205.0±2.1	222.0±1.6
CH_4 (ppb)					
Annual mean 2007	1814.8±2.9	1859.2±6.7	–	1842.6±2.4	1841.0±1.8
Annual mean 2008	1833.1±5.4	1856.1±10.4	–	1856.6±2.3	1845.6±1.5
Annual mean 2009	1830.2±1.7	1865.7±5.1	–	–	1851.8±1.9
Annual mean 2010	1830.5±2.1	1876.9±9.1	1867.5±15.4	–	1857.6±1.4
Annual mean 2011	1849.5±5.2	–	1852.0±7.6	–	1859.9±1.2
Trend (yr^{-1})	4.9±0.0	9.4±0.1	–	–	5.3±0.0
(Trend at MLO: 6.2±0.0)					
RSD	9.1	34.4	22.4	14.6	12.3
Amplitude	28.9±4.2	124.1±10.2	143.9±12.4	22.7±4.7	17.5±2.2
D_{max}	219.0±4.6	337.0±6.1	345.0±87.6	236.0±43.2	222.0±6.2
D_{min}	97.0±58.9	189.0±10.7	193.0±13.5	338.0±39.0	340.0±96.6
N_2O (ppb)					
Annual mean 2007	322.2±0.1	324.8±0.3	–		
Annual mean 2008	322.9±0.1	326.3±0.3	–		
Annual mean 2009	323.5±0.1	326.7±0.3	–		
Annual mean 2010	324.0±0.1	327.1±0.5	329.0±0.5		

Annual mean 2011	325.2±0.1	–	327.9±0.3		
Trend (yr^{-1})	0.8±0.0	0.8±0.1	–		
(Trend at MLO: 1.0±0.0)					
RSD	0.3	1.4	1.1		
Amplitude	0.6±0.1	1.2±0.5	2.2±0.6		
D_{max}	227.0±11.8	262.0±83.2	313.0±42.6		
D_{min}	115.0±16.4	141.0±48.2	65.0±33.4		
SF_6 (ppt)					
Annual mean 2007	6.26±0.03	6.19±0.01	–		
Annual mean 2008	6.54±0.03	6.49±0.02	–		
Annual mean 2009	6.79±0.01	6.77±0.01	–		
Annual mean 2010	7.17±0.01	7.08±0.02	7.10±0.07		
Annual mean 2011	7.38±0.01	–	7.45±0.03		
Trend (yr^{-1})	0.29±0.05	0.31±0.05	–		
(Trend at MLO: 0.29±0.03)					
RSD	0.07	0.05	0.12		
Amplitude	0.15±0.03	0.24±0.02	0.48±0.07		
D_{max}	320.0±8.3	327.0±12.1	342.0±59.9		
D_{min}	211.0±65.1	204.0±3.3	210.0±18.1		
CO (ppb)					
Annual mean 2007	104.7±1.4	200.5±7.8	–	121.7±1.7	141.0±4.3
Annual mean 2008	103.1±2.1	175.3±13.1	–	123.7±1.7	129.0±2.9
Annual mean 2009	98.9±1.9	174.3±4.8	–	–	131.9±3.7
Annual mean 2010	99.0±1.2	185.1±8.7	157.6±20.4	–	130.2±3.9
Annual mean 2011	99.4±2.2	–	145.9±9.9	–	124.0±2.3
Trend (yr^{-1})	-2.2±0.0	0.4±0.1	–	–	-1.9±0.0
(Trend at MLO: -1.6±0.0)					
RSD	6.5	32.0	30.8	11.8	22.5
Amplitude	28.4±2.3	78.2±11.6	144.1±16.0	37.1±4.4	38.6±5.1
D_{max}	79.0±11.4	4.0±160.2	12.0±117.9	72.0±5.0	94.0±38.2
D_{min}	297.0±5.3	238.0±46.1	213.0±23.0	318.0±6.1	331.0±6.2
H_2 (ppb)					
Annual mean 2007	539.6±2.1	574.5±2.4	–	502.4±2.0	500.9±1.5
Annual mean 2008	533.2±3.2	558.2±5.3	–	–	–
Annual mean 2009	533.3±1.6	562.4±1.6	–	–	–
Annual mean 2010	533.5±1.8	563.9±2.3	558.6±2.4	–	–
Annual mean 2011	536.9±1.5	–	555.4±1.6	–	–
Trend (yr^{-1})	-0.5±0.0	-1.3±0.1	–	–	–
RSD	6.6	8.4	7.0	13.3	9.5
Amplitude	15.8±2.2	21.6±3.4	21.3±5.0	16.7±4.0	22.8±3.0
D_{max}	120.0±8.7	96.0±9.6	99.0±8.8	120.0±34.2	51.0±13.4
D_{min}	266.0±39.6	219.0±10.3	353.0±87.8	341.0±78.3	298.0±6.5

Changes to the figures

Page 7222, change Figure 1 as follows:

Figure 1 (a) Five-day back-trajectories calculated for all sampling dates over the period 2007–2011 at Hanle (HLE), Pondicherry (PON), and Port Blair (PBL) during April–June (AMJ), July–September (JAS), October–December (OND) and January–March (JFM), respectively. Back-trajectories are colored by the elevation of air masses at hourly time step. **(b)** Map of terrain over the zoomed box in **(a)**, showing locations of HLE, PON and PBL. The digital elevation data are obtained from NASA Shuttle Radar Topographic Mission (SRTM) product at 1km resolution (http://srtm.csi.cgiar.org)

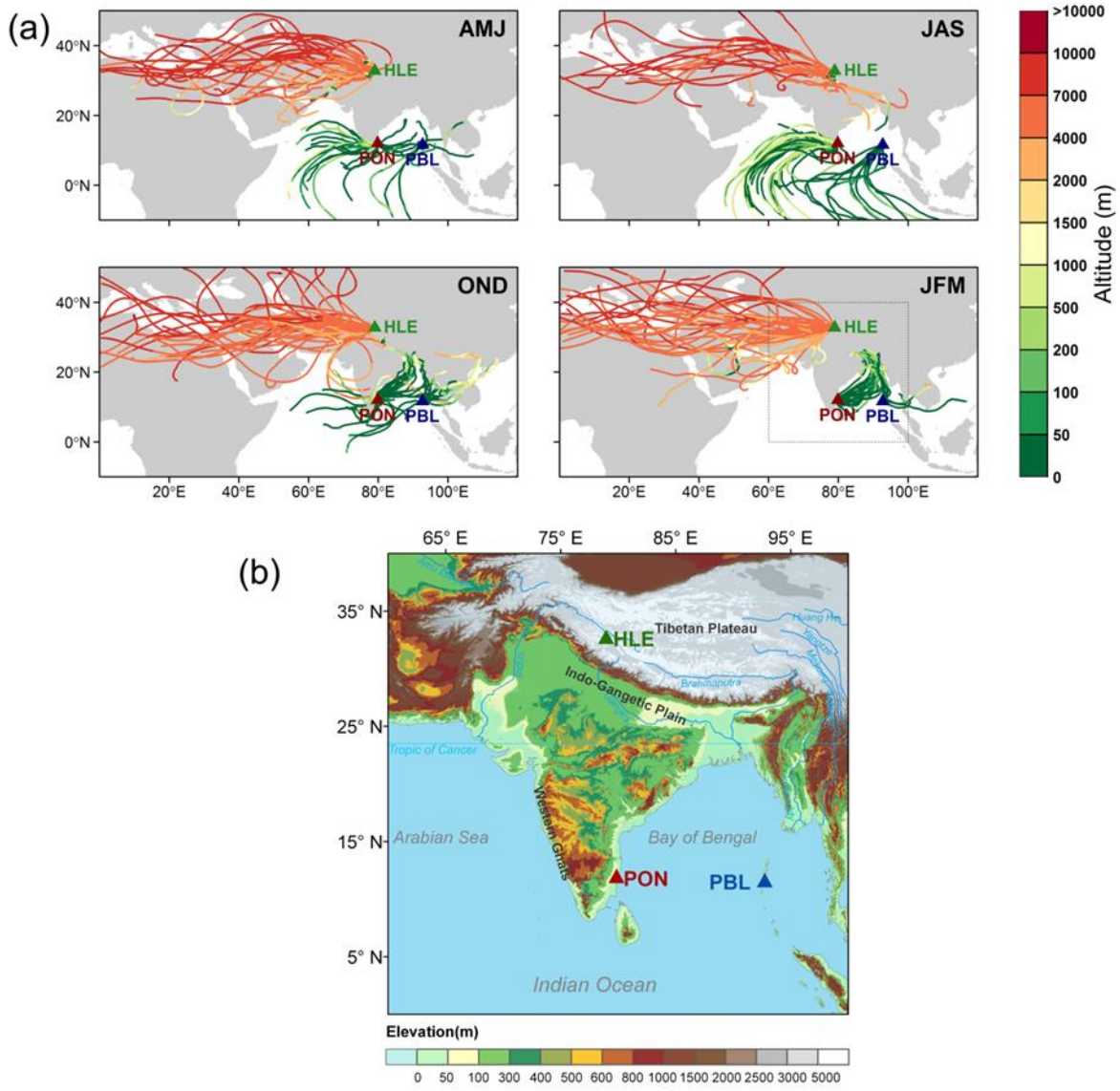

Page 7223, change the caption of Figure 2 as follows:

Figure 2 Time series of CO_2 flask measurements at **(a)** HLE and PON, **(b)** HLE and PBL, **(c)** HLE and KZM, and **(d)** HLE and WLG. The open circles denote flask data used to fit the smoothed curves, while the crosses denote discarded flask data lying outside 3 times the residual standard deviations from the smoothed curve fits. For each station, the smoothed curve is fitted using Thoning's method (Thoning et al., 1989) after removing outliers.

Page 7224, change Figure 3 as follows:

Figure 3 (a) The mean CO_2 seasonal cycle at HLE, in comparison with the mean seasonal cycles derived from the in-situ CO_2 measurements over New Delhi at different altitude bands (3–4 km, 4–5 km, and 5–6 km) by the CONTRAIL project (2006–2010). **(b)** The mean CO_2 seasonal cycles at HLE, KZM and WLG. **(c)** The mean CO_2 seasonal cycles at HLE, PON and PBL. For each station, the mean seasonal cycle is derived from the harmonics of the smoothed fitting curve in Fig. 2. Shaded area indicates the uncertainty of the mean seasonal cycle calculated from 1 s.d. of 1000 bootstrap replicates. For the CONTRAIL datasets, CO_2 measurements over New Delhi were first averaged by altitude bands. A fitting procedure was then applied to the aggregated CO_2 measurements to generate the mean season cycle for different altitude bands.

Figure 3 (cont.)

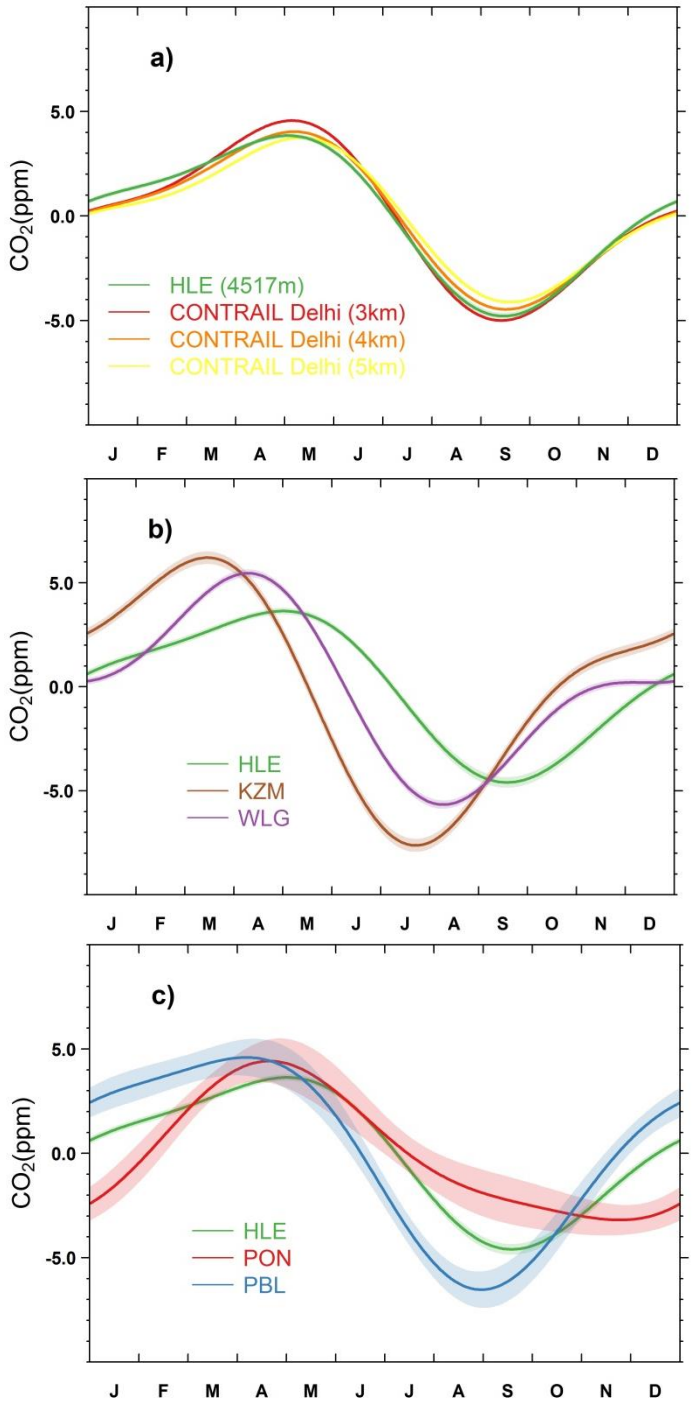

Page 7225, change the caption of Figure 4 as follows:

Figure 4 Time series of CH_4 flask measurements at (a) HLE and PON, (b) HLE and PBL, (c) HLE and KZM, and (d) HLE and WLG. The open circles denote flask data used to fit the smoothed curves, while the crosses denote discarded flask data lying outside 3 times the residual standard deviations from the smoothed curve fits. For each station, the smoothed curve is fitted using Thoning's method (Thoning et al., 1989) after removing outliers.

Page 7226, change Figure 5 as follows:

Figure 5 (a) The mean CH_4 seasonal cycles observed at HLE, KZM and WLG. The mean CH_4 seasonal cycle derived from aircraft flask measurements by the CARIBIC project is also presented. The CARIBIC flask measurements in the upper troposphere (200-300 hPa) during 2005–2012 are averaged over the Indian subcontinent (10°N-35°N, 60°E-100°E) by month to generate the mean seasonal cycle. The error bars indicate 1 standard deviation of CH_4 flask measurements within the month. **(b)** The seasonal variations of CH_4 emissions from rice paddies and wetlands over the Indian subcontinent. The CH_4 emissions from rice paddies are extracted from a global emission map for the year 2010 (EDGAR v4.2), imposed by the seasonal variation on the basis of Matthews et al. (1991). The CH_4 emissions from wetlands are extracted from outputs of a global vegetation model (BIOME4-TG, Kaplan et al., 2006). The seasonal variation of deep convection over the Indian subcontinent is also presented, indicated by convective precipitation obtained from an LMDz simulation nudged with ECMWF reanalysis (Hauglustaine et al., 2004). The CH_4 emissions and convective precipitation are averaged over the domain 10–35 °N, 70°–90°E to give a regional mean estimate. **(c)** The mean CH_4 seasonal cycles observed at HLE, PON and PBL. For each station, the mean seasonal cycle is derived from the harmonics of the smoothed fitting curve in Fig. 4. Shaded area indicates the uncertainty of the mean seasonal cycle calculated from 1 s.d. of 1000 bootstrap replicates.

Figure 5 (cont.)

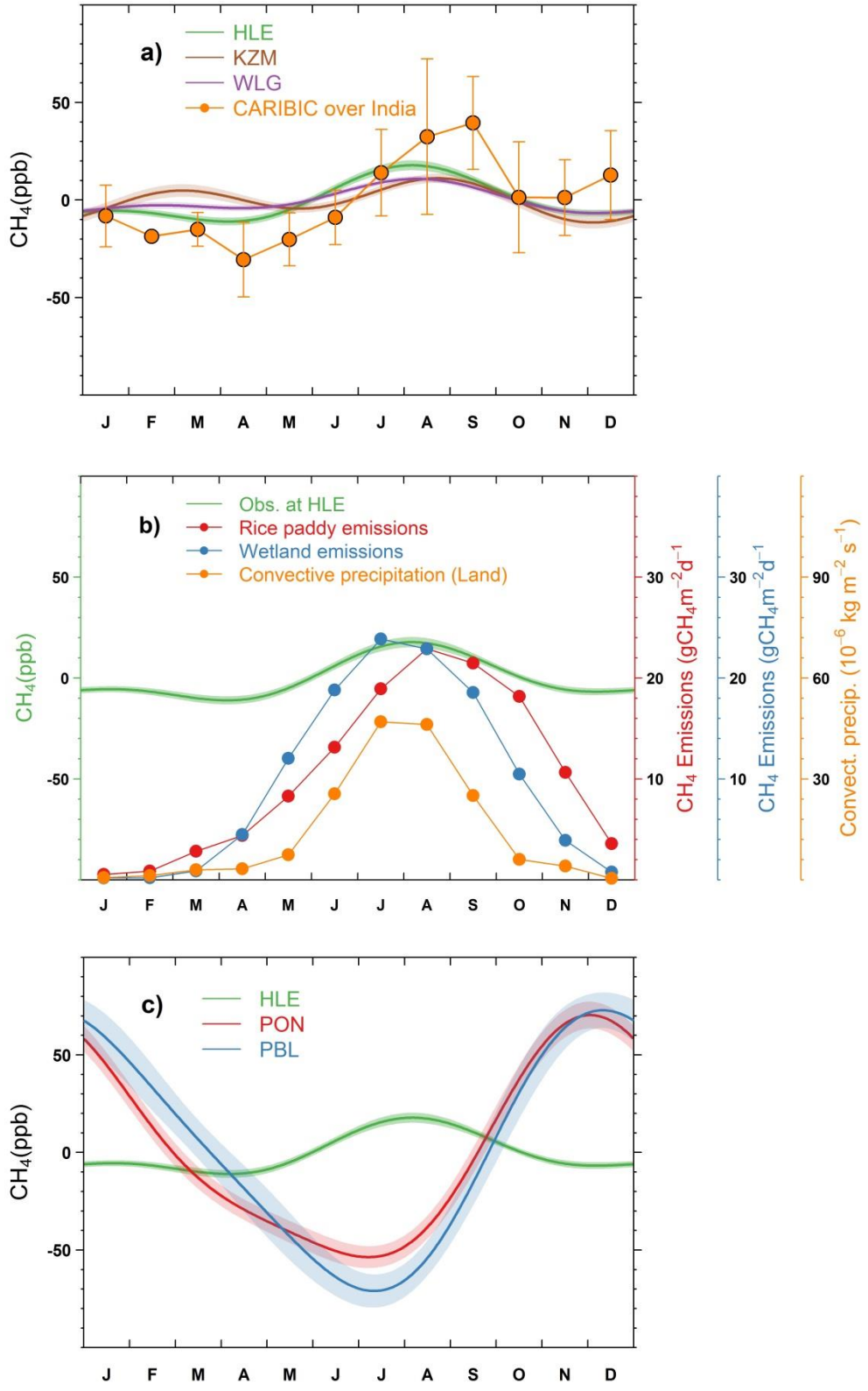

Page 7227, change the caption of Figure 6 as follows:

Figure 6 Time series of N_2O flask measurements at **(a)** HLE and PON, **(b)** HLE and PBL. The open circles denote flask data used to fit the smoothed curves, while crosses denote discarded flask data lying outside 3 times the residual standard deviations from the smoothed curve fits. For each station, the smoothed curve is fitted using Thoning's method (Thoning et al., 1989) after removing outliers.

Page 7228, change the caption of Figure 7 as follows:

Figure 7 The mean N_2O seasonal cycles observed at **(a)** HLE and PON, **(b)** HLE and PBL. For each station, the mean seasonal cycle is derived from the harmonics of the smoothed fitting curve in Fig. 6. Shaded area indicates the uncertainty of the mean seasonal cycle calculated from 1 s.d. of 1000 bootstrap replicates.

Page 7229, change the caption of Figure 8 as follows:

Figure 8 Time series of SF_6 flask measurements at **(a)** HLE and PON, **(b)** HLE and PBL, **(c)** HLE and KZM, and **(d)** HLE and WLG. The open circles denote flask data used to fit the smoothed curves. For each station, the smoothed curve is fitted using Thoning's method (Thoning et al., 1989) after removing outliers.

Page 7230, change the caption of Figure 9 as follows:

Figure 9 The mean SF_6 seasonal cycles observed at **(a)** HLE and PON, **(b)** HLE and PBL. For each station, the mean seasonal cycle is derived from the harmonics of the smoothed fitting curve in Fig. 8. Shaded area indicates the uncertainty of the mean seasonal cycle calculated from 1 s.d. of 1000 bootstrap replicates.

Page 7231, change the caption of Figure 10 as follows:

Figure 10 Time series of CO flask measurements at **(a)** HLE and PON, **(b)** HLE and PBL, **(c)** HLE and KZM, and **(d)** HLE and WLG. The open circles denote flask data used to fit the smoothed curves, while the crosses denote discarded flask data lying outside 3 times the residual standard deviations from the smoothed curve fits. For each station, the smoothed curve is fitted using Thoning's method (Thoning et al., 1989) after removing outliers.

Page 7232, change the caption of Figure 11 as follows:

Figure 11 The mean CO seasonal cycles observed at **(a)** HLE and PON, **(b)** HLE and PBL, **(c)** HLE and KZM, and **(d)** HLE and WLG. For each station, the mean seasonal cycle is derived from the harmonics of the smoothed fitting curve in Fig. 10. Shaded area indicates the uncertainty of the mean seasonal cycle calculated from 1 s.d. of 1000 bootstrap replicates.

Page 7233, change the caption of Figure 12 as follows:

Figure 12 Time series of H_2 flask measurements at **(a)** HLE and PON, **(b)** HLE and PBL, **(c)** HLE and KZM, and **(d)** HLE and WLG. The open circles denote flask data used to fit the smoothed curves, while the crosses denote discarded flask data lying outside 3 times the residual standard deviations from the smoothed curve fits. For each station, the smoothed curve is fitted using Thoning's method (Thoning et al., 1989) after removing outliers.

Page 7234, change the caption of Figure 13 as follows:

Figure 13 The mean H_2 seasonal cycles observed at **(a)** HLE and PON, **(b)** HLE and PBL, **(c)** HLE and KZM, and **(d)** HLE and WLG. For each station, the mean seasonal cycle is derived from the harmonics of the smoothed fitting curve in Fig. 12. Shaded area indicates the uncertainty of the mean seasonal cycle calculated from 1 s.d. of 1000 bootstrap replicates.

Page 7235, change Figure 14 as follows:

Figure 14 The relationships between ΔCH_4 and ΔCO at HLE **(a–d)**, PON **(e–h)**, and PBL **(i–l)** for April–June (AMJ), July–September (JAS), October–December (OND), and January–March (JFM). For each panel, ΔCH_4 and ΔCO are estimated as residuals from smoothed curves. The $\Delta CH_4/\Delta CO$ ratio is the slope of the fitting line from the orthogonal distance regression, with the SD calculated from 1000 bootstrap replications.

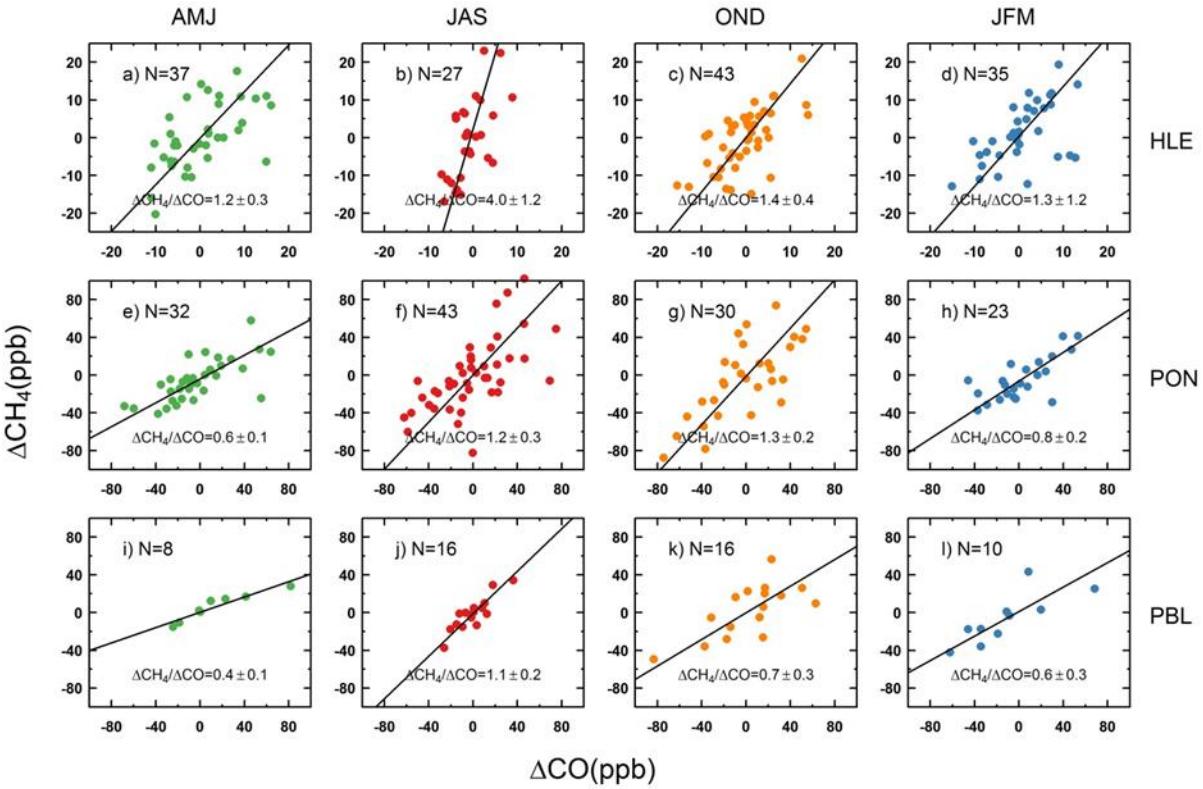

Page 7236, change Figure 15 as follows:

Figure 15 The relationships between ΔCH_4 and ΔCO_2 at HLE **(a–d)**, PON **(e–h)**, and PBL **(i–l)** for April–June (AMJ), July–September (JAS), October–December (OND), and January–March (JFM). For each panel, ΔCH_4 and ΔCO_2 are estimated as residuals from smoothed curves. The $\Delta CH_4/\Delta CO_2$ ratio is the slope of the fitting line from the orthogonal distance regression, with the SD calculated from 1000 bootstrap replications. For ΔCH_4 and ΔCO_2 that is not significantly correlated, the fitting line is not plotted.

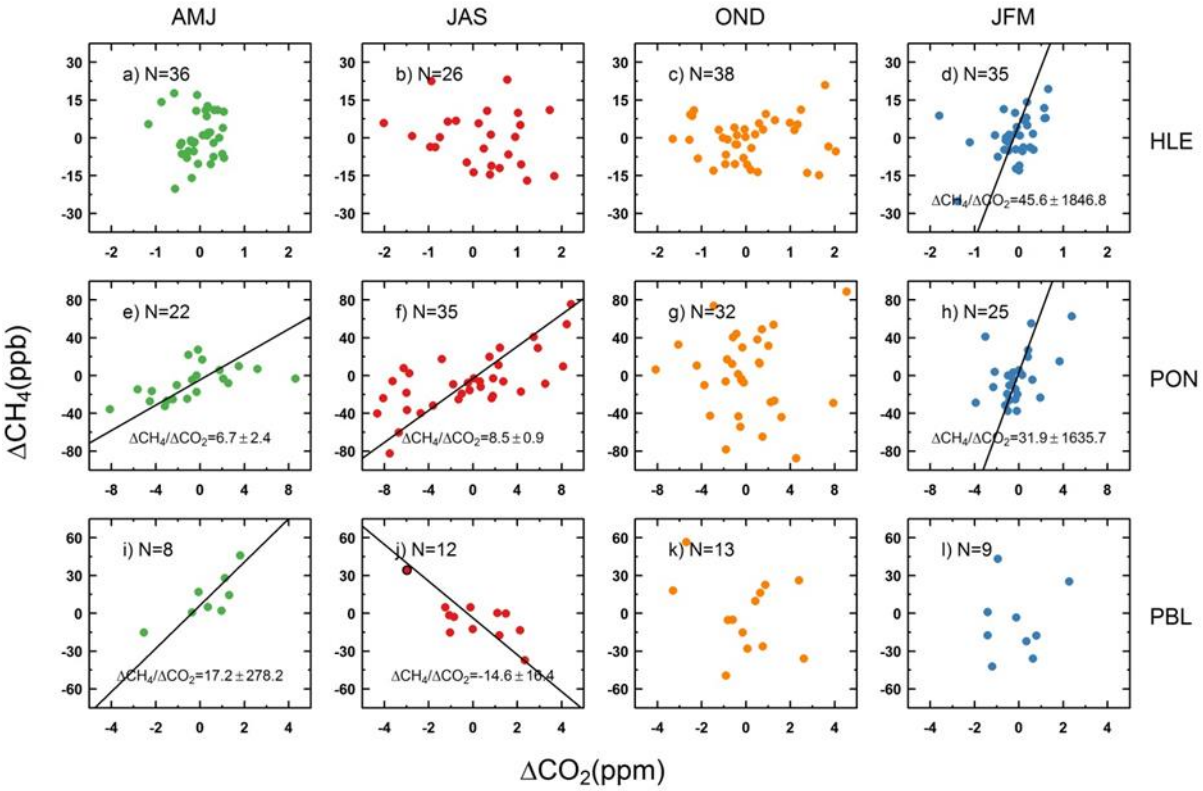

Page 7237, change Figure 16 as follows:

Figure 16 The relationships between ΔCO and ΔCO_2 at HLE **(a–d)**, PON **(e–h)**, and PBL **(i–l)** for April–June (AMJ), July–September (JAS), October–December (OND), and January–March (JFM). For each panel, ΔCO and ΔCO_2 are estimated as residuals from smoothed curves. The $\Delta CO/\Delta CO_2$ ratio is the slope of the fitting line from the orthogonal distance regression, with the SD calculated from 1000 bootstrap replications. For ΔCO and ΔCO_2 that is not significantly correlated, the fitting line is usually not plotted.

Figure 16 (cont.)

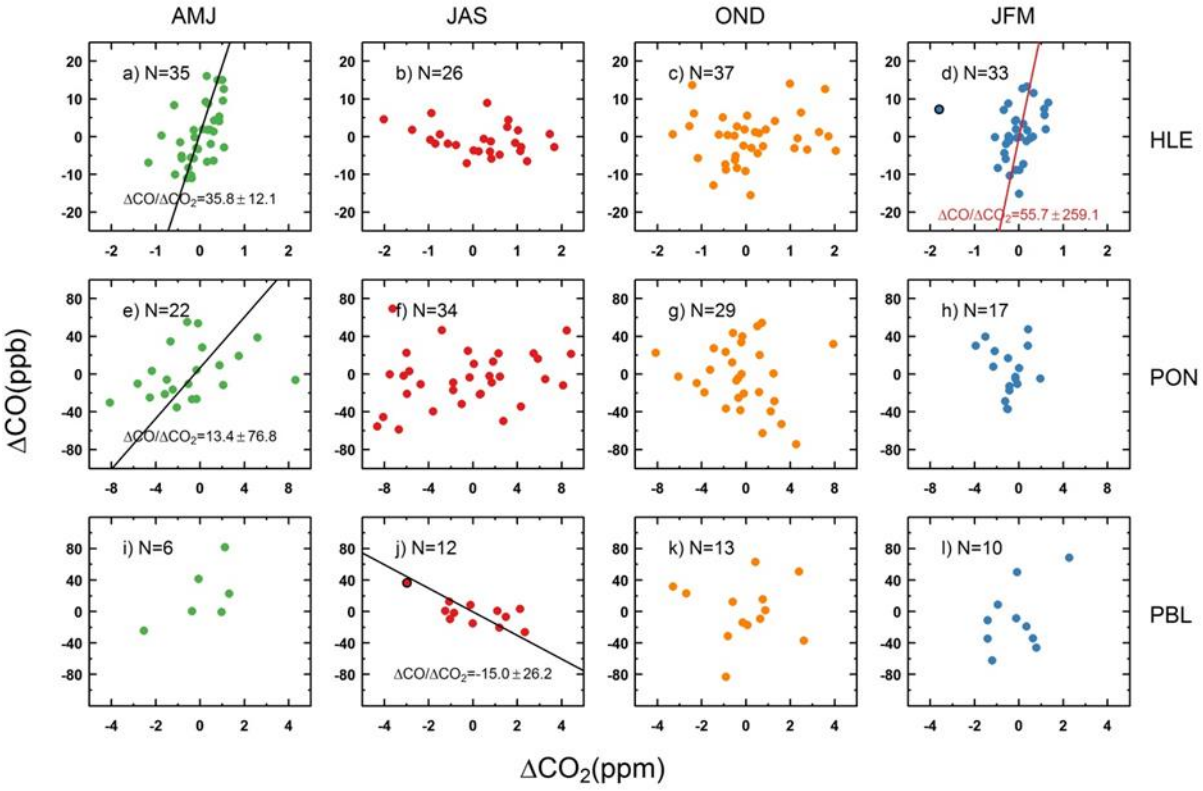

Title: Five-year flask measurements of long-lived trace gases in India

X. Lin[1], N. K. Indira[2], M. Ramonet[1], M. Delmotte[1], P. Ciais[1], B. C. Bhatt[3], M. V. Reddy[4], D. Angchuk[3], S. Balakrishnan[4], S. Jorphail[3], T. Dorjai[3], T. T. Mahey[3], S. Patnaik[4], M. Begum[5], C. Brenninkmeijer[6], S. Durairaj[5], R. Kirubagaran[7], M. Schmidt[1,8], P. S. Swathi[2], N. V. Vinithkumar[5], C. Yver Kwok[1], and V. K. Gaur[2]

[1] Laboratoire des Sciences du Climat et de l'Environnement (LSCE), UMR CEA-CNRS-UVSQ, Gif-sur-Yvette 91191, France

[2] CSIR Fourth Paradigm Institute (formerly CSIR Centre for Mathematical Modelling and Computer Simulation), NAL Belur Campus, Bangalore 560 037, India

[3] Indian Institute of Astrophysics, Bangalore 560 034, India

[4] Department of Earth Sciences, Pondicherry University, Puducherry 605 014, India

[5] Andaman and Nicobar Centre for Ocean Science and Technology (ANCOST), ESSO-NIOT, Port Blair 744103, Andaman and Nicobar Islands, India

[6] Max Planck Institute for Chemistry, Hahn-Meitner-Weg 1, D-55128 Mainz, Germany

[7] Earth System Sciences Organisation - National Institute of Ocean Technology (ESSO-NIOT), Ministry of Earth Sciences, Government of India, Tamil Nadu, Chennai 600 100, India

[8] Institut für Umweltphysik, Universität Heidelberg, INF 229, 69120 Heidelberg, Germany

Abstract

With a rapid growth in population and economic development, emissions of greenhouse gases (GHGs) from the Indian subcontinent have sharply increased during recent decades. However, evaluation of regional fluxes of GHGs and characterization of their spatial and temporal variations by atmospheric inversions remain uncertain due to a sparse regional atmospheric observation network. As a result of an Indo-French collaboration, three new atmospheric stations were established in India at Hanle (HLE), Pondicherry (PON) and Port Blair (PBL), with the objective of monitoring the atmospheric concentrations of GHGs and other trace gases. Here we present the results of the five-year measurements (2007–2011) of CO_2, CH_4, N_2O, SF_6, CO, and H_2 from regular flask sampling at these three stations. For each species, annual means, seasonal cycles and gradients between stations were calculated and related to variations in the natural GHG fluxes, anthropogenic emissions, and the monsoon circulations. Covariances between species at the synoptic scale were analyzed to investigate the likely source(s) of emissions. The flask measurements of various trace gases at the three stations show potential to constrain the inversions of fluxes over Southern and Northeastern India. However, this network of ground stations needs further extension to other parts of India to better constrain the GHG budgets at regional and continental scales.

1 Introduction

Since the pre-industrial times, anthropogenic greenhouse gas (GHG) emissions have progressively increased the radiative forcing of the atmosphere, leading to impacts on the climate system and human society (IPCC, 2013, 2014a, b). With rapid socio-economic development and urbanization during recent decades, a large and growing share of GHG emissions is contributed by emerging economies like China and India. In 2010, India became the world's third largest GHG emitter, next to China and the USA (EDGAR v4.2; Le Quéré et al., 2014). Between 1991 and 2010, anthropogenic GHG emissions in India increased by ~100% from 1.4 to 2.8 $GtCO_2eq$, much faster than rates of most developed countries and economies like the USA (9%) and EU (-14%) over the same period (EDGAR v4.2). Without a systematic effort at mitigation, this trend would continue in the coming decades, given that the per capita emission rate in India is still much below that of the more developed countries. For comparison, in 2010, the per capita GHG emission rates were 2.2, 10.9, 17.6, and 21.6 $tonCO_2eq$/capita for India, the UK, Russia, and the USA, respectively (EDGAR v4.2). In particular, non-CO_2 GHG emissions are substantial in India, most of which are contributed by agricultural activities over populous rural areas (Pathak et al., 2010). In 2010, anthropogenic CH_4 and N_2O emissions in India amounted to 29.6 $TgCH_4$ (≈0.62 $GtCO_2eq$) and 0.8 TgN_2O (≈0.23 $GtCO_2eq$), together accounting for 32% of the country's GHG emissions, of which contributions of the agricultural sector were 60 and 73%, respectively (EDGAR v4.2). Reducing emissions of these two non-CO_2 GHGs may offer a more cost-effective way to mitigate future climate change than by attempting to directly reduce CO_2 emissions (Montzka et al., 2011).

Effective climate mitigation strategies need accurate reporting of sources and sinks of GHGs. This is also a requirement of the United Nations Framework Convention on Climate Change

(UNFCCC). Current estimates of GHG budgets in India, either from the top-down approaches (based on atmospheric inversions) or bottom-up approaches (based on emission inventories or biospheric models), have larger uncertainties than for other continents. For instance, Patra et al. (2013) reported a net biospheric CO_2 sink of -104±150 $TgCyr^{-1}$ over South Asia during 2007–2008 based on global inversions from 10 TransCom-CO_2 models (Peylin et al., 2013) and a regional inversion (Patra et al., 2011b), while the bottom-up approach gave an estimate of -191±193 $TgCyr^{-1}$ over the period of 2000–2009 (Patra et al., 2013). Notably, these estimates have uncertainties as high as 100–150%, much larger compared to those of Europe (~30%, see Luyssaert et al., 2012) and North America (~60%, see King et al., 2015), where observational networks are denser and emission inventories are more accurate. Evaluation of N_2O emissions from 5 TransCom-N_2O inversions also exhibited the largest differences over South Asia (Thompson et al., 2014b). A main source of uncertainty is the lack of atmospheric observation datasets with sufficient temporal and spatial coverage (Patra et al., 2013; Thompson et al., 2014b). Networks of atmospheric stations that were used to constrain estimates of global GHG fluxes show gaps over South Asia (Patra et al., 2011a; Thompson et al., 2014b, c; Peylin et al., 2013), with Cape Rama (CRI – 15.08°N, 73.83°E, 60m a.s.l.) on the southwest coast of India being the only Indian station (Rayner et al., 2008; Patra et al., 2009; Tiwari et al., 2011; Bhattacharya et al., 2009; Saikawa et al., 2014). Recently a few other ground stations have been established in Western India and the Himalayas to monitor GHGs and atmospheric pollutants, which are located in Sinhagad (SNG – 18.35°N, 73.75°E, 1600m a.s.l.; Tiwari and Kumar, 2012; Tiwari et al., 2014), Mount Abu (24.60°N, 72.70°E, 1700m a.s.l.; S. Lal, personal communication), Ahmedabad (23.00°N, 72.50°E, 55m a.s.l.; Lal et al., 2015), Nainital (29.37°N, 79.45°E, 1958m a.s.l.; Kumar et al., 2010) and Darjeeling (27.03°N, 88.15°E, 2194m a.s.l.; Ganesan et al., 2013). Most of these stations started to measure atmospheric GHG concentrations very

recently (e.g. Sinhagad – since 2009; Ahmedabad – since 2013; Mount Abu – since 2013; Nainital – since 2006; Darjeeling – since 2011), and datasets are not always available. In addition, aircraft and satellite observations have also been carried out and provided useful constraints on estimates of GHG fluxes in this region (Park et al., 2007; Xiong et al., 2009; Schuck et al., 2010; Patra et al., 2011b; Niwa et al., 2012; Zhang et al., 2014). Although inclusion of measurements from South Asia significantly reduces uncertainties in top-down estimates of regional GHG emissions (e.g., Huang et al., 2008; Niwa et al., 2012; Zhang et al., 2014), a denser atmospheric observational network with sustained measurements is still needed over this vast and fast-growing region for an improved, more detailed, and necessary understanding of GHG budgets.

Besides the lack of a comprehensive observational network, the seasonally reversing Indian monsoon circulations and orographic effects complicate simulation of regional atmospheric transport, which contributes to uncertainty of the inverted GHG fluxes (e.g., Thompson et al., 2014b). The Indian monsoon system is a prominent meteorological phenomenon in South Asia, which, at lower altitudes, is characterized by strong southwesterlies from the Arabian Sea to the Indian subcontinent during the boreal summer, and northeasterlies during the boreal winter (Goswami, 2005). The summer monsoon is associated with deep convection, which mixes the boundary layer air into the upper troposphere and lower stratosphere (Schuck et al., 2010; Lawrence and Lelieveld, 2010). On the contrary, little deep convection occurs over South Asia during the winter monsoon period, which carries less moisture (Lawrence and Lelieveld, 2010). The Indian monsoon also impacts biogenic activities (e.g., vegetation growth, microbial activity) and GHG fluxes through its effects on rainfall variations (Tiwari et al., 2013; Valsala et al., 2013; Gadgil, 2003). Given that accurate atmospheric transport is critical for retrieving reliable inversion of GHG fluxes, an

observational network that comprises a range of altitudes including monitoring stations in mountainous regions would be valuable for validating and improving atmospheric transport models.

Since the 2000s, three new atmospheric ground stations have been established in India as part of the Indo-French collaboration, with the objective of monitoring the atmospheric concentrations of GHGs and other trace gases in flask air samples. Of the three Indian stations, Hanle (HLE) is a high-altitude station situated in the western Indian Himalayas, while Pondicherry (PON) and Port Blair (PBL) are tropical surface stations located respectively on the southeastern coast of South India and on an oceanic island in the southeastern Bay of Bengal. In this study, we briefly describe the main features of these stations and present time series of flask air sample measurements of multiple trace gases at HLE, PON, and PBL over the period 2007–2011. Descriptions of the three stations as well as methods used to analyze and calibrate the flask measurements are given in Sect. 2. For each station, four GHG species (CO_2, CH_4, N_2O, SF_6) and two additional trace gases (CO, H_2) were measured to characterize the annual means and seasonal cycles, with results and discussions presented in Sect. 3. Gradients between different stations are interpreted in the context of regional flux patterns and monsoon circulations (Sect. 3.1). We examine synoptic variations of CO_2, CH_4 and CO by analyzing the co-variances between species, using deviations from their smoothed fitting curves (Sect. 3.2). Finally, we investigate two abnormal CH_4 and CO events at PBL and propose likely sources and origins (Sect. 3.3). A summary of the paper as well as conclusions drawn from these results are given in Sect. 4.

2 Sampling stations and methods

2.1 Sampling stations

Figure 1 and S1 in the supplement show the locations of HLE, PON, and PBL. We also present five-day back-trajectories from each station for all sampling dates in April–June (AMJ; Fig. 1a), July–September (JAS; Fig. 1b), October–December (OND; Fig. 1c) and January–March (JFM; Fig. 1d), respectively. Note that this four-period classification scheme is slightly different from the climatological seasons defined by the India Meteorological Department (IMD; Attri and Tyagi, 2010), in which months of a year are categorized into the pre-monsoon season (March–May), SW monsoon season (June–September), post-monsoon season (October–December) and the winter season (January and February). We adapted the IMD classification to facilitate better display and further analyses (e.g., Sect. 3.2), making sure that samples are fairly evenly distributed across all seasons. The back-trajectories were generated using the Hybrid Single Particle Lagrangian Integrated Trajectory (HYSPLIT4) model (Draxler and Rolph, 2003), driven by wind fields from the Global Data Assimilation System (GDAS) archive data based on National Centers for Environmental Prediction (NCEP) model output (https://ready.arl.noaa.gov/gdas1.php).

The Hanle (HLE) station (32.780 °N, 78.960 °E, 4517 m a.s.l.) is located in the campus of the Indian Astronomical Observatory (IAO) atop Mt. Saraswati, about 300 m above the Nilamkhul Plain in the Hanle Valley of southeastern Ladakh in northwestern Himalayas. The station was established in 2001 as a collaborative project between the Indian Institute of Astrophysics and LSCE, France. The flask sampling inlet is installed on the top of a 3 m mast fixed on the roof of a 2m high building, and the ambient air is pumped through a Dekabon tubing with a diameter of 1/4". The area around the station is a cold mountain desert, with sparse vegetation and a small population of ~1700 distributed over an area of ~20 km^2. Anthropogenic activities are limited to small-scale crop production (e.g., barley and wheat)

and livestock farming (e.g., yaks, cows, goats, and sheep). The nearest populated city of Leh (34.25 °N, 78.00 °E, 3480 m a.s.l.) with ~27 000 inhabitants, lies 270 km to the northwest of this station. By virtue of its remoteness, high altitude, and negligible biotic and anthropogenic influences, HLE is representative of the background free tropospheric air masses in the northern mid-latitudes. Regular flask air sampling at this station has been operational since February, 2004, and continuous in-situ CO_2 measurements started in September, 2005. Over the period 2007–2011, a total of 188 flask sample pairs were collected at HLE. Back-trajectories show that, HLE dominantly samples air masses that pass over northern Africa and the Middle East throughout the year, and those coming from South and Southeast Asia during the SW monsoon season (Fig. 1a). More detailed station information of HLE would be found in several earlier publications (Babu et al., 2011; Moorthy et al., 2011).

The Pondicherry (PON) station (12.010 °N, 79.860 °E, 20 m a.s.l) is located on the southeast coast of India, about 8 km north of the city of Pondicherry with a population of ~240,000 (Census India, 2011). The station was established in collaboration with Pondicherry University in 2006. The flask sampling inlet, initially located on a 10 m mast fixed on the roof of the University Guest House, was later moved to a 30 m high tower in June, 2011. The ambient air is pumped from the top of the tower through a Dekabon tubing with a diameter of 1/4". The surrounding village Kalapet, has a population of ~9000 (Sivakumar and Anitha, 2012). A four-lane highway runs nearly 80 m to the west of the station with a low traffic flow especially during the nighttime, while the Indian Ocean stands about 100 m to the east of the station. Moreover, the two nearest megalopolises of Chennai and Bangalore, both with populations of over 6 million (Census India, 2011), are approximately 143 km to the north and 330 km to the west of the station. In order to minimize the influences of local GHG sources/sinks, flask air sampling at PON is performed between 12:00 and 18:00 local time

(LT), when the sea breeze moves clean air masses towards the land and the boundary layer air is well mixed. Flask sampling at PON began in September, 2006 and over the period 2007–2011, a total of 185 flask sample pairs were collected at the site. As shown in Fig. 1a, the air masses received at PON are strongly related to the monsoon circulations. During the boreal summer when the southwest monsoon prevails, PON is influenced by air masses originating from the Arabian Sea and South India, whereas during the boreal winter, it receives air masses from the east and northeast parts of the Indian subcontinent, and the Bay of Bengal. During the boreal spring and autumn when the monsoon changes its direction, air masses of both origins are observed.

The Port Blair (PBL) station (11.650 °N, 92.760 °E, 20 m a.s.l.) is located on the small Andaman Islands in the southeastern Bay of Bengal, ~1400 km east of Pondicherry, and roughly 600 km west of Myanmar and Thailand. The station was established in collaboration with the National Institute of Ocean Technology (NIOT), India, and flask air sampling was initiated in July, 2009. The flask sampling inlet is located on the top of a 30 m high tower, and the ambient air is pumped through a Dekabon tubing with a diameter of 1/4". The main city on the Andaman Islands, Port Blair, is about 8 km to the north of the station, with a population of ~100,000 (Census India, 2011). Due to its proximity to vegetation and a small rural community, the station is not completely free from influences of local GHG fluxes. Therefore, flask samples at PBL are obtained in the afternoon between 13:00 and 15:00 LT, when the sea breeze moves towards the land, to minimize significant local influences. Over the period 2009–2011, a total of 63 flask sample pairs were collected at PBL. Back-trajectories show that the air masses sampled at PBL are also controlled by the seasonally reversing monsoon circulations (Fig. 1a), with air masses from the Indian Ocean south of the Equator during the southwest monsoon season, and from the northeast part of the Indian

subcontinent, the Bay of Bengal, and Southeast Asia during the northeast monsoon season. As for PON, air masses of both origins are detected at PBL during the boreal spring and autumn when the monsoon changes its direction.

2.2 Flask sampling and analysis

2.2.1 Flask sampling

In principle, flask samples are taken in pairs on a weekly basis at all three stations. However, in practice air samples are collected less frequently (on average every 10-12 days) due to bad meteorological conditions or technical problems. Whole air samples are filled into pre-conditioned 1-L cylindrical borosilicate glass flasks (Normag Labor und Prozesstechnik GmbH, Germany) with valves sealed by caps made from KEL-F (PTCFE) fitted at both ends. Besides, a few flasks are equipped with valves sealed by the original Teflon PFA O-ring (Glass Expansion, Australia), accounting for ~5.0, 1.2 and 1.1% of air samples respectively for HLE, PON and PBL during the study period. For the air samples stored in flasks sealed with the original Teflon PFA O-ring, corrections are made for the loss of CO_2 (+0.0027 ppm/day) and of N_2O (+0.0035 ppb/day) after analyses of the samples. The correction factors are empirically determined based on laboratory storage tests using flasks filled with calibrated gases. Drying of the air is performed using 10 g of magnesium perchlorate ($Mg(ClO_4)_2$) confined at each end with a glass wool plug in a stainless steel cartridge, located upstream of the pump unit. To prevent entrainment of material inside the sampling unit, a 7 μm filter is attached at the end of the cartridge. The flasks are flushed prior to sampling for 10-20 min at a rate of 4–5 L min^{-1}, and the air is compressed in the flasks to about 1 bar over the ambient pressure (pump: KNF Neuberger diaphragm pump powered by a 12V DC motor,

Germany, N86KNDC with EPDM membrane). The pressurizing process lasts for less than a minute.

2.2.2 Flask analyses

On average the flasks arrive at LSCE, France about 150 days after the sampling date, and are analyzed for CO_2, CH_4, N_2O, SF_6, CO, and H_2 with two coupled gas chromatograph (GC) systems. The first gas chromatograph (HP6890, Agilent) is equipped with a flame ionization detector (FID) for CO_2 and CH_4 detection, and an electron capture detector (ECD) for N_2O and SF_6 detection. It is coupled with a second GC equipped with a reduced gas detector (RGD, Peak Laboratories, Inc., California, USA), for analyzing CO and H_2 via reduction of HgO and subsequent detection of Hg vapor through UV absorption. In the following paragraph we summarize the major configurations and parameters of the GC systems (also see Table S1). Further details on the analyzer configuration are described in Lopez (2012) and Yver et al. (2009).

Both GC systems are composed of three complementary parts: the injection device, the separation elements and the detection sensors. As flask samples are already dried during sampling, they are only passed through a 5 mL glass trap maintained in an ethanol bath kept at -55°C by a cryocooler (Thermo Neslab CC-65) to remove any remaining water vapor. The air samples are flushed with flask overpressure through a 15 mL sample loop for CO_2 and CH_4 analyses, a 15 mL sample loop for N_2O and SF_6 analyses, and a 1 mL sample loop for CO and H_2, at a flow rate of 200 mL min^{-1}. After temperature and pressure equilibration, the air sample is injected into the columns. The CO_2 and CH_4 separation is performed using a Hayesep-Q (12' × 3/16"OD, mesh 80/100) analytical column placed in an oven at 80°C, with

a N_2 5.0 carrier gas at a flow rate of 50 ml min^{-1}. Detection of CH_4 and CO_2 (after conversion to CH_4 using a Ni catalyst and H_2 gas) is performed in the FID kept at 250°C. The flame is fed with H_2 (provided by a NM-H_2 generator from F-DBS) at a flow rate of 100 ml min^{-1} and zero air (provided by a 75-82 zero air generator from Parker-Balston) at a flow rate of 300 ml min^{-1}. For N_2O and SF_6 separation, a Hayesep-Q (4' × 3/16" OD, mesh 80/100) pre-column and a Hayesep-Q (6' × 3/16" OD, mesh 80/100) analytical column, both placed in an oven at 80°C, are used together with an Ar/CH_4 carrier gas at a flow rate of 40 ml min^{-1}. Detection of N_2O and SF_6 is performed in the ECD heated at 395°C. For CO and H_2, we use a Unibeads 1S pre-column (16.5" × 1/8" OD; mesh 60/80) to separate the two gases from the air matrix, and use a Molecular Sieve 5Å analytical column (80" × 1/8" OD; mesh 60/80) to effectively separate H_2 from CO. Both columns are placed in an oven kept at 105°C. CO and H_2 are analyzed in the RGD detector heated to 265°C. A measurement takes ~5 min and calibration gases are measured at least every 0.45 hour. For CO_2, CH_4, N_2O, and SF_6, we use two calibration gases, one with a high concentration and the other with a low concentration. The calibration and quality control cylinders are filled and spiked in a matrix of synthetic air containing N_2, O_2 and Ar prepared by Deuste Steininger (Germany). The concentration of the sample is calculated using a linear regression between the two calibration gases with a time interpolation between the two measurements of the same calibration gas (Messager, 2007; Lopez, 2012). For CO and H_2, we use only one standard and apply a correction for the non-linearity of the analyzer (Yver et al., 2009; Yver, 2010). The nonlinearity is verified regularly with 5 calibration cylinders for CO and 8 calibration cylinders for H_2. All the calibration gases themselves are determined against an international primary scale (CO_2: WMOX2007; CH_4: NOAA2004; N_2O: NOAA2005A; SF_6: NOAA2005; CO: WMOX2004; H_2: WMOX2009; Hall et al., 2007; Dlugokencky et al., 2005; Jordan and Steinberg, 2011; Zhao and Tans, 2006). Finally, a "target" gas is measured every two hours after the calibration

gases as a quality control of the scales and of the analyzers. The repeatability of the GC systems estimated from the target cylinder measurements over several days is 0.06 ppm for CO_2, 1 ppb for CH_4, 0.3 ppb for N_2O, 0.1 ppt for SF_6, 1 ppb for CO and 2 ppb for H_2. Additional quality control is made by checking the values of a flask target (a flask filled with calibrated gases) placed on each measurement sequence.

For both of the GC systems, data acquisition, valve shunting, and temperature regulation are entirely processed by the Chemstation software from Agilent. Concentrations are calculated with a software developed at LSCE using peak height or area depending on the species.

2.2.3 Uncertainty of flask measurements

Uncertainties in the measured concentrations stemmed from both the sampling method and the analysis. Collecting flask samples in pairs and measuring each flask twice allow us to evaluate these uncertainties. A large discrepancy between two analyses of the same flask reveals a problem in the analysis system, while a difference between a pair of flasks reflects both analysis and sampling uncertainties. Flask pairs with differences in mole fractions beyond a certain threshold are flagged and rejected (see Table S2 in the supplement for the threshold for each species). The percentages of flask pairs retained for analyses are 65.9-88.3% for CO_2, 88.6-94.1% for CH_4, 74.6-91.5% for N_2O, 92.0-96.8% for SF_6, 68.6-88.3% for CO, and 76.2-95.2% for H_2 (Table S3). For each species, we evaluate the uncertainties by averaging differences between the two injections of the same flask (analysis uncertainty) and between the pair of flasks (analysis uncertainty + sampling uncertainty) across all retained flask pairs from the three Indian stations (Table S4). For all species except SF_6, the sampling uncertainty turns out to be the major uncertainty, while the analysis uncertainty is equivalent

to the reproducibility of the instrument. For SF_6, both uncertainties are extremely low due to the small amplitudes and variations of the signals at the three stations.

At LSCE, there are regular comparison exercises in which flasks are measured by different laboratories on the same primary scale (e.g., Inter-Comparison Project (ICP) loop, Integrated non-CO2 Greenhouse gas Observing System (InGOS) 'Cucumber' intercomparison project). These comparisons allow us to estimate possible biases in our measurements. In Table S4, the bias for each species is calculated over the sampling period using the ICP flask exercise that circulates flasks of low, medium and high concentrations between different laboratories. For CO_2, CH_4, SF_6 and CO, the biases are reported against NOAA (NOAA-LSCE) as it is the laboratory responsible for the primary scales for these species. The bias of H_2 is calculated against Max Planck Institute for Biogeochemistry (MPI-BGC) in Jena, Germany, which is responsible for the primary scale of H_2. The bias of N_2O is reported against MPI-BGC instead of NOAA. Although NOAA is responsible for the primary scale of N_2O, the instruments they use for the N_2O flask analyses and cylinder calibration are not the same as ours. For CH_4, N_2O, SF_6 and H_2, the estimated biases are within the noise level of the instrument and negligible. For CO_2 and CO, we observe a bias of -0.15±0.11 ppm and 3.5±2.2 ppb, respectively (Table S4), which could be due to the nonlinearity of the instrument and/or an improper attribution of the secondary scale values.

2.3 Data analyses

2.3.1 Curve-fitting procedures

For each time series of flask measurements, we calculated annual means and seasonal cycles using a curve-fitting routine (CCGvu) developed by NOAA/CMDL (Thoning et al., 1989). A

smoothed function was fitted to the retained data, consisting of a first-order polynomial for the growth rate and two harmonics for the annual cycle (Levin et al., 2002; Ramonet et al., 2002), as well as a low pass filter with 80 and 667 days as short-term and long-term cutoff values, respectively (Bakwin et al., 1998). Residuals were then calculated as the differences between the original data and the smoothed fitting curve. Any data lying outside three standard deviations of the residuals were regarded as outliers and discarded from the time series (Harris et al., 2000; Zhang et al., 2007). This procedure was repeated until no outliers remained. These outliers were likely a result of pollution by local emissions and not representative of regional background concentrations. The data discarded through this filtering procedure accounts for less than 4% of the retained flask pairs after flagging (Table S3). The annual means, as well as the amplitude and phases of seasonal cycles, were determined from the smoothed fitting curve and its harmonic component. We bootstrapped the curve-fitting procedures 1000 times by randomly sampling the original data with replacement to further estimate uncertainties of annual means and seasonal cycles. Since the observation records are relatively short, we used all flask measurements between 2006 and 2011 to fit the smooth curve when available (Fig. S2). For each species, we also compared results with measurements from stations outside India that belong to networks of NOAA/ESRL (http://www.esrl.noaa.gov/gmd/) and Integrated Carbon Observation System (ICOS, https://www.icos-cp.eu/). Locations and the fitting periods of these stations are also given in Table S5, Figs. S1 and S2.

2.3.2 Ratio of species

We analyzed CH_4-CO, CH_4-CO_2, and CO-CO_2 correlations using the residuals from the smoothed fitting curves that represent synoptic-scale variations (Harris et al., 2000; Ramonet et al., 2002; Grant et al., 2010). To determine the ratio between each species pair, as in

previous studies, we used the slope calculated from the orthogonal distance regression (Press et al., 2007) to equally account for variances of both species (Harris et al., 2000; Ramonet et al., 2002; Schuck et al., 2010; Baker et al., 2012). We also bootstrapped the orthogonal distance regression procedure 1000 times and estimated the 1-σ uncertainty for each ratio. The analyses were performed with R3.1.0 (R Core Team, 2014) following the recipes described in Teetor (2011).

3 Results and discussions

3.1 Annual means and seasonal cycles

3.1.1 CO_2

Figure 2 shows CO_2 flask measurements and the corresponding smooth curves fitted to the data at HLE, PON and PBL, as well as two additional NOAA/ESRL stations, namely Plateau Assy, Kazakhstan (KZM – 43.25 °N, 77.88 °E, 2519 m a.s.l.) and Waliguan, China (WLG – 36.29 °N, 100.90 °E, 3810 m a.s.l.) (Dlugokencky et al., 2014b). HLE observed an increase in CO_2 mole fractions from 382.3±0.3 to 391.4±0.3 between 2007 and 2011, with annual mean values being lower (by 0.2–1.9 ppm) than KZM and WLG (Fig. 2c and d, Table 1). At PON, the annual mean CO_2 mole fractions were generally higher than at HLE, with differences ranging 1.8–4.3 ppm (Fig. 2a, Table 1). The annual mean CO_2 gradient between PON and HLE reflects the altitudinal difference of the two stations, and a larger influence of CO_2 emissions at PON, mostly from South India (Fig. 1a, EDGAR v4.2). Besides this, as shown in Fig. 2a and Table 1, the CO_2 observations at PON are influenced by synoptic scale events, with a large variability of individual measurements relative to the fitting curve (see the relative SDs (RSD) in Table 1). At PBL, the annual mean CO_2 mole fractions were on average 1.2–1.8 ppm lower than that at HLE (Table 1). The negative gradient between PBL

and HLE is particularly large during summer, possibly due to clean air masses transported from the ocean (Figs. 1a and 2b). Note that caution should be exercised in interpreting the gradient at PBL because of the data gap and short duration of the time series.

The different CO_2 seasonal cycles observed at the five stations reflect the seasonality of carbon exchange in the northern terrestrial biosphere as well as influences of long-range transport and the monsoon circulations. At HLE, the peak-to-peak amplitude of the mean seasonal cycle was 8.2±0.4 ppm, with the maximum early May and the minimum mid-September, respectively (Fig. 3, Table 1). The mean seasonal cycle estimated from flask measurements at HLE is in good agreement with that derived from vertical profiles of in-situ aircraft measurements over New Delhi (~500 km southwest of HLE) from the Comprehensive Observation Network for Trace gases by Airliner (CONTRAIL, http://www.cger.nies.go.jp/contrail/) project at similar altitudes (R=0.98–0.99, p<0.001, Fig. 3a; Machida et al., 2008), and back-trajectories show that they represent air masses with similar origins as HLE (Fig. S7), confirming that HLE is representative of the regional free mid-troposphere background concentrations. When comparing with the two other background stations located further north in central and East Asia, a significant delay of the CO_2 phase is seen at HLE compared to KZM and WLG (Fig. 3b, Table 1). We also note that the CO_2 mean seasonal cycle at HLE is in phase with the composite zonal marine boundary layer (MBL) reference at 32°N, while for KZM and WLG, an advance in the CO_2 phase by about 1 month is observed compared to the zonal MBL reference (Fig. S3; Dlugokency et al., 2014b). The phase shifts in the CO_2 seasonal cycles mainly result from differences in the air mass origins between stations. HLE is influenced by the long-range transport of air masses from mid-latitudes around 30 °N, as well as air masses passing over the Indian subcontinent in the boreal summer (Fig. 1a), therefore its CO_2 seasonal cycle is related to the seasonality of

vegetation activity over the entire latitude band. KZM and WLG receive air masses passing over the Middle East and western Asia as HLE does, but they are also influenced by air masses of more northern origins with signals of strong CO_2 uptake over Siberia during JAS (Fig. S4). At WLG, negative CO_2 synoptic events, indicative of large-scale transport of air masses exposed to carbon sinks in Siberia in summer, were also detected by in-situ measurements during 2009-2011 (Fang et al., 2014). Moreover, the back trajectories indicate that WLG and KZM are more influenced than HLE by air masses that have exchanged with the boundary layer air being affected by vegetation CO_2 uptake (Fig. S5a,d,e). This could additionally account for the earlier CO_2 phase observed at KZM and WLG compared to HLE.

At PON and PBL, the peak-to-peak amplitudes of the CO_2 mean seasonal cycles were 7.6±1.4 and 11.1±1.3 ppm, with their maxima observed in April. The CO_2 mean seasonal cycle is controlled by changes in the monsoon circulations, in combination with the seasonality of CO_2 biotic exchange and anthropogenic emissions in India. During the boreal winter when the NE monsoon prevails, PON and PBL receive air masses enriched in CO_2 from the East and Northeast Indian subcontinent as well as from Southeast Asia, with large anthropogenic CO_2 emissions (EDGAR v4.2; Wang et al., 2013; Kurokawa et al., 2013). During April when the SW monsoon begins to develop, the two stations record a decrease in CO_2 because of the arrival of air masses depleted in CO_2 originating from the Indian Ocean south of the Equator (Fig. 1a, Fig. 3c). Compared to PBL, the CO_2 decrease at PON is less pronounced and longer, probably because of the influence of anthropogenic emissions in South India. The CO_2 mean seasonal cycle at PON is also similar to that observed at CRI (15.08°N, 73.83°E, 60m a.s.l.), another station on the southwest coast of India, yet the seasonal maximum at CRI is reached slightly earlier than at PON in March (Bhattacharya et al., 2009; Tiwari et al., 2011, 2014). The SNG station (18.35°N, 73.75°E, 1600m a.s.l.),

located over the Western Ghats, observes a larger CO_2 seasonal cycle with a peak-to-peak amplitude of ~20 ppm (Tiwari et al., 2014).

3.1.2 CH_4

Figure 4 presents the time series of CH_4 flask measurements at the three Indian stations and the two NOAA/ESRL stations (Dlugokencky et al., 2014a), with their corresponding smoothed curves for 2007–2011. At HLE, the annual mean CH_4 concentration increased from 1814.8±2.9 to 1849.5±5.2 ppb between 2007 and 2011 (Fig. 4, Table 1). The multiyear mean CH_4 value at HLE was lower than at KZM and WLG by on average 25.7±3.1 and 19.6±7.8 ppb (Fig. 4c and d, Table 1), respectively, reflecting the latitudinal and altitudinal CH_4 gradients. Indeed, KZM and WLG receive air masses transported from Siberia with large wetland CH_4 emissions in summer, as well as those from regional sources closer to the stations (Fang et al., 2013; Fig. S4), which may further contribute to the positive gradients between these two stations and HLE. At PON and PBL, the annual mean CH_4 mole fractions were higher than those at HLE by as much as 37.4±10.7 and 19.8±24.5 ppb respectively (Fig. 4a and b, Table 1). The positive gradients indicate significant regional CH_4 emissions, especially during winter when the NE monsoon transports air masses from East and Northeast India and Southeast Asia, where emissions from livestock, rice paddies and a variety of waterlogged anaerobic sources and residential biofuel burning are high (EDGAR v4.2; Baker et al., 2012; Kurokawa et al., 2013). The in-situ measurements at Darjeeling, India (27.03°N, 88.25°E, 2194 m a.s.l.), another station located in the eastern Himalayas, also showed large variability and frequent pollution events in CH_4 mole fractions, which largely result from the transport of CH_4-polluted air masses from the densely populated Indo-Gangetic Plains to the station (Ganesan et al., 2013).

The CH_4 seasonal cycles exhibit contrasting patterns across stations. As shown in Fig. 5, a distinct characteristic of the mean seasonal cycle at HLE is a CH_4 maximum from June to September. Even KZM and WLG do not show a minimum in summer that would be characteristic for the enhanced CH_4 removal rate by reaction with OH. The pronounced HLE feature is consistent with the result from the aircraft flask measurements over India at flight altitudes of 8–12.5 km by the Civil Aircraft for the Regular Investigation of the atmosphere Based on an Instrument Container (CARIBIC, http://www.caribic-atmospheric.com/) project (Schuck et al., 2010, 2012; Baker et al., 2012), although a larger seasonal cycle amplitude is found in the CARIBIC composite data due to vertical mixing between the mid- and upper troposphere (Fig. 5a). CARIBIC sampled the mid- to upper tropospheric air masses that were earlier and more strongly enriched in CH_4 due to the rapid uplift in regions of strong convection. Xiong et al. (2009) also reported enhancements of CH_4 during the summer monsoon season over South Asia based on satellite retrievals of CH_4 using the Atmospheric Infrared Sounder (AIRS) on the EOS/Aqua platform as well as model simulations. Moreover, the mean CH_4 seasonal cycle at HLE agrees well with the seasonal variations of CH_4 emissions from wetlands and rice paddies and convective precipitation over the Indian subcontinent (Fig. 5b), suggesting that the summer maximum at HLE are likely related to the enhanced biogenic CH_4 emissions from wetlands and rice paddies and deep convection that mixes surface emissions into the mid-to-upper troposphere. During the SW monsoon period (June–September), convection over the Indian subcontinent and the Bay of Bengal rapidly mixes surface polluted air with the upper troposphere, therefore concentrations of trace gases would be enhanced at higher altitudes rather than at the surface (Schuck et al., 2010; Lawrence and Lelieveld, 2010). Further analyses of carbon isotopic measurements and/or chemical transport model are needed to disentangle and quantify the contributions of

meteorology and biogenic emissions to the CH_4 summer maximum at HLE. As stated above, KZM and WLG also record CH_4 increases during summertime, but with smaller magnitudes (Fig. 5a), possibly because they are not directly influenced by deep convection from the Indian monsoon system.

In contrast to HLE, the CH_4 mean seasonal cycles at PON and PBL have distinct phases and much larger amplitudes, with minimum CH_4 values during July (Fig. 5c). These not only reflect higher rates of removal by OH, but rather the influence of southern hemispheric air transported at low altitudes from the southwest as well as the dilution effect by increased local planetary boundary layer height. In boreal winter, the maxima at PON and PBL are associated with CH_4-enriched air masses transported from East and Northeast India, and Southeast Asia, mostly polluted by agricultural-related sources (e.g., livestock, rice paddies, agricultural waste burning). As PON and PBL, the flask measurements at CRI also showed the seasonal maximum CH_4 values during the NE monsoon season, reflecting influences of air masses with elevated CH_4 from the Indian subcontinent (Bhattacharya et al., 2009; Tiwari et al., 2013).

3.1.3 N_2O

Nitrous oxide (N_2O) is a potent greenhouse gas that has the third largest contribution to anthropogenic radiative forcing after CO_2 and CH_4 (IPCC, 2013). It also becomes the dominant ozone depleting substance (ODS) emitted in the 21st century with the decline of chlorofluorocarbons (CFCs) under the Montreal Protocol (Ravishankara et al., 2009). Since the pre-industrial era, the atmospheric N_2O increased rapidly from ~270 ppb to ~325 ppb in 2011 (IPCC, 2013), largely as the result of human activities. Of the several known N_2O

sources, agricultural activities (mainly through nitrogen fertilizer use) contribute to ~58% of the global anthropogenic N_2O emissions, with a higher share in a predominantly agrarian country like India (~75%; Garg et al., 2012).

The time series of N_2O flask measurements over the period of 2007–2011 and their smoothed curves are presented in Fig. 6. At HLE, the annual mean N_2O concentration rose from 322.2±0.1 to 325.2±0.1 ppb during 2007–2011 (Table 1), with a mean annual growth rate of 0.8±0.0 ppb yr^{-1} (r^2 = 0.97, p = 0.001), smaller than that at MLO (1.0±0.0 ppb yr^{-1}, Table 1). At PON and PBL, the annual mean N_2O mole fractions are higher than at HLE by 3.1±0.3 and 3.8±1.7 ppb (Fig. 6, Table 1), respectively. The N_2O gradients between PON, PBL and HLE are larger than typical N_2O gradients observed between stations scattered in Europe or in North America. For example, Haszpra et al. (2008) presented N_2O flask measurements at a continental station – Hegyhátsál, Hungary (HUN – 46.95 °N, 16.65 °W, 248 m a.s.l.) from 1997 to 2007. The annual mean N_2O mole fraction at HUN was higher than at Mace Head (MHD) by only 1.3 ppb. We also analyzed N_2O time series of flask measurements during 2007–2011 at several European coastal stations – BGU in Spain, FIK in Greece, and LPO in France (Table S5), and the N_2O gradients between these stations and MHD were 1.1±0.2, 0.4±0.1, and 2.1±0.6 ppb, respectively (Fig. S9, Table S6). In the United States, N_2O flask measurements from the NOAA/ESRL stations at Park Falls, Wisconsin (LEF – 45.95 °N, 90.27 °W, 472 m a.s.l.), Harvard Forest, Massachusetts (HFM – 42.54 °N, 72.17 °W, 340 m a.s.l.) and a continental, high-altitude station at Niwot Ridge, Colorado (NWR – 40.05 °N, 105.58 °W, 3523 m a.s.l.) also show that, the annual mean N_2O concentrations at HFM and LEF were higher than that at NWR by only 0.5±0.1 and 0.3±0.1 ppb, respectively (Fig. S9, Table S6). Besides, the N_2O concentrations measured at PON and PBL have a notably higher variability (around the smoothed fitting curve) than that at European and US stations (see

relative SDs (RSD) in Table 1 and Table S6). The larger N_2O gradient between PON, PBL and HLE, as well as higher variability at PON and PBL, demonstrate the presence of substantial N_2O sources in South Asia and over the Indian Ocean during the observation period. The in-situ measurements at Darjeeling also exhibited N_2O enhancements to be above the background level, suggesting significant N_2O sources in this region (Ganesan et al., 2013). These sources may be related to emissions from natural and cultivated soils probably enhanced by extensive use of nitrogen fertilizers, as well as emissions from regions of coastal upwelling in the Arabian Sea (Bange et al., 2001; Garg et al., 2012; Saikawa et al., 2014).

Compared to CO_2 and CH_4, the seasonal cycle of N_2O is very small due to the long lifetime of ~120 years (Minschwaner et al., 1993; Volk et al., 1997), and has a larger uncertainty probably because synoptic events are more likely to mask the seasonal signal. At HLE, PON and PBL, the peak-to-peak amplitudes of the N_2O seasonal cycle are 0.6±0.1, 1.2±0.5, and 2.2±0.6 ppb, respectively (Table 1). HLE displays a N_2O maximum in mid-August (Student's t-test, t=1.78, p=0.06), and a secondary maximum is in January/February but not significant (Student's t-test, t=-0.84, p=0.79) (Table 1, Fig. 7, Table S7 for detailed t-test statistics). The N_2O seasonal cycle at HLE is out of phase with that at other northern background stations such as MHD (Fig. S10, Table S6), where an N_2O summer minimum is always observed, likely due to the downward transport of N_2O-depleted air from the stratosphere to the troposphere during spring and summer (Liao et al., 2004; Morgan et al., 2004; Jiang et al., 2007b). The timing of the summer N_2O maximum at HLE is consistent with that of CH_4 (Table 1; Figs. 5 and 7), giving evidence that the N_2O seasonal cycle may probably be influenced by the convective mixing of surface air, rather than by the influx of stratospheric air into the troposphere. Given that the populous Indo-Gangetic plains have high N_2O emission rates due to the intensive use of nitrogen fertilizers (Garg et al., 2012; Thompson et

al., 2014a), during summer, the surface air enriched in N_2O is vertically transported by deep convection and enhances N_2O mole fractions in the mid-to-upper troposphere. Like CH_4, the N_2O enhancement at HLE during the summer monsoon period (June-September) is consistent with the aircraft flask measurements at flight altitudes 8–12.5 km from the CARIBIC project in 2008 (Schuck et al., 2010).

At PON, N_2O also decreases during February–April and reaches a minimum at the end of May. However, the decrease of N_2O does not persist during June–September, which is in contrast with CH_4 (Table 1, Fig. 7a). One reason may be that the air masses arriving at the site during the southwest monsoon period is relatively enriched in N_2O compared to CH_4, reflecting differences in their relative emissions along the air mass route. The increase of N_2O at PON during June–August and the maximum during September–October are likely related to N_2O emissions from coastal upwelling along the southern Indian continental shelf, which peak during the SW monsoon season (Patra et al., 1999; Bange et al., 2001). According to Bange et al. (2001), the annual N_2O emission for the Arabian Sea is 0.33–0.70 Tg/yr, of which N_2O emissions during the SW monsoon account for about 64–70%. This coastal upwelling N_2O flux is significantly larger than the annual anthropogenic N_2O emissions in South India south of 15 °N, which is estimated to be on average 0.07–0.08 Tg/yr during 2000–2010 (EDGAR v4.2). At PBL, the maximum and minimum N_2O occur in November and February/March, respectively (Table 1, Fig. 7b). The late N_2O peak at PBL in November may be associated with the N_2O-enriched air masses transported from South and Southeast Asia, which could be attributed to natural and agricultural N_2O emissions from this region (Saikawa et al., 2014). It should be noted that, the mean seasonal cycles of N_2O at PON and PBL are subject to high uncertainties because of the short observation periods and data gaps (shaded area in Fig. 7). The N_2O maximum and/or minimum obtained from the mean

seasonal cycle are marginally significant for PON and PBL (Table S7 for detailed t-test statistics). Therefore, caution should be exercised in interpreting mean seasonal cycles at these stations. Sustained, long-term measurements are needed in order to generate more reliable estimates of the seasonal cycles for the two stations.

3.1.4 SF_6

Sulfur hexafluoride (SF_6) is an extremely stable greenhouse gas, with an atmospheric lifetime as long as 800–3200 year and a global warming potential (GWP) of ~23,900 over a 100-year time horizon (Ravishankara et al., 1993; Morris et al., 1995; IPCC, 2013). The main sources of atmospheric SF_6 emissions are electricity distribution systems, magnesium production, and semi-conductor manufacturing (Olivier et al., 2005), while its natural sources are negligible (Busenberg and Plummer, 2000). As its sources are almost purely anthropogenic (Maiss et al., 1996), SF_6 is widely considered as a good tracer for population density, energy consumption and anthropogenic GHG emissions (Haszpra et al., 2008).

Figure 8 presents the time series of SF_6 flask measurements and corresponding fitting curves at HLE, PON, and PBL. At HLE, the annual mean SF_6 mole fractions increased from 6.26±0.03 to 7.38±0.01 ppt between 2007 and 2011, which is in good agreement with the SF_6 trend observed at MLO during the same period (HLE: 0.29±0.05 ppt/yr, r^2=0.99, p<0.001; MLO: 0.29±0.03 ppt/yr, r^2=0.99, p<0.001; Figs. 8 and S11a, Table 1, Table S8). The annual mean SF_6 gradient between PON and HLE is -0.060±0.030 ppt, whereas the gradient between PBL and HLE is statistically insignificant (-0.002±0.097 ppt). The slight negative gradient between PON and HLE is a reversed signal compared with the SF_6 observations at stations influenced by continental emissions in Europe and United States. For example, the SF_6 mole

fractions at HUN over the years of 1997–2007 are higher than those at MHD by on average 0.19 ppt (Haszpra et al., 2008). We also analyzed the SF_6 gradients between two coastal European stations – BGU (41.97 °N, 3.3 °E, 30 m a.s.l.) and LPO (48.80 °N, 3.57 °W, 30 m a.s.l.) – and MHD, which are 0.10±0.03 and 0.05±0.02 ppt averaged over the period of 2007–2011, respectively. At HFM, the SF_6 mole fractions are higher than those of the NWR on average by 0.15±0.06 ppt during 2007–2011 (Table S8). Given the long atmospheric lifetime of SF_6, the positive gradients between continental European and US stations and background reference stations suggest significant sources in Europe and the US. On the contrary, the slight negative gradient between PON and HLE implies weak SF_6 emissions over the Indian subcontinent, which is also indicated by recent high-frequency in-situ SF_6 measurements at Darjeeling (Ganesan et al., 2013). It is also worthwhile to note that high SF_6 values occur repeatedly at HLE and PBL in winter, which is likely related to episodic SF_6 pollution events from the Middle East, South/Southeast Asia and China (Figs. 8b and S6d).

The annual mean SF_6 seasonal cycles for HLE, PON, and PBL are presented in Fig. 9. The peak-to-peak amplitudes at the three stations are 0.15±0.03, 0.24±0.02, and 0.48±0.07 ppt, respectively (Table 1). At HLE, the SF_6 seasonal cycle is bimodal as for N_2O, with an absolute maximum occurring in November (Student's t-test, t=2.425, p=0.014) and a secondary maximum in May (Student's t-test, t=2.443, p=0.016) (Table S9 for detailed t-test statistics). Given that SF_6 increases monotonously and that its sources are purely anthropogenic and not subject to seasonally variations (Maiss et al., 1996), the seasonal cycle of SF_6 should be driven by changes in atmospheric circulations, e.g., the SW monsoon convection and stratosphere-atmosphere exchange (Levin et al., 2002). We note that, at HLE, no enhancement of SF_6 during the SW monsoon season is recorded, unlike what is observed for CH_4 and N_2O (Figs. 5 and 7). Although the CARIBIC aircraft flask measurements over

630 the Indian region demonstrated SF_6 enhancements in the upper troposphere at ~30 °N
631 (approximately where HLE is located) in August, 2008, back-trajectories from the CARIBIC
632 flights showed that the summer enhancements in SF_6 were more related to the influences of
633 westerly jet transport in the upper troposphere, rather than the SW monsoon and sources from
634 India that contributed to the summer maxima in CH_4 and N_2O (Schuck et al., 2010, Fig. S8).
635 The absence of SF_6 enhancement in summer at HLE confirms weak SF_6 emissions in India.
636 At PBL, the SF_6 seasonal cycle is related to the monsoon circulation and convection (Figs. 9b
637 and S6d). The maximum during November–December (Student's t-test, $t=5.138$, $p<0.001$;
638 Table S9) is likely due to frequent episodic SF_6 polluted air masses transported from
639 Southeast Asia and China (Fig. S6d).
640
641 **3.1.5 CO**
642 Carbon monoxide (CO) plays important roles in atmospheric chemistry, as the dominant sink
643 for the hydroxyl radical (OH, the main tropospheric oxidant) and a precursor of tropospheric
644 ozone under high NO_x ($NO+NO_2$) concentrations (Logan et al., 1981; Novelli et al., 1998;
645 Seinfeld and Pandis, 2006). Although CO does not act as a greenhouse gas, it modulates the
646 atmospheric concentrations of CH_4 (the second anthropogenic greenhouse gas after CO_2)
647 through competition for the OH radicals. At the global scale, it contributes to an indirect
648 positive radiative forcing of $0.23\pm0.07 Wm^{-2}$ (IPCC, 2013). Besides, CO is an excellent tracer
649 for combustion processes, with emission sources mainly contributed by incomplete
650 combustion of fossil fuel and biofuels, and by biomass burning (Granier et al., 2011). In India,
651 biofuel and agricultural waste burning account for 70–80% of the total anthropogenic CO
652 emissions (EDGAR v4.2; Streets et al., 2003b; Yevich and Logan, 2003).
653

654 The time series of CO flask measurements and corresponding smoothed curves are shown in
655 Fig. 10. Over the period of 2007–2011, HLE recorded a slight decrease in CO mole fractions
656 from 104.7±1.4 to 99.4±2.2 ppb, with an annual rate of -2.2±0.0 ppb yr^{-1} (r^2 = 0.65, p = 0.06).
657 The CO mole fractions at HLE are lower than those at KZM and WLG (Novelli et al., 2014b),
658 by on average 18.8±2.5 and 30.2±7.4 ppb, respectively (Table 1, Fig. 10c and d). The
659 positive gradient between KZM, WLG and HLE does not only reflect decreasing CO with
660 altitude and the N-S global gradient, but also suggests differences in regional emission
661 sources. For example, compared to HLE, the CO signals at WLG are more influenced by
662 transport of polluted air, especially during summer when about 30% air masses pass over
663 industrialized and urbanized areas southeast of the station (Zhang et al., 2011). Besides, the
664 positive CO gradient between KZM, WLG and HLE may be further contributed by air
665 masses of northern Siberia origin in summer (Fig. S4), with higher CO emissions from
666 biomass burning and secondary CO from the oxidation of CH_4 and non-CH_4 hydrocarbons
667 (Konovalov et al., 2014). At PON and PBL, the annual mean CO mole fractions are higher
668 than that at HLE by on average 82.4±10.7 and 52.5±8.5 ppb, respectively (Table 1, Fig. 10a
669 and b). The PON and PBL stations are influenced by CO regional emissions, mainly due to
670 biofuel and agricultural burning over South and Southeast Asia (Lelieveld et al., 2001; Streets
671 et al., 2003a, b; Yevich and Logan, 2003). We also note that, for all the five stations, the CO
672 time series show larger variability with respect to their corresponding smoothed curves than
673 other species do (see the residual SD (RSD) in Table 1, Fig. 10), as a result of the unevenly
674 distributed CO sources and short atmospheric lifetime (Novelli et al., 1992).

675

676 As shown in Fig. 11, the CO seasonal cycle at HLE reaches a maximum in mid-March and a
677 minimum by the end of October, with a peak-to-peak amplitude of 28.4±2.3 ppb (Table 1,
678 Fig. 11). The phase of the mean CO seasonal cycle at HLE generally agrees with the ones

observed at KZM and WLG, with a lag of up to 1 month in the timing of seasonal minimum at the two stations (Table 1, Fig. 11c and d). In contrast with the three stations representative of large-scale free tropospheric air masses, the stations at the maritime boundary layer in the mid-to-high Northern Hemisphere observe the lowest CO values in July or August (Novelli et al., 1992, 1998), when the concentration of OH – the major sink of CO – is highest (Logan et al., 1981). The delay in timing of the seasonal CO minimum at the three free troposphere stations in Central and South Asia compared to those boundary layer stations is probably due to the mixing time of regional surface CO emissions and the relatively short lifetime of CO (1-2 months on average). During summer, KZM and WLG sample air masses from Siberia impacted by CO fire emissions (Duncan et al., 2003; Kasischke et al., 2005), as well as CO-polluted air from urbanized and industrialized area (Zhang et al., 2011), while HLE is influenced by convective mixing of CO emissions from India, either from anthropogenic sources or oxidation of VOCs. It is interesting to note that the CO seasonal cycle at HLE does not show an enhancement during JAS as CH_4 and N_2O do (Figs. 5 and 7), possibly as a result of OH oxidation that reduces CO and acts oppositely to vertical transport, and/or differences in seasonal emission patterns between CO and the other two species (Baker et al., 2012). However, the CO enhancement during summer was observed in the upper troposphere over South Asia from the CARIBIC aircraft measurements at flight altitudes 8-12.5 km and Microwave Limb Sounder observations at 100–200 hPa (Li et al., 2005; Jiang et al., 2007a; Schuck et al., 2010). The differences in the CO seasonal cycles at different altitudes suggest faster transport (and younger air masses) at 10 km than at 5 km due to convection, controlling the vertical profile of CO, which makes it difficult to directly compare aircraft measurements in the upper troposphere and column remote sensing observations with surface data.

At PON and PBL, the mean CO seasonal cycles show maxima in the boreal winter and minima in the boreal summer, with peak-to-peak amplitudes of 78.2±11.6 and 144.1±16.0 ppb, respectively (Fig. 11a and b). A strong and positive correlation is found between detrended CO and CH_4 at PON ($r=0.70$, $p<0.001$) and PBL ($r=0.84$, $p<0.001$), suggesting that the seasonal cycles of both species are dominated by the seasonally varying atmospheric transport. During summer when the southwest monsoon prevails, the surface CO concentrations at PON and PBL are low due to rapid convective uplifting and advection of clean air masses from the ocean. During winter, the two stations are influenced by northeasterly air masses enriched in CO from Northeast India, Southeast Asia and China (back-trajectories in Fig. S6e), probably influenced by biofuel and agricultural waste burning in these regions (Yevich and Logan, 2003; Lelieveld et al., 2001).

3.1.6 H_2

Hydrogen (H_2) is the second most abundant reduced trace gas in the troposphere after CH_4, with an average mole fraction of ~530 ppb (Novelli et al., 1999). It plays important roles in tropospheric and stratospheric chemistry and indirectly impacts budgets of CH_4, CO and non-methane hydrocarbons (NMHCs) through reaction with the OH radicals (Novelli et al., 1999; Ehhalt and Rohrer, 2009). Like CO, H_2 is also a good tracer for incomplete combustion emissions from fossil fuel and biomass/biofuel burning, which is quite extensive in India (Streets et al., 2003b; Yevich and Logan, 2003).

Figure 12 shows the time series of H_2 flask measurements with smoothed curves at HLE, PON, and PBL, respectively. No significant trend was observed at any of the three stations (Table 1, Fig. 12), consistent with the long-term H_2 measurements at other background

727 stations during the last three decades (Novelli et al., 1999; Ehhalt and Rohrer, 2009; Grant et
728 al., 2010). For the year 2008, comparing to KZM and WLG (Novelli et al., 2014a), HLE
729 recorded higher H_2 mole fractions by ~40 ppb, reflecting the latitudinal gradient of H_2 with
730 lower concentrations towards northern high latitudes, due to land uptake by soils (Novelli et
731 al., 1999; Price et al., 2007; Hauglustaine and Ehhalt, 2002; Ehhalt and Rohrer, 2009). Note
732 that these results based on only one-year comparison need to be confirmed by extended data
733 more up-to-date, which are not available yet. At PON and PBL, the annual mean H_2 mole
734 fractions were higher than at HLE by 29.8±4.1 and 21.8±4.6 ppb, respectively (Table 1; Fig.
735 12). Comparisons with H_2 measurements at Mariana Island, Guam (GMI – 13.39 °N,
736 144.66 °E, 0.00 m a.s.l.) (Novelli et al., 2014a), another maritime station in the western
737 Pacific at a similar latitude as PON and PBL, also showed positive gradients of ~40 ppb (Fig.
738 S12c and d; Table S10), suggesting substantial regional H_2 sources over the footprint area of
739 PBL and PON. During October–March when the NE monsoon prevails, both PON and PBL
740 receive H_2-enriched air masses from South and Southeast Asia, mainly influenced by fossil
741 fuel combustion and biomass burning (Fig. S6f; GFED v3.1; Hauglustaine and Ehhalt, 2002;
742 Price et al., 2007; Ehhalt and Rohrer, 2009; van der Werf et al., 2010). During April–
743 September, with the northward movement of Intertropical Convergence Zone (ITCZ), the two
744 stations are influenced by advection of air from south of the Equator. For PON, H_2-polluted
745 air masses are occasionally sampled during JAS when the SW monsoon moves over the
746 continent of South India with high population and heavy industry (Fig. S6f; Census India,
747 2011).
748
749 The mean H_2 seasonal cycles for HLE, PON, and PBL are presented in Fig. 13. At HLE, the
750 peak-to-peak H_2 seasonal amplitude is 15.8±2.2 ppb, less than half of the seasonal amplitudes
751 at BMW (39.6±2.6 ppb) and MID (38.0±2.4 ppb) of similar latitudes (Novelli et al., 2014a),

and that at WLG (22.8±3.0 ppb) (Figs. 13d and S13a, Tables 1 and S10). The maximum and minimum of H_2 occur in April and September, respectively. The dampening of the H_2 seasonal amplitude with increasing altitude was previously found for another high-altitude continental station at Jungfraujoch, Switzerland (JUN – 46.53 °N, 7.98 °E, 3580.00 m a.s.l.) (Bond et al., 2011), and was also captured by the GEOS-Chem global chemical transport model (Price et al., 2007). Since the soil sink dominates much of the surface H_2 seasonal cycle in the mid-to-high Northern Hemisphere (Hauglustaine and Ehhalt, 2002; Price et al., 2007; Bousquet et al., 2011; Yver et al., 2011; Yashiro et al., 2011), the smaller amplitude in the H_2 seasonal cycle at HLE may be attributed to the weakened soil sink with increasing altitude due to vertical mixing (Price et al., 2007; Bond et al., 2011).

At PON and PBL, the mean H_2 seasonal cycles are characterized by the peak-to-peak amplitudes of 21.6±3.4 and 21.3±5.0 ppb respectively, comparable to that at GMI (21.5±1.2 ppb) (Tables 1 and S10, Figs. 13a and b and S13b). At PBL, the H_2 maximum in March–April and a secondary increase during September–October coincide with the double biomass burning peaks in each hemisphere – in March for northern tropics, in August/September for southern tropics (van der Werf et al., 2006; Price et al., 2007; Bousquet et al., 2011; Yver et al., 2011). Given that the seasonal variation of soil H_2 uptake is probably small in the tropics (Price et al., 2007; Bousquet et al., 2011; Yver et al., 2011; Yashiro et al., 2011), this bimodal H_2 seasonal cycle at PBL could be related to biomass burning.

3.2 Synoptic variations

In this section we analyze synoptic variations of CO_2, CH_4, and CO by examining correlations between species, after subtracting the smoothed curve from the original data.

776 Ratios of trace gas mole fractions or their enhancements have been widely used in previous
777 studies to partition contributions from different source types and origins (Langenfelds et al.,
778 2002; Paris et al., 2008, Lopez et al., 2012), to estimate emissions of one species given
779 emissions of another one that is better-known (Gamnitzer et al., 2006; Rivier et al., 2006;
780 Turnbull et al., 2006; Schuck et al., 2010), and to provide valuable constraints on inversion of
781 sources and sinks of trace gases (Xiao et al., 2004; Pison et al., 2009).

782

783 **3.2.1 $\Delta CH_4/\Delta CO$**

784 Figure 14 shows scatterplots of CH_4 and CO residuals with the orthogonal distance regression
785 lines at HLE, PON, and PBL for different seasons. A significant and positive correlation
786 between CH_4 and CO residuals (hereafter $\Delta CH_4/\Delta CO$, unit ppb ppb^{-1}) is found for all three
787 stations throughout the year. Furthermore, the $\Delta CH_4/\Delta CO$ ratio also shows seasonal variation
788 at each of the three stations. The most prominent feature is the occurrence of maximum
789 slopes in July–September (also October–December at PON), especially at HLE and the
790 generally higher ratios at this station. Wada et al. (2011) and Niwa et al. (2014) also reported
791 increased summer $\Delta CH_4/\Delta CO$ over the western North Pacific, according to the in-situ
792 measurements at several surface stations and aircraft flask measurements in the mid-
793 troposphere. The main process for this seasonal variation of $\Delta CH_4/\Delta CO$ might be the
794 enhanced emissions of biogenic CH_4 in summer (e.g., wetland and rice paddy emissions;
795 Streets et al., 2003a;Yan et al., 2003) combined with concurrent lower anthropogenic CO
796 emissions in summer than in winter (due to less residential fuel use for heating, see Streets et
797 al., 2003a). The faster photochemical destruction of CO by increased OH during summer
798 cannot explain such large changes (less than 15% according to Wada et al. (2011)).

799

800 At HLE, the $\Delta CH_4/\Delta CO$ ratio varies from 1.2±0.3 to 4.0±1.2 ppb ppb^{-1} throughout the year,
801 with a maximum in JAS, corresponding to the summer monsoon season (Fig. 14a-d). Based
802 on the CARIBIC flights between 10 and 12 km from Frankfurt, Germany to Chennai, India,
803 Baker et al. (2012) derived a $\Delta CH_4/\Delta CO$ ratio in the range 1.88(±0.22) to 4.43(±0.56) in JAS
804 over South Asia. The maximum $\Delta CH_4/\Delta CO$ observed during summer in the mid-to-upper
805 troposphere may be the result of higher biogenic CH_4 emission over the Indian subcontinent,
806 lower CO emissions, combined with frequent widespread convective uplift of surface air
807 during the SW monsoon (Schuck et al., 2010; Baker et al., 2012). The CARIBIC flights
808 recorded similar $\Delta CH_4/\Delta CO$ values to HLE, confirming that convection plays a dominant
809 role compared to advection during the SW monsoon season. Outside the SW monsoon season,
810 both the CARIBIC flights and HLE do generally not record strong effects of surface
811 emissions due to the weakened vertical transport. With respect to the $\Delta CH_4/\Delta CO$ ratios for
812 January–March, April–June and October–December, our estimates are 1.5 to 4 times that of
813 the ratios determined for air masses with signatures of fossil fuel combustion, according to
814 several aircraft and ground observations in East and Southeast Asia (Table S11; Sawa et al.,
815 2004; Lai et al., 2010; Wada et al., 2011; Niwa et al., 2014), which rules out fossil fuel
816 combustion as an explanation for the higher ratios. Our ratios are comparable to the
817 $\Delta CH_4/\Delta CO$ values inferred for air masses of Siberian origin during winter (Table S11; Harris
818 et al., 2000; Chi et al., 2013), and we also obtain similar estimates of $\Delta CH_4/\Delta CO$ from the
819 flask measurements at KZM over the study period (The $\Delta CH_4/\Delta CO$ ratios for KZM are
820 0.8±0.2, 1.7±0.2 and 1.5±0.3 ppb ppb^{-1} for AMJ, OND and JFM, respectively), which are
821 influenced by air masses originating from North Africa, the Middle East, and Central Asia as
822 seen at HLE (see back-trajectories in Fig. S4). Given that oil and gas production accounts for
823 50–70% of CH_4 emissions in these regions (EDGAR v4.2) and that over dry areas the
824 daytime boundary layer is higher which favors injection of surface emissions into the

825 troposphere, the preferential enrichment in CH_4 relative to CO at HLE may tentatively be
826 attributed to fossil CH_4 emissions over gas extraction regions and transported eastwards by
827 westerlies (Harris et al., 2000; Tohjima et al., 1996).

828

829 At PON and PBL, the $\Delta CH_4/\Delta CO$ ratios are in general considerably higher than 0.3 for all
830 seasons, putting them in the range of ratios indicative of urban/industrial sources (Table S11;
831 Harriss et al., 1994; Sawa et al., 2004; Xiao et al., 2004; Bakwin et al., 1995; Lai et al., 2010;
832 Wada et al., 2011; Niwa et al., 2014). However, this does not rule out contributions from
833 biomass/biofuel burning with emissions having a typical $\Delta CH_4/\Delta CO$ ratio less than 0.3
834 (Mauzerall et al., 1998; Andreae and Merlet, 2001; Mühle et al., 2002). Considering that
835 biofuel and agriculture waste burning are the primary energy sources in rural India (Streets et
836 al., 2003a; Yevich and Logan, 2003; Venkataraman et al., 2005), CO emissions from biofuel
837 burning must be substantial (Lelieveld et al., 2001). This is the case for NE India located
838 upwind of PON and PBL when the NE monsoon prevails during December–March.
839 Nevertheless, the relatively low $\Delta CH_4/\Delta CO$ derived from biomass/biofuel burning could be
840 increased by CH_4 emissions from livestock with similarly distributed sources (EDGAR v4.2).
841 Emissions of both trace gases from livestock and biomass/biofuel burning in the Indian
842 subcontinent compiled by EDGAR v4.2 also indicate a CH_4 to CO ratio of 0.64–0.69 over the
843 period of 2000–2008, close to the atmospheric measurements of $\Delta CH_4/\Delta CO$ at PON and PBL
844 during JFM (Fig. 14h and l).

845

846 **3.2.2 $\Delta CH_4/\Delta CO_2$**

847 The $\Delta CH_4/\Delta CO_2$ ratios are strongly influenced by the high variability of CO_2 and the
848 interpretation is complex. Unlike the positive correlation between CH_4 and CO consistently

observed at all three stations, the relationships between CH_4 and CO_2 residuals exhibit scattered and differences in the residual slopes for different stations and seasons (Fig. 15). At HLE, no significant correlations are found during AMJ, JAS, and OND (Fig. 15a–c), because CH_4 and CO_2 have distinct biogenic and/or photochemical sources and sinks over the northern mid-latitudes. During JFM when biogenic CO_2 fluxes and anthropogenic emissions are positive to the atmosphere, there is a significant and positive relationship between CH_4 and CO_2, with a $\Delta CH_4/\Delta CO_2$ ratio of 45.6±1846.8 ppb ppm^{-1} (r=0.37, p=0.03; Fig. 15d). This value is close to the ratio of CH_4 and CO_2 anthropogenic emissions over North Africa (39.1–46.2 mmol mol^{-1}), Central Asia (44.4–49.5 mmol mol^{-1}) and to a lesser degree the Middle East (25.8–28.4 mmol mol^{-1}) during the period of 2000–2010 (EDGAR v4.2), corresponding to the back-trajectories reaching HLE (Fig. 1a). It should be noted that this estimate of $\Delta CH_4/\Delta CO_2$ is subject to large uncertainty according to the standard deviation calculated with 1000 bootstrap replications (Fig. 15d), implying that CH_4 and CO_2 sources of various types and origins influence the HLE records.

At PON, in contrast to HLE, positive correlations occur between CH_4 and CO_2 residuals for all seasons except OND, with a $\Delta CH_4/\Delta CO_2$ ratio of 6.7±2.4 ppb ppm^{-1} (r=0.72, p<0.001) in AMJ and 8.5±0.9 ppb ppm^{-1} in JAS (r=0.74, p<0.001), respectively (Fig. 15e and f). The relatively narrow ranges of slopes compared to that for HLE and PBL likely suggest co-located urban and industrial sources in South India upwind of PON during April–September (see back-trajectories in Fig. 1a). Emissions from biofuel burning could be a common source for both CH_4 and CO_2, given the substantial biofuel use in South India (Yevich and Logan, 2003) and the biofuel burning emission ratio of CH_4 and CO_2 derived from previous studies (5–10 mmol mol^{-1}; Andreae and Merlet, 2001). Note that the CARIBIC flask measurements over India south of 20°N indicate a negative correlation between CH_4 and CO_2 at the altitudes

of 10-12 km during July–September, 2008 (r=-0.80, p=0.002; Fig. S14a), interpreted as the concurrent strong uptake of CO_2 with enhanced emissions of CH_4 during the SW monsoon. During JFM when the NE monsoon predominates, CH_4 is positively correlated with CO_2 with a $\Delta CH_4/\Delta CO_2$ ratio of 31.9±1635.7 ppb ppm^{-1} (r=0.45, p=0.02; Fig. 15h). Like at HLE, this ratio is subject to large uncertainty due to variability in CH_4 and CO_2 sources. The ratio based on the CARIBIC observations in the upper troposphere (10-12 km) is 23.5±41.4 ppb ppm^{-1} (r=0.67, p=0.004; Fig. S14b). The inconsistency of the $\Delta CH_4/\Delta CO_2$ ratios estimated from the two datasets suggest that the flask measurements at the surface station PON do provide information more specific for constraining estimates of regional CH_4 and CO_2 fluxes.

Finally, at PBL, the prominent feature of the CH_4–CO_2 relationship is the significant and negative correlation observed during JAS, with a $\Delta CH_4/\Delta CO_2$ ratio of -14.6±16.4 ppb ppm^{-1} (r=-0.73, p=0.007; Fig. 15j). Since the time series of flask measurements at PBL is relatively short and has large data gaps (Fig. S2), correlations between trace gases could be influenced by abnormal pollution events. For example, excluding the event with CH_4 residuals > +20 ppb (corresponding to the observation at PBL on 16 September 2009, the point marked with black circle in Fig. 15j) would substantially decrease the strength of negative correlation between CH_4 and CO_2 (r=-0.54, p=0.09). We will investigate the CH_4 enriched event further in Sect. 3.3.

3.2.3 $\Delta CO/\Delta CO_2$

As shown in Fig. 16, at HLE, CO is positively correlated with CO_2 during AMJ, with a $\Delta CO/\Delta CO_2$ ratio of 35.8±12.1 ppb ppm^{-1} (r=0.53, p=0.001; Fig. 16a). During JFM, there is no significant relationship between CO and CO_2 (r=0.15, p=0.39; Fig. 16d). However,

898 excluding an abnormal event with ΔCO_2 = -1.8 ppm on 8 January 2007 (the point marked
899 with black circle in Fig. 16d) would give a significant and positive correlation between CO
900 and CO_2, with a $\Delta CO/\Delta CO_2$ ratio of 55.7±259.1 ppb ppm^{-1} (r=0.40, p=0.02; the red solid line
901 in Fig. 16d). This ratio is less than half the emission ratio of CO to CO_2 from forest/grassland
902 biomass burning (Mauzerall et al., 1998; Andreae and Merlet, 2001), but higher than ratios of
903 anthropogenic combustion sources in developed countries that are typically in the range of
904 10–15 ppb ppm^{-1} (e.g., Suntharalingam et al., 2004; Wada et al., 2011; Takegawa et al., 2004).
905 This could be attributed not only to the lower combustion efficiency of fuels in North Africa,
906 the Middle East, and Central Asia where air masses at HLE originate from, but also to
907 additional contribution from biofuel burning with relatively high CO to CO_2 emission ratios
908 (e.g., fuelwood, charcoal, agricultural residuals; Andreae and Merlet, 2001). Besides, the
909 relatively high $\Delta CO/\Delta CO_2$ in JFM compared to AMJ may further indicate a contribution of
910 CO emissions from residential biofuel burning in winter (Wada et al., 2011), especially in
911 developing countries within the footprint area.

912

913 At PON, a positive and significant correlation between CO and CO_2 is found during AMJ,
914 with a $\Delta CO/\Delta CO_2$ ratio of 13.4±76.8 ppb ppm^{-1} (r=0.46, p=0.03; Fig. 16e). This ratio is
915 similar to the ratios determined for air masses influenced by both fossil fuel emissions and
916 biomass/biofuel burning during the same seasons. For example, based on the in-situ
917 measurements in the upper troposphere during the CARIBIC flights between South China
918 and Philippines in April 2007, Lai et al. (2010) reported the $\Delta CO/\Delta CO_2$ ratios of 15.6–29.3
919 ppb ppm^{-1} during pollution events influenced by both biomass/biofuel burning and fossil fuel
920 combustion in Indochinese Peninsula. At PBL, CO is significantly and negatively correlated
921 with CO_2 during JAS (r=-0.68, p=0.01; Fig. 16j). However, we note that the CH_4 abnormal
922 event discussed in Sect. 3.2.2 is enriched in CO as well, and the negative relationship

between CO and CO_2 would no longer exist if we removed the event (r=-0.45, p=0.16). The simultaneous enhancement of CO and CH_4 may suggest possible influences of biomass burning episodes, which we will explore in detail in Sect. 3.3. During JFM, no significant relationship is found between CO and CO_2 for PON or PBL (Fig. 16h and l).

3.3 Elevated CH_4 and CO events at PBL

In this section, we discuss two elevated CH_4 and CO events at PBL during the SW monsoon season. Significant enhancements of CH_4 and CO were observed on September 16, 2009 (July 29, 2011), with residuals from smoothed curves as high as 34.2 (29.2) ppb and 36.2 (17.9) ppb for CH_4 and CO, respectively. We further analyzed CH_4 and CO measurements at Bukit Kototabang (BKT – 0.20 °S, 100.32 °E, 845.00 m a.s.l.), Indonesia, located upwind of PBL when the southwest monsoon prevails. The flask measurements at BKT detected enhanced CH_4 and CO with a magnitude of 38.0 and 66.1 ppb on September 8, 2009, about one week before the occurrence of the first CH_4 and CO event at PBL (Fig. 17a). The in-situ measurements at BKT also showed CH_4 and CO enhancements about one week before the second event at PBL, lasting over the period of 17 July–21 July 2011 (Fig. 17b). The coincidence of the two abnormal CH_4 and CO events at PBL and BKT possibly suggests influences of polluted air masses with common sources and origins. Moreover, the fire radiative power (FRP, mWm^{-2}) during the sampling dates implies that the two abnormal CH_4 and CO events could be related to fire emissions in Indonesia (GFAS product version 1.0; Kaiser et al. 2012; Fig. S15). Note that the mechanisms we propose for the abnormal CH_4 and CO events and the possible linkage between PBL and BKT during the SW monsoon season are still speculative. Model experiments are needed to further confirm these hypotheses.

4 Conclusions

In this paper we present the results of flask measurements of CO_2, CH_4, N_2O, SF_6, CO, and H_2 at three stations in India: Hanle (HLE), Pondicherry (PON) and Port-Blair (PBL), over the period of 2007–2011. Of these three stations, HLE is located at a high altitude and regarded as a continental background station in the mid-latitude of the Northern Hemisphere; PON is a tropical surface station located on the southwest coast of India, while PBL is an oceanic station located on the Andaman Islands, of similar latitude to PON. With a total of 188, 185, and 63 flask pair samples collected respectively from HLE, PON and PBL between 2007 and 2011 (for PBL between 2009 and 2011), and analyzed at LSCE, the program represents an important logistical and analytical effort to produce a unique dataset of atmospheric trace gas observations over the Indian subcontinent. The observed records will serve as an important source of information to infer regional patterns of trace gas fluxes and atmospheric transport in this under-documented region. Several conclusions and implications are drawn from the first analyses of the datasets.

The annual gradients of the atmospheric mole fractions observed at PON and PBL, with respect to HLE as a reference, suggest significant emission sources of CO_2, CH_4, N_2O, CO, and H_2 over the footprints of those stations, whereas SF_6 emission sources are weak. In particular, the annual mean N_2O mole fractions at PON and PBL are higher than at HLE by 3.1±0.3 and 3.8±1.7 ppb, notably larger than the typical N_2O gradients observed between stations in Europe or North America, indicating substantial N_2O emissions. The analyses of the atmospheric mole fractions with back-trajectories at the three stations further confirmed emission sources from South and NE India, and SE Asia, all of which are populous with high demand for food and energy, and thus high emissions from industrial, residential, and/or agricultural sectors.

The seasonal cycles for each trace gas reflect not only the seasonal variations of natural sources/sinks and anthropogenic emissions over the Indian subcontinent, but also the seasonally varying atmospheric transport, especially the monsoon circulations (including convection). Strong influences of the monsoon circulations are well depicted by the contrasting phases of CH_4 seasonal cycles between HLE and PON/PBL. At HLE, the distinct CH_4 maximum during June-September is likely related to the enhanced biogenic CH_4 emissions from wetlands and rice paddies in summer, combined with deep convection associated with the SW monsoon that mixes surface emissions into the mid-to-upper troposphere. By contrast, the CH_4 seasonal cycles at PON and PBL have seasonal minima during the SW monsoon season, reflecting influences of southern hemispheric air depleted in CH_4 transported at low altitudes, as well as high rates of OH oxidation. Covariance between species variations at the synoptic scale further helps identification and attribution of different sources and sinks, like fossil fuel combustion, biofuel burning and biogenic emissions. Besides, measurements of $\delta^{13}C$-CO_2 have been recently started for HLE, and the 4-D distributions of CO_2 and CH_4 have been realistically simulated using a chemical transport model (LMDz-OR-INCA, Hauglustaine et al., 2004; Folberth et al., 2006) with zoom over South and East Asia (manuscript in preparation). Both of them may serve as valuable tools to disentangle and quantify contributions of different sources and meteorology to trace gas signals.

Apart from the flask measurements of trace gases presented in this study for the three stations, in-situ continuous measurements of CO_2 and CH_4 have also been deployed at HLE, PON and PBL in parallel, which would considerably contribute to the value of the stations through high-frequency air sampling. While the three stations have the potential to provide useful

constraints on estimates of trace gas fluxes over South and NE India (for example, Swathi et al. (2013) reported considerable reduction in the uncertainty of inverted CO_2 fluxes over temperate Eurasia by the inclusion of measurements at HLE), the monitoring network requires further expansion to sample air masses from other parts of the Indian subcontinent. Recently a few other atmospheric ground stations have been established in western India (Bhattacharya et al., 2009; Tiwari et al., 2011; Tiwari et al., 2014; Tiwari and Kumar, 2012) and the Himalayas (Kumar et al., 2010; Ganesan et al., 2013), with their concentration footprints covering Central India (e.g., the Sinhagad station; Tiwari et al., 2014; Tiwari and Kumar, 2012), the Indo-Gangetic Plains and a large extent of the Himalayas (e.g., the Dajeeling station; Ganesan et al., 2013). More efforts are needed to develop a comprehensive observation network with adequate spatial and temporal coverage in this region.

Acknowledgement

This study has been initiated within the framework of CaFICA-CEFIPRA project (2809-1). X. Lin acknowledges PhD funding support from AIRBUS D&S and ESF TTorch Short Visiting Grant for the 1st ICOS Science Conference (No. 6849). P. Ciais acknowledges support of the Synergy grant ERC-2013-SyG-610028 IMBALANCE-P of the European Research Council. The authors thank the engineers and staff from Indian Astronomical Observatory, Hanle, who have been helpful at the station in Hanle, and Mr. Manil Kumar, Mr. Shambhulinga and Mr. Prabhath Prabhu, who helped in flask sampling at Pondicherry University, Mr. B. Parmeshwar from National Institute of Ocean Technology for operating and maintaining the facilities in the stations. We also acknowledge the LSCE staff (L. Klenov, A. Crevier, B. Gal, C. Peureux, M. Grand, L. Hogrel, V. Bazantay and A. Orgun) taking in charge the RAMCES network logistics, measurements, and data processing.

References

Attri, S. D., and Tyagi, A.: Climate Profile of India: Contribution to the Indian Network of Climate Change Assessment (NATIONAL COMMUNICATION-II) Minitry of Environment and Forests, Met Monograph No. Environment Meteorology-01/2010, India Meteorological Department, Ministry of Earth Sciences, New Delhi, 2010.

Andreae, M. O., and Merlet, P.: Emission of trace gases and aerosols from biomass burning, Global Biogeochem. Cy., 15, 955-966, 10.1029/2000gb001382, 2001.

Babu, S. S., Chaubey, J. P., Krishna Moorthy, K., Gogoi, M. M., Kompalli, S. K., Sreekanth, V., Bagare, S. P., Bhatt, B. C., Gaur, V. K., Prabhu, T. P., and Singh, N. S.: High altitude (4520 m amsl) measurements of black carbon aerosols over western trans-Himalayas: Seasonal heterogeneity and source apportionment, J. Geophys. Res.-Atmos., 116, D24201, 10.1029/2011jd016722, 2011.

Baker, A. K., Schuck, T. J., Brenninkmeijer, C. A. M., Rauthe-Schöch, A., Slemr, F., van Velthoven, P. F. J., and Lelieveld, J.: Estimating the contribution of monsoon-related biogenic production to methane emissions from South Asia using CARIBIC observations, Geophys. Res. Lett., 39, L10813, 10.1029/2012gl051756, 2012.

Bakwin, P. S., Tans, P. P., Zhao, C., Ussler, W., and Quesnell, E.: Measurements of carbon dioxide on a very tall tower, Tellus B, 47, 535-549, 10.1034/j.1600-0889.47.issue5.2.x, 1995.

Bakwin, P. S., Tans, P. P., Hurst, D. F., and Zhao, C.: Measurements of carbon dioxide on very tall towers: results of the NOAA/CMDL program, Tellus B, 50B, 401-415, 1998.

Bange, H. W., Andreae, M. O., Lal, S., Law, C. S., Naqvi, S. W. A., Patra, P. K., Rixen, T., and Upstill-Goddard, R. C.: Nitrous oxide emissions from the Arabian Sea: A synthesis, Atmos. Chem. Phys., 1, 61-71, 10.5194/acp-1-61-2001, 2001.

Bhattacharya, S. K., Borole, D. V., Francey, R. J., Allison, C. E., Steele, L. P., Krummel, P. B., Langenfelds, R., Masarie, K. A., Tiwari, Y. K., and Patra, P. K.: Trace gases and CO_2 isotope records from Cabo de Rama, India, Curr. Sci., 97, 1336-1344, 2009.

Bond, S. W., Vollmer, M. K., Steinbacher, M., Henne, S., and Reimann, S.: Atmospheric molecular hydrogen (H_2): observations at the high-altitude site Jungfraujoch, Switzerland, Tellus B, 63, 64-76, 10.1111/j.1600-0889.2010.00509.x, 2011.

Bousquet, P., Yver, C., Pison, I., Li, Y. S., Fortems, A., Hauglustaine, D., Szopa, S., Rayner, P. J., Novelli, P., Langenfelds, R., Steele, P., Ramonet, M., Schmidt, M., Foster, P., Morfopoulos, C., and Ciais, P.: A three-dimensional synthesis inversion of the molecular hydrogen cycle: Sources and sinks budget and implications for the soil uptake, J. Geophys. Res.-Atmos., 116, D01302, 10.1029/2010jd014599, 2011.

Busenberg, E. and Plummer, L. N.: Dating young groundwater with sulfur hexafluoride: Natural and anthropogenic sources of sulfur hexafluoride, Water Resour. Res., 36(10), 3011–3030, doi:10.1029/2000WR900151, 2000.

Chi, X., Winderlich, J., Mayer, J. C., Panov, A. V., Heimann, M., Birmili, W., Heintzenberg, J., Cheng, Y., and Andreae, M. O.: Long-term measurements of aerosol and carbon monoxide at the ZOTTO tall tower to characterize polluted and pristine air in the Siberian taiga, Atmos. Chem. Phys., 13, 12271-12298, 10.5194/acp-13-12271-2013, 2013.

Dlugokencky, E. J., Myers, R. C., Lang, P. M., Masarie, K. A., Crotwell, A. M., Thoning, K. W., Hall, B. D., Elkins, J. W., and Steele, L. P.: Conversion of NOAA atmospheric dry air CH_4 mole fractions to a gravimetrically prepared standard scale, J. Geophys. Res.-Atmos., 110, D18306, 10.1029/2005jd006035, 2005.

Dlugokencky, E.J., P.M. Lang, A.M. Crotwell, K.A. Masarie, and Crotwell, M. J.: Atmospheric Methane Dry Air Mole Fractions from the NOAA ESRL Carbon Cycle Cooperative Global Air Sampling Network, 1983-2013, Version: 2014-06-24, Path: ftp://aftp.cmdl.noaa.gov/data/trace_gases/ch4/flask/surface/ (last access: 11 December 2014), 2014a.

Dlugokencky, E.J., P.M. Lang, K.A. Masarie, A.M. Crotwell, and Crotwell, M.J.: Atmospheric Carbon Dioxide Dry Air Mole Fractions from the NOAA ESRL Carbon Cycle Cooperative Global Air Sampling Network, 1968-2013, Version: 2014-06-27, Path: ftp://aftp.cmdl.noaa.gov/data/trace_gases/co2/flask/surface/ (last access: 11 December 2014), 2014b.

Draxler, R. R., and Rolph, G. D.: HYSPLIT (HYbrid Single-Particle Lagrangian Integrated Trajectory), Model access via NOAA ARL READY website http://www.arl.noaa.gov/ready/hysplit4.html (last access: 9 January 2014), NOAA Air Resources Laboratory, Silver Spring, MD, 2003.

Duncan, B. N., Martin, R. V., Staudt, A. C., Yevich, R., and Logan, J. A.: Interannual and seasonal variability of biomass burning emissions constrained by satellite observations, , J. Geophys. Res.-Atmos., 108, 4100, 10.1029/2002jd002378, 2003.

EC-JRC/PBL (European Commission, Joint Research Centre/Netherlands Environmental Assessment Agency): Emission Database for Global Atmospheric Research (EDGAR), release version 4.2: available at: http://edgar.jrc.ec.europa.eu (last access: 16 August 2014), 2011

Ehhalt, D. H., and Rohrer, F.: The tropospheric cycle of H_2: a critical review, Tellus B, 61, 500-535, 10.1111/j.1600-0889.2009.00416.x, 2009.

Fang, S.-X., Zhou, L.-X., Masarie, K. A., Xu, L. and Rella, C. W.: Study of atmospheric CH_4 mole fractions at three WMO/GAW stations in China, J. Geophys. Res.-Atmos., 118(10), 4874–4886, doi:10.1002/jgrd.50284, 2013.

Fang, S. X., Zhou, L. X., Tans, P. P., Ciais, P., Steinbacher, M., Xu, L., and Luan, T.: In situ measurement of atmospheric CO_2 at the four WMO/GAW stations in China, Atmos. Chem. Phys., 14, 2541-2554, 10.5194/acp-14-2541-2014, 2014.

Folberth, G. A., Hauglustaine, D. A., Lathière, J. and Brocheton, F.: Interactive chemistry in the Laboratoire de Météorologie Dynamique general circulation model: model description and impact analysis of biogenic hydrocarbons on tropospheric chemistry, Atmos. Chem. Phys., 6(8), 2273–2319, doi:10.5194/acp-6-2273-2006, 2006.

Gadgil, S.: The Indian Monsoon and its variability, Annu. Rev. Earth Planet Sci., 31, 429-467, 10.1146/annurev.earth.31.100901.141251, 2003.

Gamnitzer, U., Karstens, U., Kromer, B., Neubert, R. E. M., Meijer, H. A. J., Schroeder, H., and Levin, I.: Carbon monoxide: A quantitative tracer for fossil fuel CO_2?, J. Geophys. Res.-Atmos., 111, D22302, 10.1029/2005jd006966, 2006.

Ganesan, A. L., Chatterjee, A., Prinn, R. G., Harth, C. M., Salameh, P. K., Manning, A. J., Hall, B. D., Mühle, J., Meredith, L. K., Weiss, R. F., O'Doherty, S., and Young, D.: The variability of methane, nitrous oxide and sulfur hexafluoride in Northeast India, Atmos. Chem. Phys., 13, 10633-10644, 10.5194/acp-13-10633-2013, 2013.

Garg, A., Shukla, P. R., Kapshe, M., and Menon, D.: Indian methane and nitrous oxide emissions and mitigation flexibility, Atmos. Environ., 38, 1965-1977, http://dx.doi.org/10.1016/j.atmosenv.2003.12.032, 2004.

Garg, A., Shukla, P. R., and Upadhyay, J.: N_2O emissions of India: an assessment of temporal, regional and sector trends, Clim. Change, 110, 755-782, 10.1007/s10584-011-0094-9, 2012.

Goswami, B. N.: South Asian Monsoon, in: Intraseasonal variability in the Atmosphere-Ocean Climate System, edited by: Lau, W. K. M., and Waliser, D. E., Springer & Praxis Publishing, Chichester, UK, 2005.

Granier, C., Bessagnet, B., Bond, T., D'Angiola, A., Denier van der Gon, H., Frost, G., Heil, A., Kaiser, J., Kinne, S., Klimont, Z., Kloster, S., Lamarque, J.-F., Liousse, C., Masui, T., Meleux, F., Mieville, A., Ohara, T., Raut, J.-C., Riahi, K., Schultz, M., Smith, S., Thompson, A., van Aardenne, J., van der Werf, G. and van Vuuren, D.: Evolution of anthropogenic and biomass burning emissions of air pollutants at global and regional scales during the 1980–2010 period, Clim. Change, 109(1-2), 163–190, doi:10.1007/s10584-011-0154-1, 2011.

Grant, A., Witham, C. S., Simmonds, P. G., Manning, A. J., and O'Doherty, S.: A 15 year record of high-frequency, in situ measurements of hydrogen at Mace Head, Ireland, Atmos. Chem. Phys., 10, 1203-1214, 10.5194/acp-10-1203-2010, 2010.

Hall, B. D., Dutton, G. S., and Elkins, J. W.: The NOAA nitrous oxide standard scale for atmospheric observations, J. Geophys. Res.-Atmos., 112, D09305, 10.1029/2006jd007954, 2007.

Harris, J. M., Dlugokencky, E. J., Oltmans, S. J., Tans, P. P., Conway, T. J., Novelli, P. C., Thoning, K. W., and Kahl, J. D. W.: An interpretation of trace gas correlations during Barrow, Alaska, winter dark periods, 1986–1997, J. Geophys. Res.-Atmos., 105, 17267-17278, 10.1029/2000jd900167, 2000.

Harriss, R. C., Sachse, G. W., Collins, J. E., Wade, L., Bartlett, K. B., Talbot, R. W., Browell, E. V., Barrie, L. A., Hill, G. F., and Burney, L. G.: Carbon monoxide and methane over Canada: July–August 1990, J. Geophys. Res.-Atmos., 99, 1659-1669, 10.1029/93jd01906, 1994.

Haszpra, L., Barcza, Z., Hidy, D., Szilágyi, I., Dlugokencky, E., and Tans, P.: Trends and temporal variations of major greenhouse gases at a rural site in Central Europe, Atmos. Environ., 42, 8707-8716, http://dx.doi.org/10.1016/j.atmosenv.2008.09.012, 2008.

Hauglustaine, D. A., and Ehhalt, D. H.: A three-dimensional model of molecular hydrogen in the troposphere, J. Geophys. Res.- Atmos., 107, 4330, 10.1029/2001jd001156, 2002.

Hauglustaine, D. A., Hourdin, F., Jourdain, L., Filiberti, M. A., Walters, S., Lamarque, J. F., and Holland, E. A.: Interactive chemistry in the Laboratoire de Météorologie Dynamique general circulation model: Description and background tropospheric chemistry evaluation, J. Geophys. Res.-Atmos., 109, D04314, 10.1029/2003jd003957, 2004.

Huang, J., Golombek, A., Prinn, R., Weiss, R., Fraser, P., Simmonds, P., Dlugokencky, E. J., Hall, B., Elkins, J., Steele, P., Langenfelds, R., Krummel, P., Dutton, G. and Porter, L.: Estimation of regional emissions of nitrous oxide from 1997 to 2005 using multinetwork measurements, a chemical transport model, and an inverse method, J. Geophys. Res.-Atmos., 113(D17), D17313, doi:10.1029/2007JD009381, 2008.

IPCC: Climate Change 2013: The Physical Science Basis. Contribution of Working Group I to the Fifth Assessment Report of the Intergovernmental Panel on Climate Change, Cambridge University Press, Cambridge, 2013.

IPCC: Climate Change 2014: Impacts, Adaptation, and Vulnerability. Part A: Global and Sectoral Aspects. Contribution of Working Group II to the Fifth Assessment Report of the Intergovernmental Panel on Climate Change [Field, C.B., V.R. Barros, D.J. Dokken, K.J. Mach, M.D. Mastrandrea, T.E. Bilir, M. Chatterjee, K.L. Ebi, Y.O. Estrada, R.C. Genova, B. Girma, E.S. Kissel, A.N. Levy, S. MacCracken, P.R. Mastrandrea, and L.L. White (eds.)], Cambridge University Press, Cambridge, United Kingdom and New York, NY, USA, 2014a.

IPCC: Climate Change 2014: Impacts, Adaptation, and Vulnerability. Part B: Regional Aspects. Contribution of Working Group II to the Fifth Assessment Report of the Intergovernmental Panel on Climate Change [Barros, V.R., C.B. Field, D.J. Dokken, M.D. Mastrandrea, K.J. Mach, T.E. Bilir, M. Chatterjee, K.L. Ebi, Y.O. Estrada, R.C. Genova, B. Girma, E.S. Kissel, A.N. Levy, S. MacCracken, P.R. Mastrandrea, and L.L. White (eds.)], Cambridge University Press, Cambridge, United Kingdom and New York, NY, USA, 2014b.

Jiang, J. H., Livesey, N. J., Su, H., Neary, L., McConnell, J. C., and Richards, N. A. D.: Connecting surface emissions, convective uplifting, and long-range transport of carbon monoxide in the upper troposphere: New observations from the Aura Microwave Limb Sounder, Geophys. Res. Lett., 34, L18812, 10.1029/2007gl030638, 2007a.

Jiang, X., Ku, W. L., Shia, R.-L., Li, Q., Elkins, J. W., Prinn, R. G., and Yung, Y. L.: Seasonal cycle of N_2O: Analysis of data, Global Biogeochemical Cycles, 21, GB1006, 10.1029/2006gb002691, 2007b.

Jordan, A., and Steinberg, B.: Calibration of atmospheric hydrogen measurements, Atmos. Meas. Tech., 4, 509-521, 10.5194/amt-4-509-2011, 2011.

Kaiser, J. W., Heil, A., Andreae, M. O., Benedetti, A., Chubarova, N., Jones, L., Morcrette, J. J., Razinger, M., Schultz, M. G., Suttie, M., and van der Werf, G. R.: Biomass burning emissions

estimated with a global fire assimilation system based on observed fire radiative power, Biogeosciences, 9, 527-554, 10.5194/bg-9-527-2012, 2012.

Kaplan, J. O., Folberth, G. and Hauglustaine, D. A.: Role of methane and biogenic volatile organic compound sources in late glacial and Holocene fluctuations of atmospheric methane concentrations, Global Biogeochem. Cycles, 20(2), GB2016, doi:10.1029/2005GB002590, 2006.

Kasischke, E. S., Hyer, E. J., Novelli, P. C., Bruhwiler, L. P., French, N. H. F., Sukhinin, A. I., Hewson, J. H., and Stocks, B. J.: Influences of boreal fire emissions on Northern Hemisphere atmospheric carbon and carbon monoxide, Global Biogeochem. Cy., 19, GB1012, 10.1029/2004gb002300, 2005.

King, A. W., Andres, R. J., Davis, K. J., Hafer, M., Hayes, D. J., Huntzinger, D. N., de Jong, B., Kurz, W. A., McGuire, A. D., Vargas, R., Wei, Y., West, T. O. and Woodall, C. W.: North America's net terrestrial CO_2 exchange with the atmosphere 1990–2009, Biogeosciences, 12(2), 399–414, doi:10.5194/bg-12-399-2015, 2015.

Konovalov, I. B., Berezin, E. V., Ciais, P., Broquet, G., Beekmann, M., Hadji-Lazaro, J., Clerbaux, C., Andreae, M. O., Kaiser, J. W., and Schulze, E. D.: Constraining CO_2 emissions from open biomass burning by satellite observations of co-emitted species: a method and its application to wildfires in Siberia, Atmos. Chem. Phys., 14, 10383-10410, 10.5194/acp-14-10383-2014, 2014.

Kumar, R., Naja, M., Venkataramani, S., and Wild, O.: Variations in surface ozone at Nainital: A high-altitude site in the central Himalayas, J. Geophys. Res.-Atmos., 115, D16302, 10.1029/2009jd013715, 2010.

Kurokawa, J., Ohara, T., Morikawa, T., Hanayama, S., Janssens-Maenhout, G., Fukui, T., Kawashima, K., and Akimoto, H.: Emissions of air pollutants and greenhouse gases over Asian regions during 2000–2008: Regional Emission inventory in ASia (REAS) version 2, Atmos. Chem. Phys., 13, 11019-11058, 10.5194/acp-13-11019-2013, 2013.

Lai, S. C., Baker, A. K., Schuck, T. J., van Velthoven, P., Oram, D. E., Zahn, A., Hermann, M., Weigelt, A., Slemr, F., Brenninkmeijer, C. A. M., and Ziereis, H.: Pollution events observed during CARIBIC flights in the upper troposphere between South China and the Philippines, Atmos. Chem. Phys., 10, 1649-1660, 10.5194/acp-10-1649-2010, 2010.

Lal, S., Chandra, N., Venkataramani, S.: A study of CO_2 and related trace gases using a laser based technique at an urban site in western India. Submitted to Curr. Sci., 2015.

Langenfelds, R. L., Francey, R. J., Pak, B. C., Steele, L. P., Lloyd, J., Trudinger, C. M., and Allison, C. E.: Interannual growth rate variations of atmospheric CO_2 and its $\delta^{13}C$, H_2, CH_4, and CO between 1992 and 1999 linked to biomass burning, Global Biogeochem. Cy., 16, 1048, 10.1029/2001gb001466, 2002.

Lawrence, M. G., and Lelieveld, J.: Atmospheric pollutant outflow from southern Asia: a review, Atmos. Chem. Phys., 10, 11017-11096, 10.5194/acp-10-11017-2010, 2010.

Lelieveld, J., Crutzen, P. J., Ramanathan, V., Andreae, M. O., Brenninkmeijer, C. A. M., Campos, T., Cass, G. R., Dickerson, R. R., Fischer, H., de Gouw, J. A., Hansel, A., Jefferson, A., Kley, D., de Laat, A. T. J., Lal, S., Lawrence, M. G., Lobert, J. M., Mayol-Bracero, O. L., Mitra, A. P., Novakov, T., Oltmans, S. J., Prather, K. A., Reiner, T., Rodhe, H., Scheeren, H. A., Sikka, D., and Williams, J.: The Indian Ocean Experiment: Widespread Air Pollution from South and Southeast Asia, Science, 291, 1031-1036, 2001.

Le Quéré, C., Moriarty, R., Andrew, R. M., Peters, G. P., Ciais, P., Friedlingstein, P., Jones, S. D., Sitch, S., Tans, P., Arneth, A., Boden, T. A., Bopp, L., Bozec, Y., Canadell, J. G., Chevallier, F., Cosca, C. E., Harris, I., Hoppema, M., Houghton, R. A., House, J. I., Jain, A. K., Johannessen, T., Kato, E., Keeling, R. F., Kitidis, V., Klein Goldewijk, K., Koven, C., Landa, C. S., Landschützer, P., Lenton, A., Lima, I. D., Marland, G. H., Mathis, J. T., Metzl, N., Nojiri, Y., Olsen, A., Ono, T., Peters, W., Pfeil, B., Poulter, B., Raupach, M. R., Regnier, P., Rödenbeck, C., Saito, S., Sailsbury, J. E., Schuster, U., Schwinger, J., Séférian, R., Segschneider, J., Steinhoff, T., Stocker, B. D., Sutton,

A. J., Takahashi, T., Tilbrook, B., van der Werf, G. R., Viovy, N., Wang, Y.-P., Wanninkhof, R., Wiltshire, A., and Zeng, N.: Global Carbon Budget 2014. Earth Syst. Sci. Data Discuss., doi:10.5194/essdd-7-521-2014, 2014

Levin, I., Ciais, P., Langenfelds, R., Schmidt, M., Ramonet, M., Sidorov, K., Tchebakova, N., Gloor, M., Heimann, M., Schulze, E. D., Vygodskaya, N. N., Shibistova, O., and Lloyd, J.: Three years of trace gas observations over the EuroSiberian domain derived from aircraft sampling — a concerted action, Tellus B, 54, 696-712, 10.1034/j.1600-0889.2002.01352.x, 2002.

Li, Q., Jiang, J. H., Wu, D. L., Read, W. G., Livesey, N. J., Waters, J. W., Zhang, Y., Wang, B., Filipiak, M. J., Davis, C. P., Turquety, S., Wu, S., Park, R. J., Yantosca, R. M., and Jacob, D. J.: Convective outflow of South Asian pollution: A global CTM simulation compared with EOS MLS observations, Geophys. Res. Lett., 32, L14826, 10.1029/2005gl022762, 2005.

Liao, T., Camp, C. D., and Yung, Y. L.: The seasonal cycle of N_2O, Geophys. Res. Lett., 31, L17108, 10.1029/2004gl020345, 2004.

Logan, J. A., Prather, M. J., Wofsy, S. C., and McElroy, M. B.: Tropospheric chemistry: A global perspective, J. Geophys. Res.-Oceans, 86, 7210-7254, 10.1029/JC086iC08p07210, 1981.

Lopez, M.: Estimation des émissions de gaz à effet de serre à différentes échelles en France à l'aide d'observations de haute précision, Ph.D, Université Paris-Sud, 2012.

Lopez, M., Schmidt, M., Ramonet, M., Bonne, J.-L., Colomb, A., Kazan, V., Laj, P., and Pichon, J.-M.: A gas chromatograph system for semi-continuous greenhouse gas measurements at Puy de Dôme station, Centeral France, Atmos. Meas. Tech. Discuss., 8(3), 3121–3170, doi:10.5194/amtd-8-3121-2015, 2015.

Luyssaert, S., Abril, G., Andres, R., Bastviken, D., Bellassen, V., Bergamaschi, P., Bousquet, P., Chevallier, F., Ciais, P., Corazza, M., Dechow, R., Erb, K.-H., Etiope, G., Fortems-Cheiney, A., Grassi, G., Hartmann, J., Jung, M., Lathière, J., Lohila, A., Mayorga, E., Moosdorf, N., Njakou, D. S., Otto, J., Papale, D., Peters, W., Peylin, P., Raymond, P., Rödenbeck, C., Saarnio, S., Schulze, E.-D., Szopa, S., Thompson, R., Verkerk, P. J., Vuichard, N., Wang, R., Wattenbach, M. and Zaehle, S.: The European land and inland water CO_2, CO, CH_4 and N_2O balance between 2001 and 2005, Biogeosciences, 9(8), 3357–3380, doi:10.5194/bg-9-3357-2012, 2012.

Machida, T., Matsueda, H., Sawa, Y., Nakagawa, Y., Hirotani, K., Kondo, N., Goto, K., Nakazawa, T., Ishikawa, K., and Ogawa, T.: Worldwide Measurements of Atmospheric CO_2 and Other Trace Gas Species Using Commercial Airlines, J. Atmos. Ocean. Tech., 25, 1744-1754, 10.1175/2008jtecha1082.1, 2008.

Maiss, M., Steele, L. P., Francey, R. J., Fraser, P. J., Langenfelds, R. L., Trivett, N. B. A., and Levin, I.: Sulfur hexafluoride—A powerful new atmospheric tracer, Atmos. Environ., 30, 1621-1629, http://dx.doi.org/10.1016/1352-2310(95)00425-4, 1996.

Matthews, E., Fung, I. and Lerner, J.: Methane emission from rice cultivation: Geographic and seasonal distribution of cultivated areas and emissions, Global Biogeochem. Cycles, 5(1), 3–24, doi:10.1029/90GB02311, 1991.

Mauzerall, D. L., Logan, J. A., Jacob, D. J., Anderson, B. E., Blake, D. R., Bradshaw, J. D., Heikes, B., Sachse, G. W., Singh, H., and Talbot, B.: Photochemistry in biomass burning plumes and implications for tropospheric ozone over the tropical South Atlantic, J. Geophys. Res.-Atmos., 103, 8401-8423, 10.1029/97jd02612, 1998.

Messager, C.: Estimation des flux de gaz à effet de serre à l'échelle régionale à partir de mesures atmosphériques, Université Paris 7 - Denis Diderot, 2007.

Minschwaner, K., Salawitch, R. J., and McElroy, M. B.: Absorption of solar radiation by O_2: Implications for O_3 and lifetimes of N_2O, $CFCl_3$, and CF_2Cl_2, J. Geophys. Res.-Atmos., 98, 10543-10561, 10.1029/93jd00223, 1993.

Montzka, S. A., Dlugokencky, E. J., and Butler, J. H.: Non-CO_2 greenhouse gases and climate change, Nature, 476, 43-50, 2011.

Moorthy, K. K., Sreekanth, V., Chaubey, J. P., Gogoi, M. M., Babu, S. S., Kompalli, S. K., Bagare, S. P., Bhatt, B. C., Gaur, V. K., Prabhu, T. P., Singh, N. S.: Fine and ultrafine particles at near-free

tropospheric environment over the high-altitude station Hanle in the Trans-Himalaya: New particle formation and size distribution, J. Geophys. Res.-Atmos., 116, D20212, doi: 10.1029/2011JD016343, 2011

Morgan, C. G., Allen, M., Liang, M. C., Shia, R. L., Blake, G. A., and Yung, Y. L.: Isotopic fractionation of nitrous oxide in the stratosphere: Comparison between model and observations, J. Geophys. Res.-Atmos., 109, D04305, 10.1029/2003jd003402, 2004.

Morris, R. A., Miller, T. M., Viggiano, A. A., Paulson, J. F., Solomon, S., and Reid, G.: Effects of electron and ion reactions on atmospheric lifetimes of fully fluorinated compounds, J. Geophys. Res.-Atmos., 100, 1287-1294, 10.1029/94jd02399, 1995.

Mühle, J., Brenninkmeijer, C. A. M., Rhee, T. S., Slemr, F., Oram, D. E., Penkett, S. A., and Zahn, A.: Biomass burning and fossil fuel signatures in the upper troposphere observed during a CARIBIC flight from Namibia to Germany, Geophys. Res. Lett., 29, 1910, 10.1029/2002gl015764, 2002.

Niwa, Y., Machida, T., Sawa, Y., Matsueda, H., Schuck, T. J., Brenninkmeijer, C. A. M., Imasu, R., and Satoh, M.: Imposing strong constraints on tropical terrestrial CO_2 fluxes using passenger aircraft based measurements, J. Geophys. Res.-Atmos., 117, D11303, 10.1029/2012jd017474, 2012.

Niwa, Y., Tsuboi, K., Matsueda, H., Sawa, Y., Machida, T., Nakamura, M., Kawasato, T., Saito, K., Takatsuji, S., Tsuji, K., Nishi, H., Dehara, K., Baba, Y., Kuboike, D., Iwatsubo, S., Ohmori, H., and Hanamiya, Y.: Seasonal Variations of CO_2, CH_4, N_2O and CO in the Mid-Troposphere over the Western North Pacific Observed Using a C-130H Cargo Aircraft, J. Meteor. Soc. Japan. Ser. II, 92, 55-70, 10.2151/jmsj.2014-104, 2014.

Novelli, P. C., Steele, L. P., and Tans, P. P.: Mixing ratios of carbon monoxide in the troposphere, J. Geophys. Res.-Atmos., 97, 20731-20750, 10.1029/92jd02010, 1992.

Novelli, P. C., Masarie, K. A., and Lang, P. M.: Distributions and recent changes of carbon monoxide in the lower troposphere, J. Geophys. Res.-Atmos., 103, 19015-19033, 10.1029/98jd01366, 1998.

Novelli, P. C., Lang, P. M., Masarie, K. A., Hurst, D. F., Myers, R., and Elkins, J. W.: Molecular hydrogen in the troposphere: Global distribution and budget, J. Geophys. Res.-Atmos., 104, 30427-30444, 10.1029/1999jd900788, 1999.

Novelli, P. C., Lang, P. M., and Masarie, K. A.: Atmospheric Hydrogen Dry Air Mole Fractions from the NOAA ESRL Carbon Cycle Cooperative Global Air Sampling Network, 1988-2009, Version: 2014-08-27, Path: ftp://aftp.cmdl.noaa.gov/data/trace_gases/h2/flask/surface/ (last access: 11 December 2014), 2014a.

Novelli, P.C. and Masarie, K.A.: Atmospheric Carbon Monoxide Dry Air Mole Fractions from the NOAA ESRL Carbon Cycle Cooperative Global Air Sampling Network, 1988-2013, Version: 2014-07-02, Path: ftp://aftp.cmdl.noaa.gov/data/trace_gases/co/flask/surface/ (last access: 11 December 2014), 2014b.

Olivier, J. G. J., Van Aardenne, J. A., Dentener, F., Ganzeveld, L. and Peters, J. A. H. W.: Recent trends in global greenhouse gas emissions: regional trends and spatial distribution of key sources, in Non-CO_2 Greenhouse Gases (NCGG-4), edited by A. Van Amstel, pp. 325–330, Millpress, Rotterdam, The Netherlands., 2005.

Paris, J. D., Ciais, P., NÉDÉLec, P., Ramonet, M., Belan, B. D., Arshinov, M. Y., Golitsyn, G. S., Granberg, I., Stohl, A., Cayez, G., Athier, G., Boumard, F., and Cousin, J. M.: The YAK-AEROSIB transcontinental aircraft campaigns: new insights on the transport of CO_2, CO and O_3 across Siberia, Tellus B, 60, 551-568, 10.1111/j.1600-0889.2008.00369.x, 2008.

Park, M., Randel, W. J., Gettelman, A., Massie, S. T., and Jiang, J. H.: Transport above the Asian summer monsoon anticyclone inferred from Aura Microwave Limb Sounder tracers, J. Geophys. Res.-Atmos., 112, D16309, 10.1029/2006jd008294, 2007.

Pathak, H., Bhatia, A., Jain, N., and Aggarwal, P. K.: Greenhouse Gas Emission and Mitigation in Indian Agriculture - A Review, in: ING Bulletins on Regional Assessment of Reactive Nitrogen, Bulletin No. 19, edited by: Singh, B., SCON-ING, New Delhi, i-iv & 1-34, 2010.

Patra, P., Takigawa, M., Ishijima, K., Choi, B.-C., Cunnold, D., J. Dlugokencky, E., Fraser, P., J. Gomez-Pelaez, A., Goo, T.-Y., Kim, J.-S., Krummel, P., Langenfelds, R., Meinhardt, F., Mukai, H., O'Doherty, S., Prinn, R. G., Simmonds, P., Steele, P., Tohjima, Y., Tsuboi, K., Uhse, K., Weiss, R., Worthy, D., and Nakazawa, T.: Growth Rate, Seasonal, Synoptic, Diurnal Variations and Budget of Methane in the Lower Atmosphere, J. Meteor. Soc. Japan. Ser. II, 87, 635-663, 2009.

Patra, P. K., Lal, S., Venkataramani, S., de Sousa, S. N., Sarma, V. V. S. S., and Sardesai, S.: Seasonal and spatial variability in N_2O distribution in the Arabian Sea, Deep Sea Res. Part I: Oceanogr Res. Pap., 46, 529-543, http://dx.doi.org/10.1016/S0967-0637(98)00071-5, 1999.

Patra, P. K., Houweling, S., Krol, M., Bousquet, P., Belikov, D., Bergmann, D., Bian, H., Cameron-Smith, P., Chipperfield, M. P., Corbin, K., Fortems-Cheiney, A., Fraser, A., Gloor, E., Hess, P., Ito, A., Kawa, S. R., Law, R. M., Loh, Z., Maksyutov, S., Meng, L., Palmer, P. I., Prinn, R. G., Rigby, M., Saito, R., and Wilson, C.: TransCom model simulations of CH_4 and related species: linking transport, surface flux and chemical loss with CH_4 variability in the troposphere and lower stratosphere, Atmos. Chem. Phys., 11, 12813-12837, 10.5194/acp-11-12813-2011, 2011a.

Patra, P. K., Niwa, Y., Schuck, T. J., Brenninkmeijer, C. A. M., Machida, T., Matsueda, H., and Sawa, Y.: Carbon balance of South Asia constrained by passenger aircraft CO_2 measurements, Atmos. Chem. Phys., 11, 4163-4175, 10.5194/acp-11-4163-2011, 2011b.

Patra, P. K., Canadell, J. G., Houghton, R. A., Piao, S. L., Oh, N. H., Ciais, P., Manjunath, K. R., Chhabra, A., Wang, T., Bhattacharya, T., Bousquet, P., Hartman, J., Ito, A., Mayorga, E., Niwa, Y., Raymond, P. A., Sarma, V. V. S. S., and Lasco, R.: The carbon budget of South Asia, Biogeosciences, 10, 513-527, 10.5194/bg-10-513-2013, 2013.

Peylin, P., Law, R. M., Gurney, K. R., Chevallier, F., Jacobson, A. R., Maki, T., Niwa, Y., Patra, P. K., Peters, W., Rayner, P. J., Rödenbeck, C., and Zhang, X.: Global atmospheric carbon budget: results from an ensemble of atmospheric CO_2 inversions, Biogeosciences Discuss., 10, 5301-5360, 10.5194/bgd-10-5301-2013, 2013.

Pison, I., Bousquet, P., Chevallier, F., Szopa, S., and Hauglustaine, D.: Multi-species inversion of CH_4, CO and H_2 emissions from surface measurements, Atmos. Chem. Phys., 9, 5281-5297, 10.5194/acp-9-5281-2009, 2009.

Press, W.H., Teukolsky, S.A., Vetterling, W.T., Flannery, B.P., 2007. Straight-Line Data with Errors in Both Coordinates, in: Numerical Recipes: The Art of Scientific Computing. Cambridge University Press, New York, pp. 785–788.

Price, H., Jaeglé, L., Rice, A., Quay, P., Novelli, P. C., and Gammon, R.: Global budget of molecular hydrogen and its deuterium content: Constraints from ground station, cruise, and aircraft observations, J. Geophys. Res.-Atmos., 112, D22108, 10.1029/2006jd008152, 2007.

R Core Team: R: A language and environment for statistical computing. R Foundation for Statistical computing, Vienna, Austria. Available from: http://www.r-project.org/, 2014.

Ramonet, M., Ciais, P., Nepomniachii, I., Sidorov, K., Neubert, R. E. M., Langendörfer, U., Picard, D., Kazan, V., Biraud, S., Gusti, M., Kolle, O., Schulze, E. D., and Lloyd, J.: Three years of aircraft-based trace gas measurements over the Fyodorovskoye southern taiga forest, 300 km north-west of Moscow, Tellus B, 54, 713-734, 10.1034/j.1600-0889.2002.01358.x, 2002.

Ravishankara, A. R., Daniel, J. S. and Portmann, R. W.: Nitrous oxide (N_2O): The dominant ozone-depleting substance emitted in the 21st century, Science, 326(5949), 123–125, doi:10.1126/science.1176985, 2009.

Ravishankara, A. R., Solomon, S., Turnipseed, A. A., and Warren, R. F.: Atmospheric lifetimes of long-lived halogenated species, Science, 259, 194-199, 1993.

Rayner, P. J., Law, R. M., Allison, C. E., Francey, R. J., Trudinger, C. M., and Pickett-Heaps, C.: Interannual variability of the global carbon cycle (1992–2005) inferred by inversion of

atmospheric CO_2 and $\delta^{13}CO_2$ measurements, Global Biogeochem. Cy., 22, GB3008, 10.1029/2007gb003068, 2008.

Rivier, L., Ciais, P., Hauglustaine, D. A., Bakwin, P., Bousquet, P., Peylin, P., and Klonecki, A.: Evaluation of SF_6, C_2Cl_4, and CO to approximate fossil fuel CO_2 in the Northern Hemisphere using a chemistry transport model, J. Geophys. Res.-Atmos., 111, D16311, 10.1029/2005jd006725, 2006.

Saikawa, E., Prinn, R. G., Dlugokencky, E., Ishijima, K., Dutton, G. S., Hall, B. D., Langenfelds, R., Tohjima, Y., Machida, T., Manizza, M., Rigby, M., O'Doherty, S., Patra, P. K., Harth, C. M., Weiss, R. F., Krummel, P. B., van der Schoot, M., Fraser, P. J., Steele, L. P., Aoki, S., Nakazawa, T., and Elkins, J. W.: Global and regional emissions estimates for N_2O, Atmos. Chem. Phys., 14, 4617-4641, 10.5194/acp-14-4617-2014, 2014.

Sawa, Y., Matsueda, H., Makino, Y., Inoue, H. Y., Murayama, S., Hirota, M., Tsutsumi, Y., Zaizen, Y., Ikegami, M., and Okada, K.: Aircraft Observation of CO_2, CO, O_3 and H_2 over the North Pacific during the PACE-7 Campaign, Tellus B, 56, 2-20, 10.1111/j.1600-0889.2004.00088.x, 2004.

Schuck, T. J., Brenninkmeijer, C. A. M., Baker, A. K., Slemr, F., von Velthoven, P. F. J., and Zahn, A.: Greenhouse gas relationships in the Indian summer monsoon plume measured by the CARIBIC passenger aircraft, Atmos. Chem. Phys., 10, 3965-3984, 10.5194/acp-10-3965-2010, 2010.

Schuck, T. J., Ishijima, K., Patra, P. K., Baker, A. K., Machida, T., Matsueda, H., Sawa, Y., Umezawa, T., Brenninkmeijer, C. A. M., and Lelieveld, J.: Distribution of methane in the tropical upper troposphere measured by CARIBIC and CONTRAIL aircraft, J. Geophys. Res.-Atmos., 117, D19304, 10.1029/2012jd018199, 2012.

Seinfeld, J. H. and Pandis, S. N.: Atmospheric Chemistry and Physics: From Air Pollution to Climate Change, John Wiley and Sons, Hoboken, New Jersey, USA., 2006.

Sivakumar, I., and Anitha, M.: Education and girl children in Puducherry region: Problems and perspective, Int. J. Soc. Sci. Interdiscipl. Res., 1, 175-184, 2012.

Streets, D. G., Bond, T. C., Carmichael, G. R., Fernandes, S. D., Fu, Q., He, D., Klimont, Z., Nelson, S. M., Tsai, N. Y., Wang, M. Q., Woo, J. H., and Yarber, K. F.: An inventory of gaseous and primary aerosol emissions in Asia in the year 2000, J. Geophys. Res.-Atmos., 108, 8809, 10.1029/2002jd003093, 2003a.

Streets, D. G., Yarber, K. F., Woo, J. H., and Carmichael, G. R.: Biomass burning in Asia: Annual and seasonal estimates and atmospheric emissions, Global Biogeochem. Cy., 17, 1099, 10.1029/2003gb002040, 2003b.

Suntharalingam, P., Jacob, D. J., Palmer, P. I., Logan, J. A., Yantosca, R. M., Xiao, Y., Evans, M. J., Streets, D. G., Vay, S. L., and Sachse, G. W.: Improved quantification of Chinese carbon fluxes using CO_2/CO correlations in Asian outflow, J. Geophys. Res.-Atmos., 109, D18S18, 10.1029/2003jd004362, 2004.

Swathi, P. S., Indira, N. K., Rayner, P. J., Ramonet, M., Jagadheesha, D., Bhatt, B. C., Gaur, V. K.: Robust inversion of carbon dioxide fluxes over temperate Eurasia in 2006-2008, Curr. Sci., 105, 201-208, 2013.

Takegawa, N., Kondo, Y., Koike, M., Chen, G., Machida, T., Watai, T., Blake, D. R., Streets, D. G., Woo, J. H., Carmichael, G. R., Kita, K., Miyazaki, Y., Shirai, T., Liley, J. B., and Ogawa, T.: Removal of NO_x and NO_y in Asian outflow plumes: Aircraft measurements over the western Pacific in January 2002, J. Geophys. Res.-Atmos., 109, D23S04, 10.1029/2004jd004866, 2004.

Teetor, P., 2011. Performing Simple Orthogonal Regression, in: Loukides, M. (Ed.), R Cookbook. O'Reilly Media, Sebastopol, pp. 340–341.

Thompson, R. L., Chevallier, F., Crotwell, A. M., Dutton, G., Langenfelds, R. L., Prinn, R. G., Weiss, R. F., Tohjima, Y., Nakazawa, T., Krummel, P. B., Steele, L. P., Fraser, P., O'Doherty, S., Ishijima, K., and Aoki, S.: Nitrous oxide emissions 1999 to 2009 from a global atmospheric inversion, Atmos. Chem. Phys., 14, 1801-1817, 10.5194/acp-14-1801-2014, 2014a.

Thompson, R. L., Ishijima, K., Saikawa, E., Corazza, M., Karstens, U., Patra, P. K., Bergamaschi, P., Chevallier, F., Dlugokencky, E., Prinn, R. G., Weiss, R. F., O'Doherty, S., Fraser, P. J., Steele, L. P., Krummel, P. B., Vermeulen, A., Tohjima, Y., Jordan, A., Haszpra, L., Steinbacher, M., Van der Laan, S., Aalto, T., Meinhardt, F., Popa, M. E., Moncrieff, J., and Bousquet, P.: TransCom N_2O model inter-comparison – Part 2: Atmospheric inversion estimates of N_2O emissions, Atmos. Chem. Phys., 14, 6177-6194, 10.5194/acp-14-6177-2014, 2014b.

Thompson, R. L., Patra, P. K., Ishijima, K., Saikawa, E., Corazza, M., Karstens, U., Wilson, C., Bergamaschi, P., Dlugokencky, E., Sweeney, C., Prinn, R. G., Weiss, R. F., O'Doherty, S., Fraser, P. J., Steele, L. P., Krummel, P. B., Saunois, M., Chipperfield, M., and Bousquet, P.: TransCom N_2O model inter-comparison – Part 1: Assessing the influence of transport and surface fluxes on tropospheric N_2O variability, Atmos. Chem. Phys., 14, 4349-4368, 10.5194/acp-14-4349-2014, 2014c.

Thoning, K. W., Tans, P. P., and Komhyr, W. D.: Atmospheric carbon dioxide at Mauna Loa Observatory: 2. Analysis of the NOAA GMCC data, 1974–1985, J. Geophys. Res.-Atmos., 94, 8549-8565, 10.1029/JD094iD06p08549, 1989.

Tiwari, Y. K., Patra, P. K., Chevallier, F., Francey, R. J., Krummel, P. B., Allison, C. E., Revadekar, J. V., Chakraborty, S., Langenfelds, R. L., Bhattacharya, S. K., Borole, D. V., Kumar, K. R., and Steele, L. P.: Carbon dioxide observations at Cape Rama, India for the period 1993-2002: implications for constraining Indian emissions, Curr. Sci., 101, 1562-1568, 2011.

Tiwari, Y. K., and Kumar, K. R.: GHG observation programs in India, in: Asian GAW greenhouse gases Newsletter, Volume No. 3, Korea Meteorological Administration, Chungnam, South Korea, 2012.

Tiwari, Y. K., Revadekar, J. V., and Ravi Kumar, K.: Variations in atmospheric Carbon Dioxide and its association with rainfall and vegetation over India, Atmos. Environ., 68, 45-51, http://dx.doi.org/10.1016/j.atmosenv.2012.11.040, 2013.

Tiwari, Y. K., Vellore, R. K., Ravi Kumar, K., van der Schoot, M., and Cho, C.-H.: Influence of monsoons on atmospheric CO_2 spatial variability and ground-based monitoring over India, Sci. Total Environ., 490, 570-578, http://dx.doi.org/10.1016/j.scitotenv.2014.05.045, 2014.

Tohjima, Y., Maksyutov, S., Machida, T., and Inoue, G.: Airborne measurements of atmospheric methane over oil fields in western Siberia, Geophys. Res. Lett., 23, 1621-1624, 10.1029/96gl01027, 1996.

Turnbull, J. C., Miller, J. B., Lehman, S. J., Tans, P. P., Sparks, R. J., and Southon, J.: Comparison of 14CO2, CO, and SF6 as tracers for recently added fossil fuel CO2 in the atmosphere and implications for biological CO_2 exchange, Geophys. Res. Lett., 33, L01817, 10.1029/2005gl024213, 2006.

Valsala, V., Tiwari, Y. K., Pillai, P., Roxy, M., Maksyutov, S., and Murtugudde, R.: Intraseasonal variability of terrestrial biospheric CO_2 fluxes over India during summer monsoons, J. Geophys. Res.-Biogeo., 118, 752-769, 10.1002/jgrg.20037, 2013.

van der Werf, G. R., Randerson, J. T., Giglio, L., Collatz, G. J., Kasibhatla, P. S., and Arellano Jr, A. F.: Interannual variability in global biomass burning emissions from 1997 to 2004, Atmos. Chem. Phys., 6, 3423-3441, 10.5194/acp-6-3423-2006, 2006.

van der Werf, G. R., Randerson, J. T., Giglio, L., Collatz, G. J., Mu, M., Kasibhatla, P. S., Morton, D. C., DeFries, R. S., Jin, Y., and van Leeuwen, T. T.: Global fire emissions and the contribution of deforestation, savanna, forest, agricultural, and peat fires (1997–2009), Atmos. Chem. Phys., 10, 11707-11735, 10.5194/acp-10-11707-2010, 2010.

Venkataraman, C., Habib, G., Eiguren-Fernandez, A., Miguel, A. H., and Friedlander, S. K.: Residential Biofuels in South Asia: Carbonaceous Aerosol Emissions and Climate Impacts, Science, 307, 1454-1456, 2005.

Volk, C. M., Elkins, J. W., Fahey, D. W., Dutton, G. S., Gilligan, J. M., Loewenstein, M., Podolske, J. R., Chan, K. R., and Gunson, M. R.: Evaluation of source gas lifetimes from stratospheric observations, J. Geophys. Res.-Atmos., 102, 25543-25564, 10.1029/97jd02215, 1997.

Wada, A., Matsueda, H., Sawa, Y., Tsuboi, K., and Okubo, S.: Seasonal variation of enhancement ratios of trace gases observed over 10 years in the western North Pacific, Atmos. Environ., 45, 2129-2137, http://dx.doi.org/10.1016/j.atmosenv.2011.01.043, 2011.

Wang, R., Tao, S., Ciais, P., Shen, H. Z., Huang, Y., Chen, H., Shen, G. F., Wang, B., Li, W., Zhang, Y. Y., Lu, Y., Zhu, D., Chen, Y. C., Liu, X. P., Wang, W. T., Wang, X. L., Liu, W. X., Li, B. G., and Piao, S. L.: High-resolution mapping of combustion processes and implications for CO_2 emissions, Atmos. Chem. Phys., 13, 5189-5203, 10.5194/acp-13-5189-2013, 2013.

Xiao, Y., Jacob, D. J., Wang, J. S., Logan, J. A., Palmer, P. I., Suntharalingam, P., Yantosca, R. M., Sachse, G. W., Blake, D. R., and Streets, D. G.: Constraints on Asian and European sources of methane from CH_4-C_2H_6-CO correlations in Asian outflow, J. Geophys. Res.-Atmos., 109, D15S16, 10.1029/2003jd004475, 2004.

Xiong, X., Houweling, S., Wei, J., Maddy, E., Sun, F., and Barnet, C.: Methane plume over south Asia during the monsoon season: satellite observation and model simulation, Atmos. Chem. Phys., 9, 783-794, 10.5194/acp-9-783-2009, 2009.

Yan, X., Cai, Z., Ohara, T., and Akimoto, H.: Methane emission from rice fields in mainland China: Amount and seasonal and spatial distribution, J. Geophys. Res.-Atmos., 108, 4505, 10.1029/2002jd003182, 2003.

Yashiro, H., Sudo, K., Yonemura, S., and Takigawa, M.: The impact of soil uptake on the global distribution of molecular hydrogen: chemical transport model simulation, Atmos. Chem. Phys., 11, 6701-6719, 10.5194/acp-11-6701-2011, 2011.

Yevich, R., and Logan, J. A.: An assessment of biofuel use and burning of agricultural waste in the developing world, Global Biogeochem. Cy., 17, 1095, 10.1029/2002gb001952, 2003.

Yver, C., Schmidt, M., Bousquet, P., Zahorowski, W., and Ramonet, M.: Estimation of the molecular hydrogen soil uptake and traffic emissions at a suburban site near Paris through hydrogen, carbon monoxide, and radon-222 semicontinuous measurements, J. Geophys. Res.-Atmos., 114, D18304, 10.1029/2009jd012122, 2009.

Yver, C.: Estimation des sources et puits du dihydrogène troposphérique - développements instrumentaux, mesures atmosphériques et assimilation variationnelle, Ph.D dissertation, Université de Versailles - Saint Quentin, 2010.

Yver, C. E., Pison, I. C., Fortems-Cheiney, A., Schmidt, M., Chevallier, F., Ramonet, M., Jordan, A., Søvde, O. A., Engel, A., Fisher, R. E., Lowry, D., Nisbet, E. G., Levin, I., Hammer, S., Necki, J., Bartyzel, J., Reimann, S., Vollmer, M. K., Steinbacher, M., Aalto, T., Maione, M., Arduini, J., O'Doherty, S., Grant, A., Sturges, W. T., Forster, G. L., Lunder, C. R., Privalov, V., Paramonova, N., Werner, A., and Bousquet, P.: A new estimation of the recent tropospheric molecular hydrogen budget using atmospheric observations and variational inversion, Atmos. Chem. Phys., 11, 3375-3392, 10.5194/acp-11-3375-2011, 2011.

Zhang, F., Zhou, L. X., Novelli, P. C., Worthy, D. E. J., Zellweger, C., Klausen, J., Ernst, M., Steinbacher, M., Cai, Y. X., Xu, L., Fang, S. X., and Yao, B.: Evaluation of in situ measurements of atmospheric carbon monoxide at Mount Waliguan, China, Atmos. Chem. Phys., 11, 5195-5206, 10.5194/acp-11-5195-2011, 2011.

Zhang, H. F., Chen, B. Z., Machida, T., Matsueda, H., Sawa, Y., Fukuyama, Y., Langenfelds, R., van der Schoot, M., Xu, G., Yan, J. W., Cheng, M. L., Zhou, L. X., Tans, P., and Peters, W.: Estimating Asian terrestrial carbon fluxes from CONTRAIL aircraft and surface CO_2 observations for the period 2006-2010, Atmos. Chem. Phys., 14, 5807-5824, 10.5194/acp-14-5807-2014, 2014.

Zhang, X. I. A., Nakazawa, T., Ishizawa, M., Aoki, S., Nakaoka, S.-I., Sugawara, S., Maksyutov, S., Saeki, T., and Hayasaka, T.: Temporal variations of atmospheric carbon dioxide in the southernmost part of Japan, Tellus B, 59, 654-663, 10.1111/j.1600-0889.2007.00288.x, 2007.

Zhao, C. L., and Tans, P. P.: Estimating uncertainty of the WMO mole fraction scale for carbon dioxide in air, J. Geophys. Res.-Atmos., 111, D08S09, 10.1029/2005jd006003, 2006.

Table

Table 1 Annual mean values, trend, and average peak-to-peak amplitudes of trace gases at HLE, PON, PBL and the two additional NOAA/ESRL stations – KZM and WLG. For each species at each station, the annual mean values and average peak-to-peak amplitude are calculated from the smoothed curve and mean seasonal cycle, respectively. The residual standard deviation (RSD) around the smoothed curve and the Julian days corresponding to the maximum (D_{max}) and minimum (D_{min}) of the mean seasonal cycle are given as well. Uncertainty of each estimate is calculated from 1 s.d. of 1000 bootstrap replicates.

	HLE	PON	PBL	KZM	WLG
CO_2 (ppm)					
Annual mean 2007	382.3±0.3	386.6±0.9	–	382.7±0.2	384.2±0.2
Annual mean 2008	384.6±0.5	388.1±0.9	–	385.7±0.2	386.0±0.2
Annual mean 2009	387.2±0.2	389.0±0.6	–	–	387.4±0.2
Annual mean 2010	389.4±0.1	391.3±1.5	387.6±0.7	–	390.1±0.2
Annual mean 2011	391.4±0.3	–	390.2±0.6	–	392.2±0.2
Trend (yr^{-1})	2.1±0.0	1.7±0.1	–	–	2.0±0.0
(Trend at MLO: 2.0±0.0)					
RSD	0.7	4.0	1.5	1.5	1.4
Amplitude	8.2±0.4	7.6±1.4	11.1±1.3	13.8±0.5	11.1±0.4
D_{max}	122.0±2.9	111.0±13.4	97.0±26.0	75.0±2.6	100.0±1.5
D_{min}	261.0±3.0	327.0±54.3	242.0±7.7	205.0±2.1	222.0±1.6
CH_4 (ppb)					
Annual mean 2007	1814.8±2.9	1859.2±6.7	–	1842.6±2.4	1841.0±1.8
Annual mean 2008	1833.1±5.4	1856.1±10.4	–	1856.6±2.3	1845.6±1.5
Annual mean 2009	1830.2±1.7	1865.7±5.1	–	–	1851.8±1.9
Annual mean 2010	1830.5±2.1	1876.9±9.1	1867.5±15.4	–	1857.6±1.4
Annual mean 2011	1849.5±5.2	–	1852.0±7.6	–	1859.9±1.2
Trend (yr^{-1})	4.9±0.0	9.4±0.1	–	–	5.3±0.0
(Trend at MLO: 6.2±0.0)					
RSD	9.1	34.4	22.4	14.6	12.3
Amplitude	28.9±4.2	124.1±10.2	143.9±12.4	22.7±4.7	17.5±2.2
D_{max}	219.0±4.6	337.0±6.1	345.0±87.6	236.0±43.2	222.0±6.2
D_{min}	97.0±58.9	189.0±10.7	193.0±13.5	338.0±39.0	340.0±96.6
N_2O (ppb)					
Annual mean 2007	322.2±0.1	324.8±0.3	–		
Annual mean 2008	322.9±0.1	326.3±0.3	–		
Annual mean 2009	323.5±0.1	326.7±0.3	–		
Annual mean 2010	324.0±0.1	327.1±0.5	329.0±0.5		
Annual mean 2011	325.2±0.1	–	327.9±0.3		

Trend (yr^{-1})	0.8±0.0	0.8±0.1	–		
(Trend at MLO: 1.0±0.0)					
RSD	0.3	1.4	1.1		
Amplitude	0.6±0.1	1.2±0.5	2.2±0.6		
D_{max}	227.0±11.8	262.0±83.2	313.0±42.6		
D_{min}	115.0±16.4	141.0±48.2	65.0±33.4		
SF_6 (ppt)					
Annual mean 2007	6.26±0.03	6.19±0.01	–		
Annual mean 2008	6.54±0.03	6.49±0.02	–		
Annual mean 2009	6.79±0.01	6.77±0.01	–		
Annual mean 2010	7.17±0.01	7.08±0.02	7.10±0.07		
Annual mean 2011	7.38±0.01	–	7.45±0.03		
Trend (yr^{-1})	0.29±0.05	0.31±0.05	–		
(Trend at MLO: 0.29±0.03)					
RSD	0.07	0.05	0.12		
Amplitude	0.15±0.03	0.24±0.02	0.48±0.07		
D_{max}	320.0±8.3	327.0±12.1	342.0±59.9		
D_{min}	211.0±65.1	204.0±3.3	210.0±18.1		
CO (ppb)					
Annual mean 2007	104.7±1.4	200.5±7.8	–	121.7±1.7	141.0±4.3
Annual mean 2008	103.1±2.1	175.3±13.1	–	123.7±1.7	129.0±2.9
Annual mean 2009	98.9±1.9	174.3±4.8	–	–	131.9±3.7
Annual mean 2010	99.0±1.2	185.1±8.7	157.6±20.4	–	130.2±3.9
Annual mean 2011	99.4±2.2	–	145.9±9.9	–	124.0±2.3
Trend (yr^{-1})	-2.2±0.0	0.4±0.1	–	–	-1.9±0.0
(Trend at MLO: -1.6±0.0)					
RSD	6.5	32.0	30.8	11.8	22.5
Amplitude	28.4±2.3	78.2±11.6	144.1±16.0	37.1±4.4	38.6±5.1
D_{max}	79.0±11.4	4.0±160.2	12.0±117.9	72.0±5.0	94.0±38.2
D_{min}	297.0±5.3	238.0±46.1	213.0±23.0	318.0±6.1	331.0±6.2
H_2 (ppb)					
Annual mean 2007	539.6±2.1	574.5±2.4	–	502.4±2.0	500.9±1.5
Annual mean 2008	533.2±3.2	558.2±5.3	–	–	–
Annual mean 2009	533.3±1.6	562.4±1.6	–	–	–
Annual mean 2010	533.5±1.8	563.9±2.3	558.6±2.4	–	–
Annual mean 2011	536.9±1.5	–	555.4±1.6	–	–
Trend (yr^{-1})	-0.5±0.0	-1.3±0.1	–	–	–
RSD	6.6	8.4	7.0	13.3	9.5
Amplitude	15.8±2.2	21.6±3.4	21.3±5.0	16.7±4.0	22.8±3.0
D_{max}	120.0±8.7	96.0±9.6	99.0±8.8	120.0±34.2	51.0±13.4
D_{min}	266.0±39.6	219.0±10.3	353.0±87.8	341.0±78.3	298.0±6.5

Figures

Figure 1 **(a)** Five-day back-trajectories calculated for all sampling dates over the period 2007–2011 at Hanle (HLE), Pondicherry (PON), and Port Blair (PBL) during April–June (AMJ), July–September (JAS), October–December (OND) and January–March (JFM), respectively. Back-trajectories are colored by the elevation of air masses at hourly time step. **(b)** Map of terrain over the zoomed box in **(a)**, showing locations of HLE, PON and PBL. The digital elevation data are obtained from NASA Shuttle Radar Topographic Mission (SRTM) product at 1km resolution (http://srtm.csi.cgiar.org)

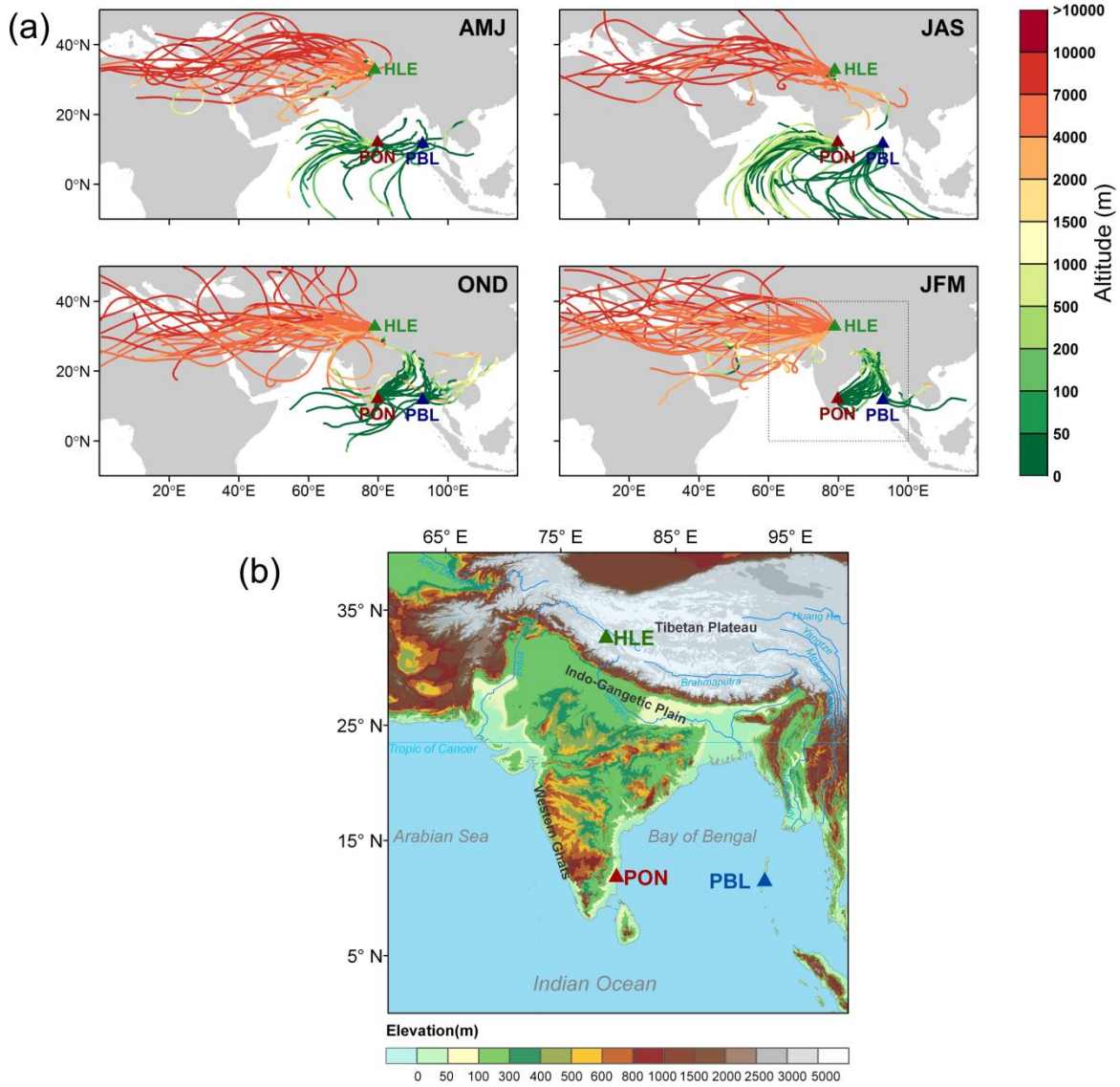

Figure 2 Time series of CO_2 flask measurements at **(a)** HLE and PON, **(b)** HLE and PBL, **(c)** HLE and KZM, and **(d)** HLE and WLG. The open circles denote flask data used to fit the smoothed curves, while the crosses denote discarded flask data lying outside 3 times the residual standard deviations from the smoothed curve fits. For each station, the smoothed curve is fitted using Thoning's method (Thoning et al., 1989) after removing outliers.

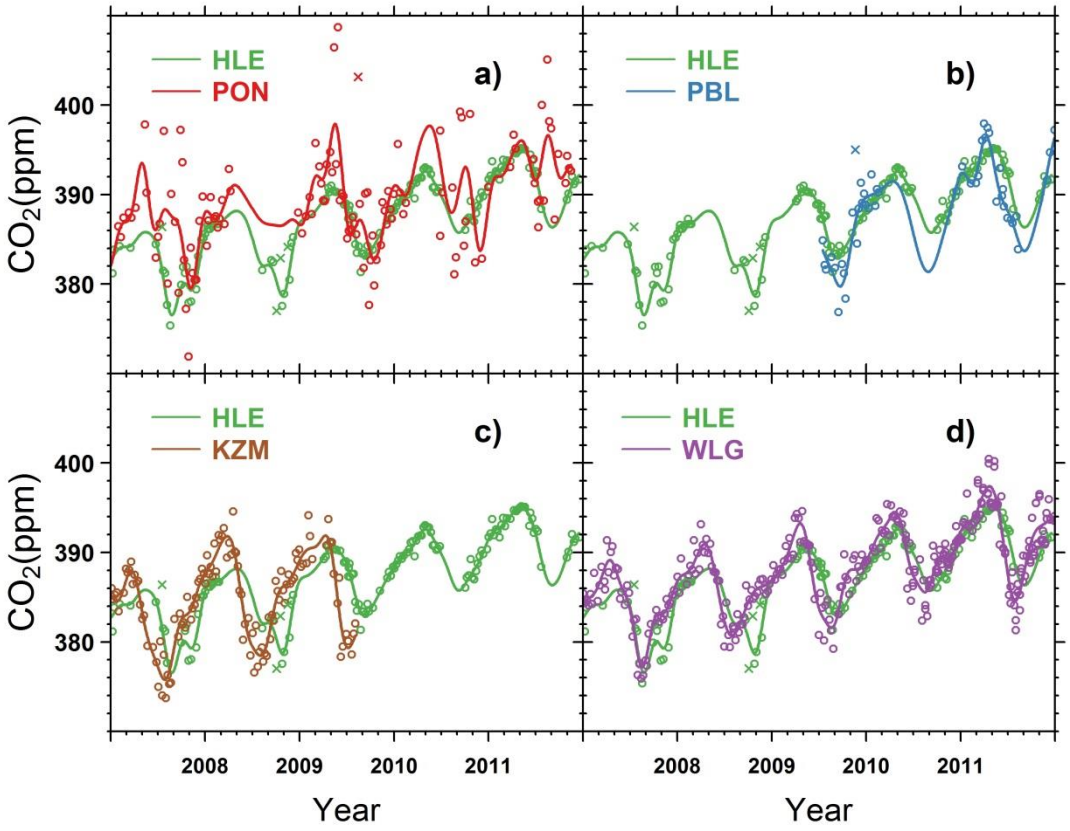

Figure 3 (a) The mean CO_2 seasonal cycle at HLE, in comparison with the mean seasonal cycles derived from the in-situ CO_2 measurements over New Delhi at different altitude bands (3–4 km, 4–5 km, and 5–6 km) by the CONTRAIL project (2006–2010). **(b)** The mean CO_2 seasonal cycles at HLE, KZM and WLG. **(c)** The mean CO_2 seasonal cycles at HLE, PON and PBL. For each station, the mean seasonal cycle is derived from the harmonics of the smoothed fitting curve in Fig. 2. Shaded area indicates the uncertainty of the mean seasonal cycle calculated from 1 s.d. of 1000 bootstrap replicates. For the CONTRAIL datasets, CO_2 measurements over New Delhi were first averaged by altitude bands. A fitting procedure was then applied to the aggregated CO_2 measurements to generate the mean season cycle for different altitude bands.

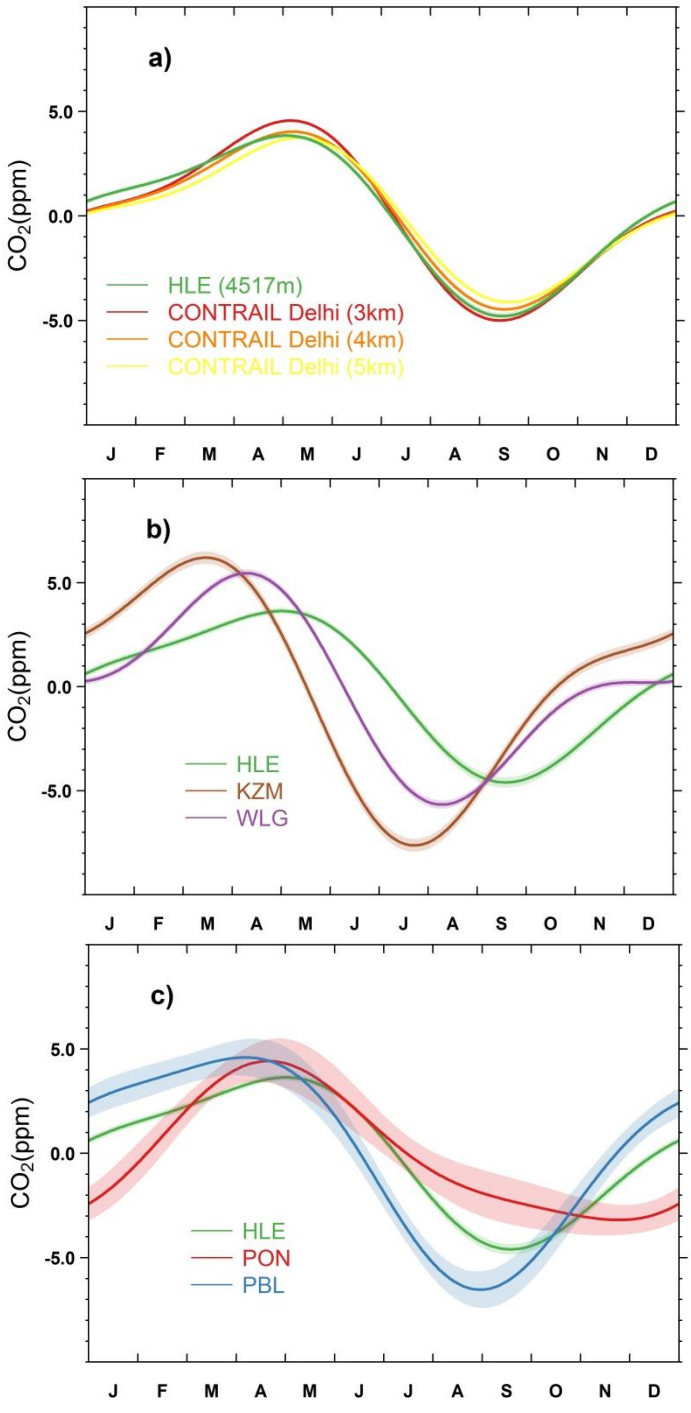

Figure 4 Time series of CH_4 flask measurements at **(a)** HLE and PON, **(b)** HLE and PBL, **(c)** HLE and KZM, and **(d)** HLE and WLG. The open circles denote flask data used to fit the smoothed curves, while the crosses denote discarded flask data lying outside 3 times the residual standard deviations from the smoothed curve fits. For each station, the smoothed curve is fitted using Thoning's method (Thoning et al., 1989) after removing outliers.

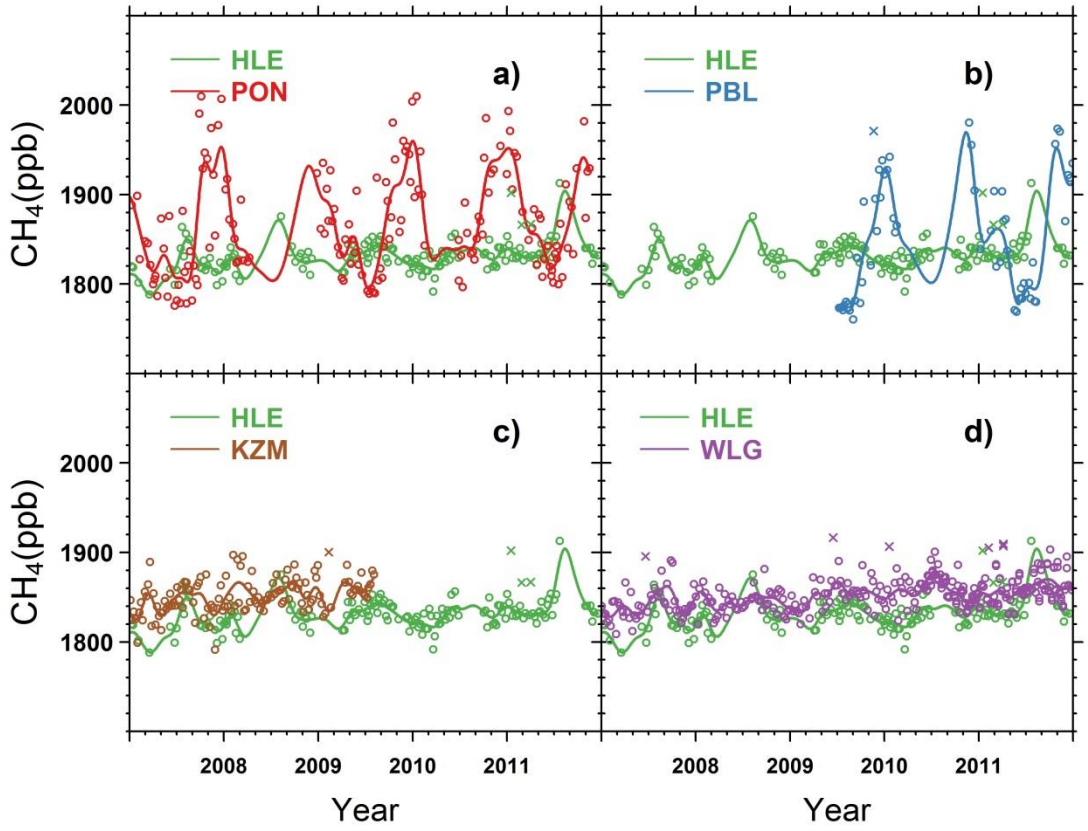

Figure 5 **(a)** The mean CH_4 seasonal cycles observed at HLE, KZM and WLG. The mean CH_4 seasonal cycle derived from aircraft flask measurements by the CARIBIC project is also presented. The CARIBIC flask measurements in the upper troposphere (200-300 hPa) during 2005–2012 are averaged over the Indian subcontinent (10°N-35°N, 60°E-100°E) by month to generate the mean seasonal cycle. The error bars indicate 1 standard deviation of CH_4 flask measurements within the month. **(b)** The seasonal variations of CH_4 emissions from rice paddies and wetlands over the Indian subcontinent. The CH_4 emissions from rice paddies are extracted from a global emission map for the year 2010 (EDGAR v4.2), imposed by the seasonal variation on the basis of Matthews et al. (1991). The CH_4 emissions from wetlands are extracted from outputs of a global vegetation model (BIOME4-TG, Kaplan et al., 2006). The seasonal variation of deep convection over the Indian subcontinent is also presented, indicated by convective precipitation obtained from an LMDz simulation nudged with ECMWF reanalysis (Hauglustaine et al., 2004). The CH_4 emissions and convective precipitation are averaged over the domain 10–35 °N, 70°–90°E to give a regional mean estimate. **(c)** The mean CH_4 seasonal cycles observed at HLE, PON and PBL. For each station, the mean seasonal cycle is derived from the harmonics of the smoothed fitting curve in Fig. 4. Shaded area indicates the uncertainty of the mean seasonal cycle calculated from 1 s.d. of 1000 bootstrap replicates.

1585

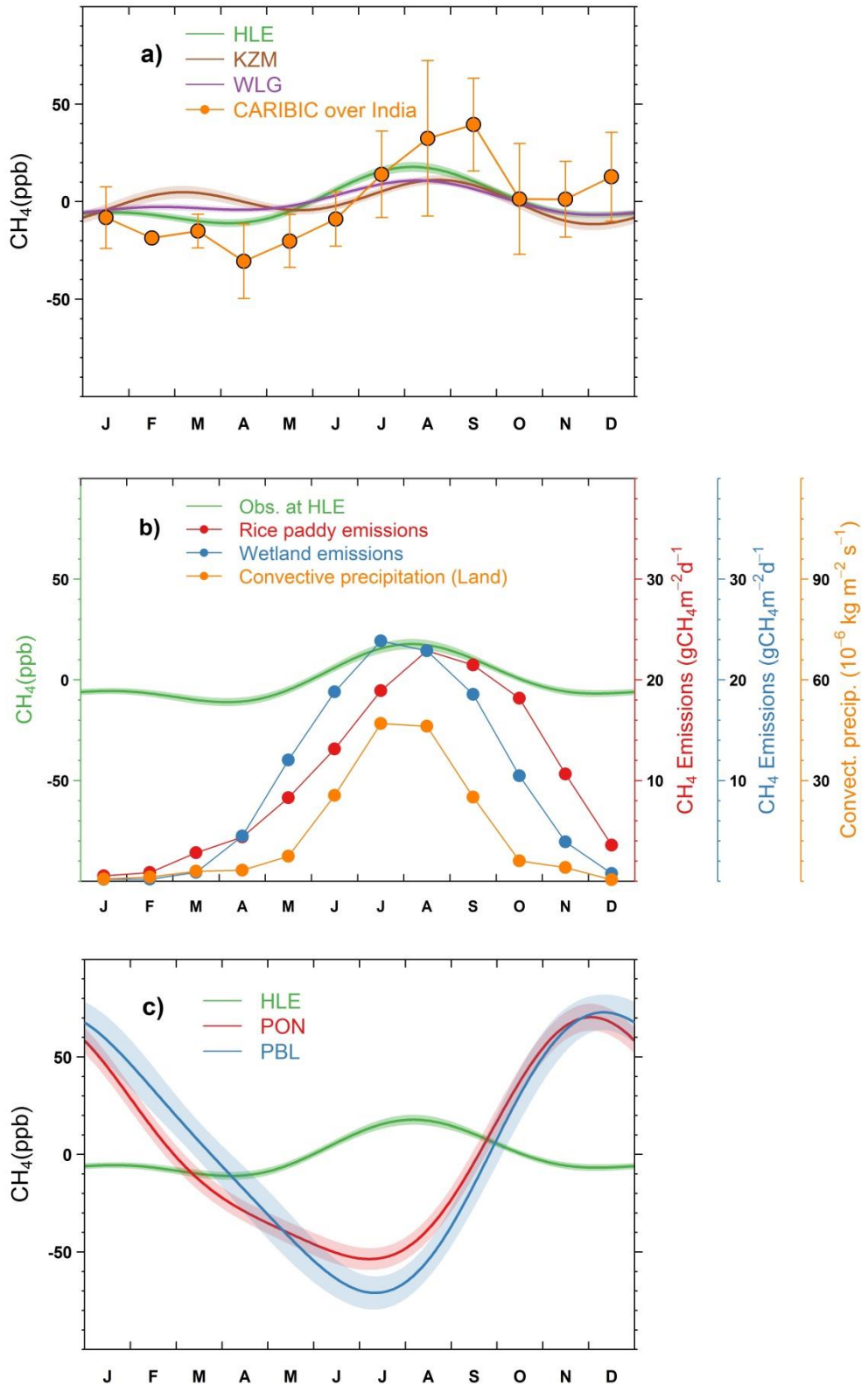
a)
HLE
KZM
WLG
CARIBIC over India
CH4(ppb)
50
0
-50
J F M A M J J A S O N D
b)
Obs. at HLE
Rice paddy emissions
Wetland emissions
Convective precipitation (Land)
CH4(ppb)
CH4 Emissions (gCH4m-2d-1
CH4 Emissions (gCH4m-2d-1
Convect. precip. (10-6 kg m-2 s-1)
30
20
10
90
60
c)
HLE
PON
PBL
CH4(ppb)

Figure 6 Time series of N_2O flask measurements at **(a)** HLE and PON, **(b)** HLE and PBL. The open circles denote flask data used to fit the smoothed curves, while crosses denote discarded flask data lying outside 3 times the residual standard deviations from the smoothed curve fits. For each station, the smoothed curve is fitted using Thoning's method (Thoning et al., 1989) after removing outliers.

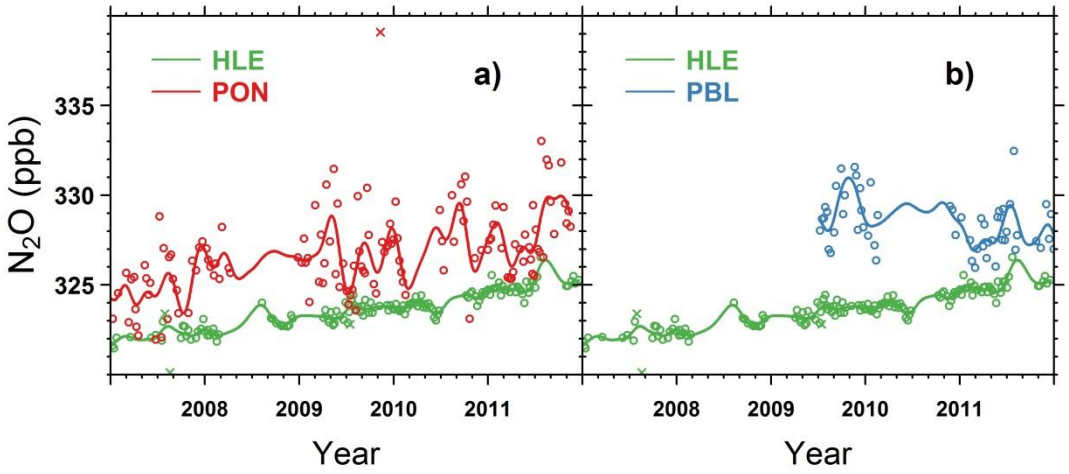

Figure 7 The mean N_2O seasonal cycles observed at **(a)** HLE and PON, **(b)** HLE and PBL. For each station, the mean seasonal cycle is derived from the harmonics of the smoothed fitting curve in Fig. 6. Shaded area indicates the uncertainty of the mean seasonal cycle calculated from 1 s.d. of 1000 bootstrap replicates.

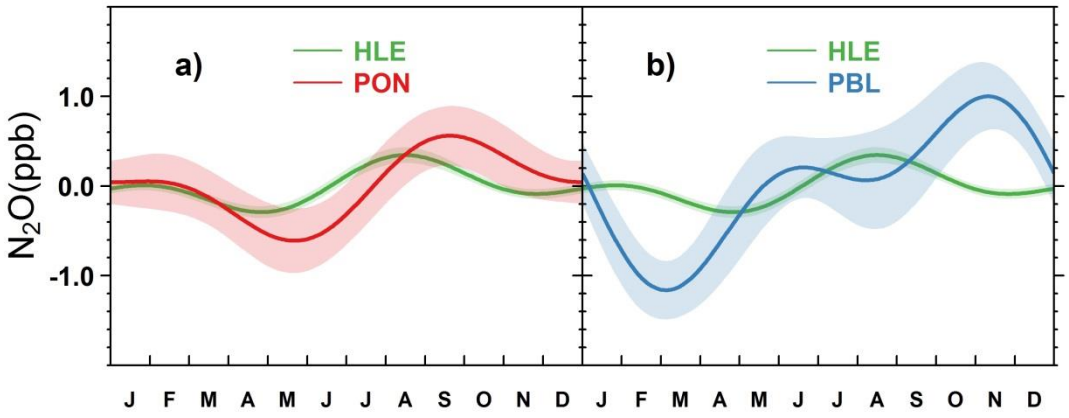

Figure 8 Time series of SF_6 flask measurements at **(a)** HLE and PON, **(b)** HLE and PBL, **(c)** HLE and KZM, and **(d)** HLE and WLG. The open circles denote flask data used to fit the smoothed curves. For each station, the smoothed curve is fitted using Thoning's method (Thoning et al., 1989) after removing outliers.

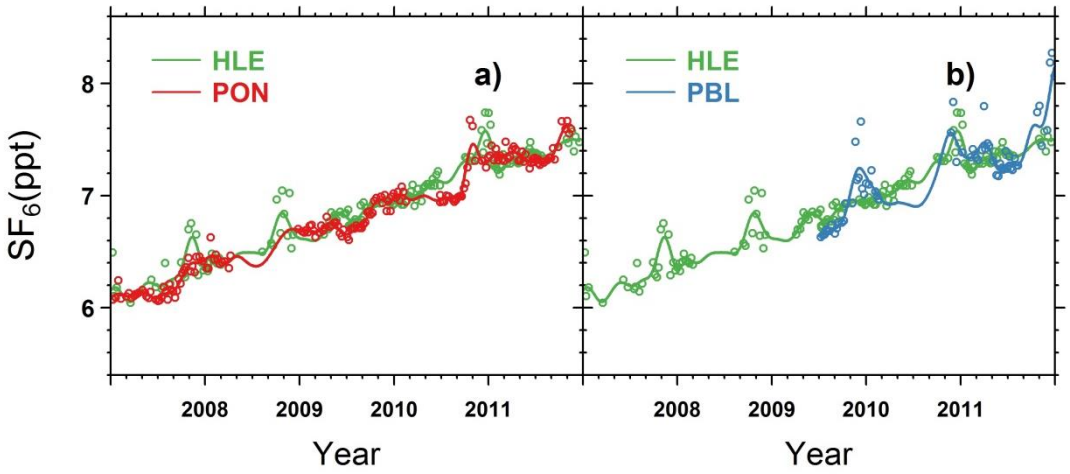

Figure 9 The mean SF_6 seasonal cycles observed at **(a)** HLE and PON, **(b)** HLE and PBL. For each station, the mean seasonal cycle is derived from the harmonics of the smoothed fitting curve in Fig. 8. Shaded area indicates the uncertainty of the mean seasonal cycle calculated from 1 s.d. of 1000 bootstrap replicates.

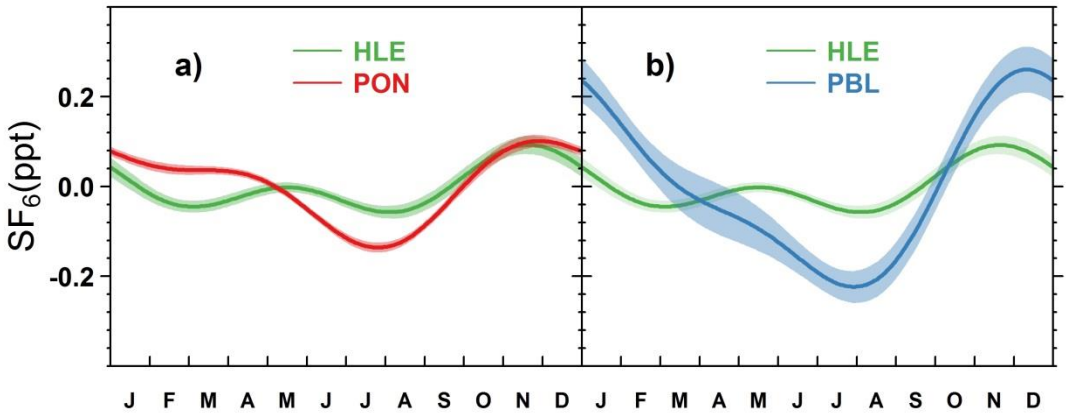

Figure 10 Time series of CO flask measurements at **(a)** HLE and PON, **(b)** HLE and PBL, **(c)** HLE and KZM, and **(d)** HLE and WLG. The open circles denote flask data used to fit the smoothed curves, while the crosses denote discarded flask data lying outside 3 times the residual standard deviations from the smoothed curve fits. For each station, the smoothed curve is fitted using Thoning's method (Thoning et al., 1989) after removing outliers.

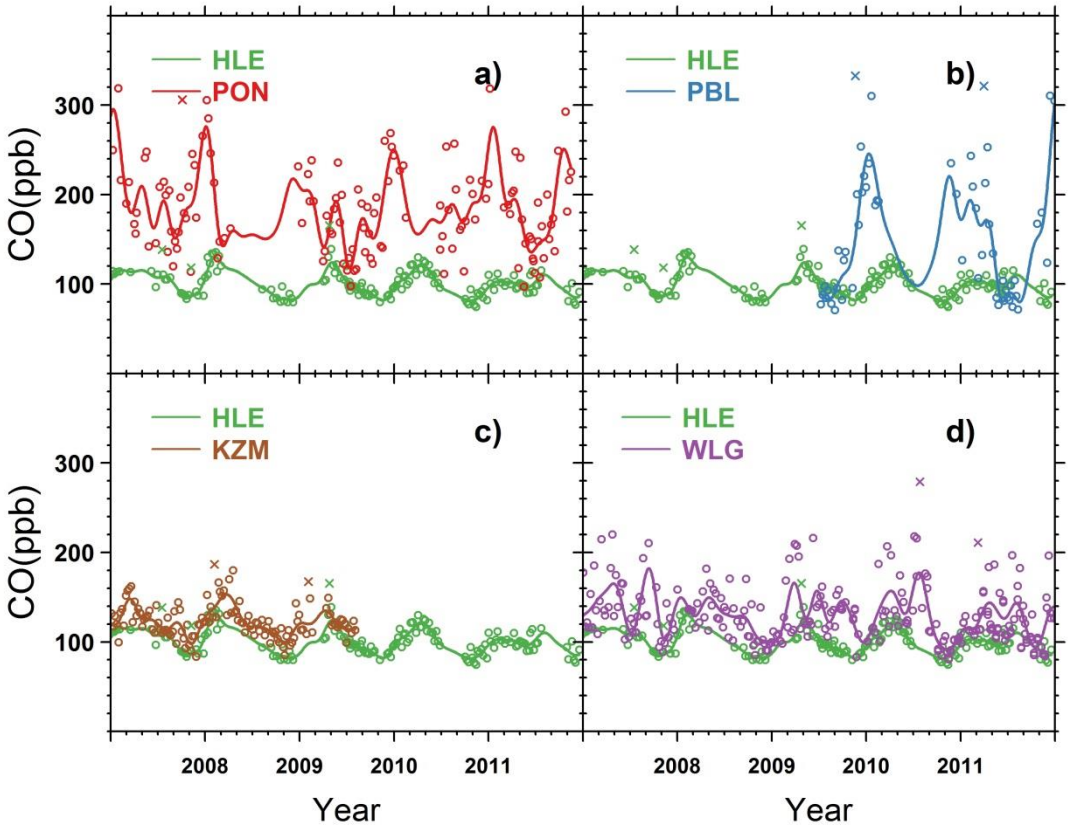

Figure 11 The mean CO seasonal cycles observed at **(a)** HLE and PON, **(b)** HLE and PBL, **(c)** HLE and KZM, and **(d)** HLE and WLG. For each station, the mean seasonal cycle is derived from the harmonics of the smoothed fitting curve in Fig. 10. Shaded area indicates the uncertainty of the mean seasonal cycle calculated from 1 s.d. of 1000 bootstrap replicates.

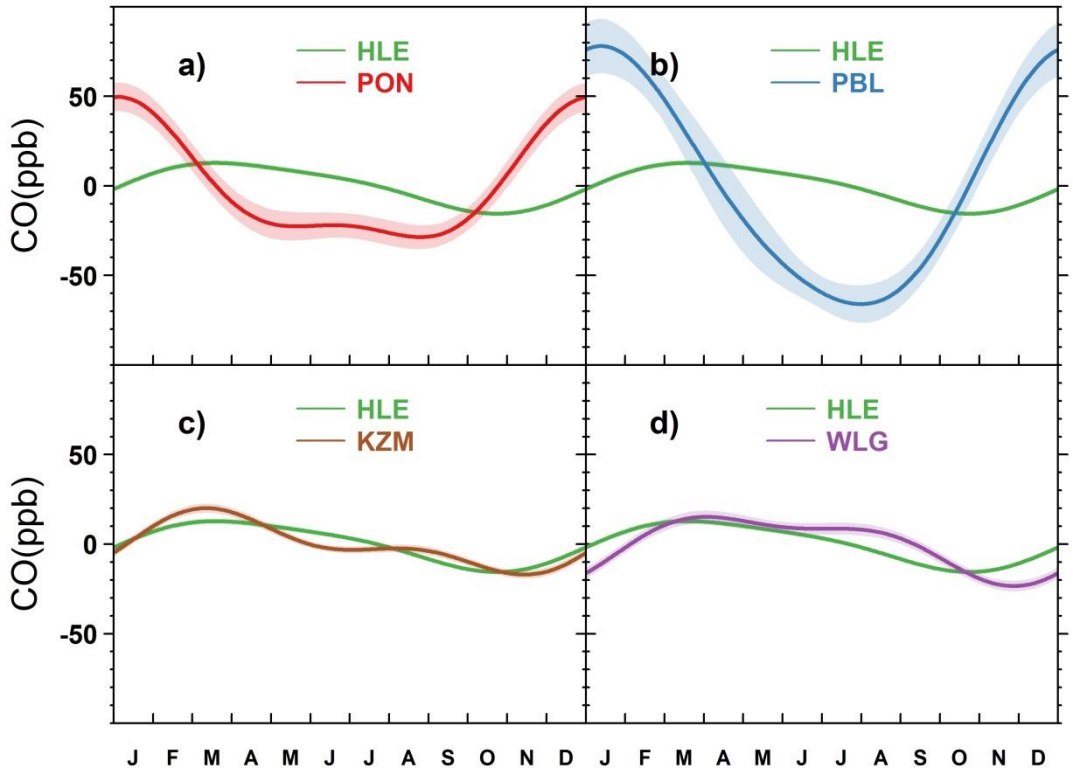

Figure 12 Time series of H_2 flask measurements at **(a)** HLE and PON, **(b)** HLE and PBL, **(c)** HLE and KZM, and **(d)** HLE and WLG. The open circles denote flask data used to fit the smoothed curves, while the crosses denote discarded flask data lying outside 3 times the residual standard deviations from the smoothed curve fits. For each station, the smoothed curve is fitted using Thoning's method (Thoning et al., 1989) after removing outliers.

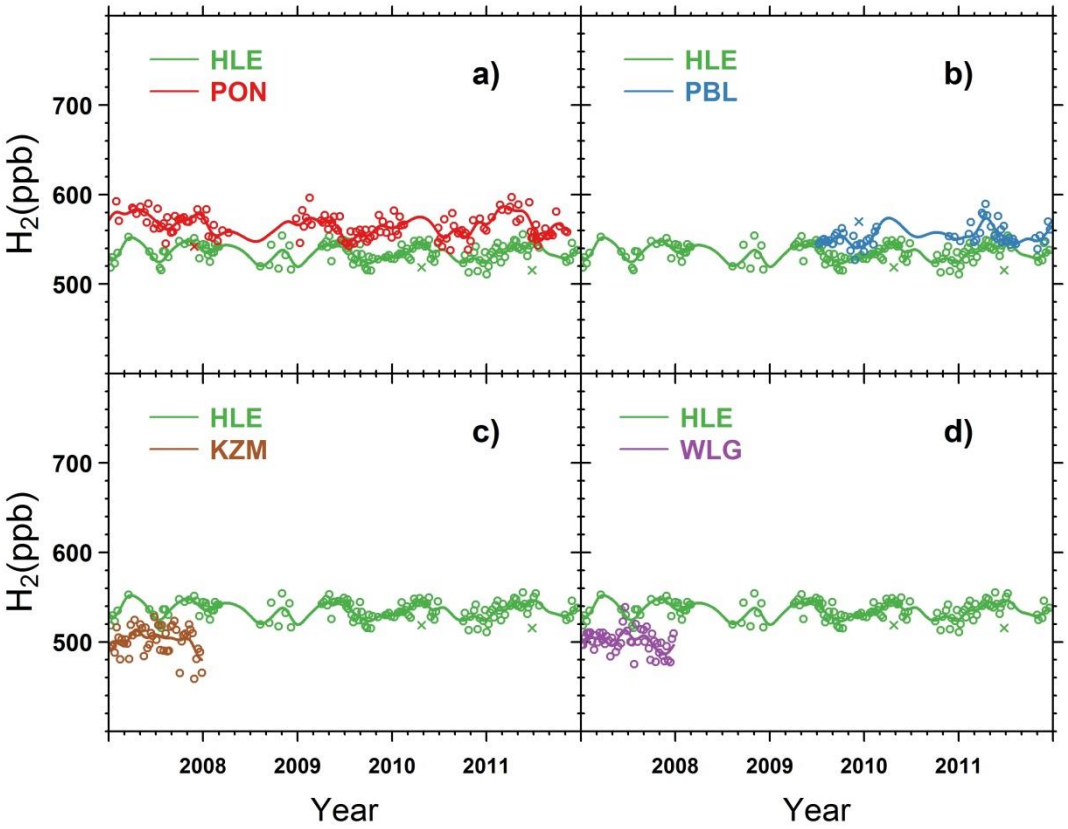

Figure 13 The mean H_2 seasonal cycles observed at **(a)** HLE and PON, **(b)** HLE and PBL, **(c)** HLE and KZM, and **(d)** HLE and WLG. For each station, the mean seasonal cycle is derived from the harmonics of the smoothed fitting curve in Fig. 12. Shaded area indicates the uncertainty of the mean seasonal cycle calculated from 1 s.d. of 1000 bootstrap replicates.

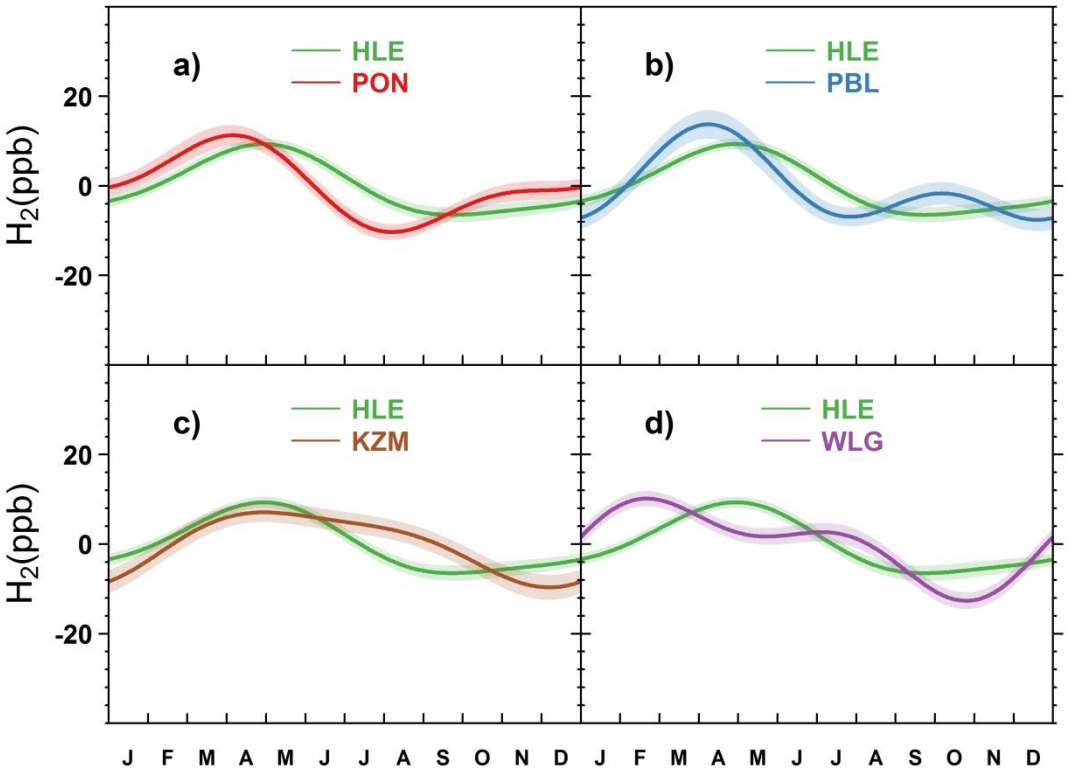

Figure 14 The relationships between ΔCH_4 and ΔCO at HLE **(a–d)**, PON **(e–h)**, and PBL **(i–l)** for April–June (AMJ), July–September (JAS), October–December (OND), and January–March (JFM). For each panel, ΔCH_4 and ΔCO are estimated as residuals from smoothed curves. The $\Delta CH_4/\Delta CO$ ratio is the slope of the fitting line from the orthogonal distance regression, with the SD calculated from 1000 bootstrap replications.

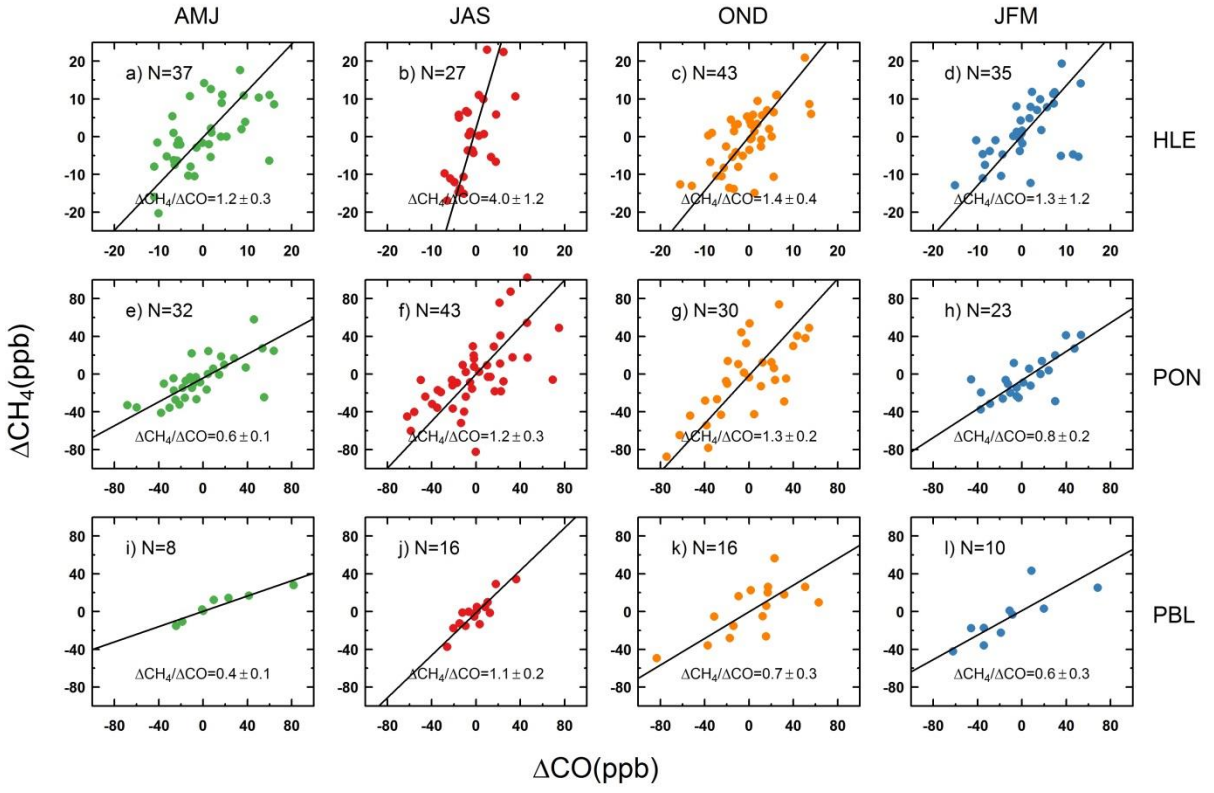

Figure 15 The relationships between ΔCH_4 and ΔCO_2 at HLE **(a–d)**, PON **(e–h)**, and PBL **(i–l)** for April–June (AMJ), July–September (JAS), October–December (OND), and January–March (JFM). For each panel, ΔCH_4 and ΔCO_2 are estimated as residuals from smoothed curves. The $\Delta CH_4/\Delta CO_2$ ratio is the slope of the fitting line from the orthogonal distance regression, with the SD calculated from 1000 bootstrap replications. For ΔCH_4 and ΔCO_2 that is not significantly correlated, the fitting line is not plotted.

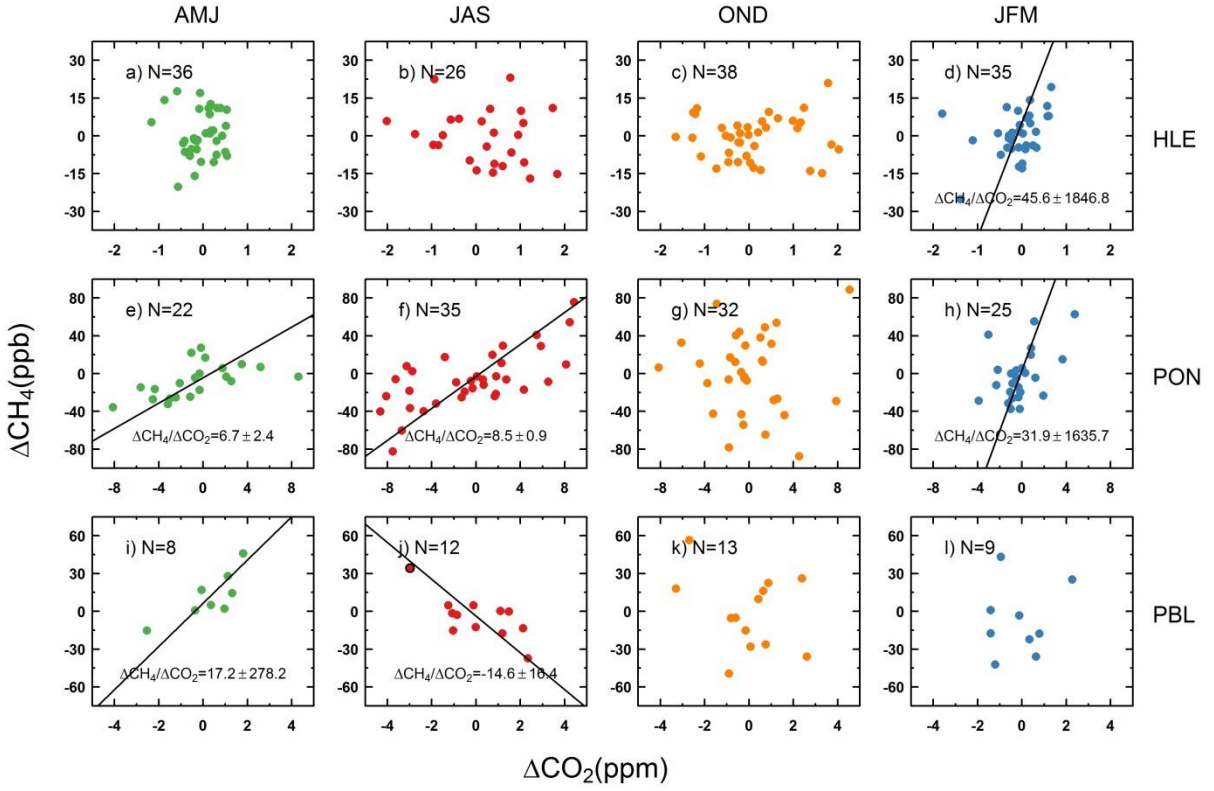

Figure 16 The relationships between ΔCO and ΔCO_2 at HLE **(a–d)**, PON **(e–h)**, and PBL **(i–l)** for April–June (AMJ), July–September (JAS), October–December (OND), and January–March (JFM). For each panel, ΔCO and ΔCO_2 are estimated as residuals from smoothed curves. The $\Delta CO/\Delta CO_2$ ratio is the slope of the fitting line from the orthogonal distance regression, with the SD calculated from 1000 bootstrap replications. For ΔCO and ΔCO_2 that is not significantly correlated, the fitting line is usually not plotted.

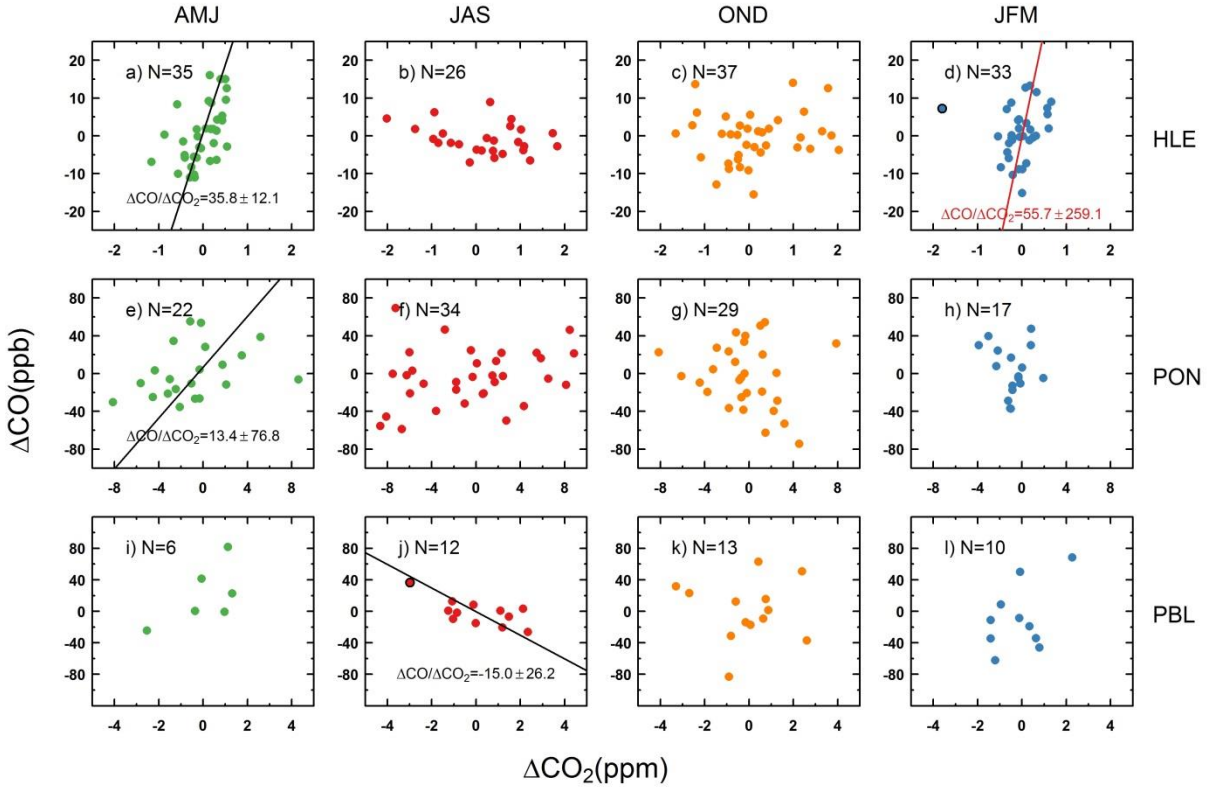

Figure 17 (a) The relationship between ΔCH_4 and ΔCO at PBL (colored by red) and BKT (colored by grey) during July–September (JAS) over the period of 2007–2011. ΔCH_4 and ΔCO are estimated as residuals from smoothed curves. The $\Delta CH_4/\Delta CO$ ratio is the slope of the fitting line from orthogonal distance regression (ODR), with the SD calculated from 1000 bootstrap replications. Two abnormal events at PBL are labeled, with enhancements of CH_4 and CO on September 16, 2009 and July 29, 2011, respectively. Enhancements of CH_4 and CO are also observed at BKT on Sep. 8, 2009. **(b)** Hourly CH_4 and CO measurements at BKT in July, 2011 (BMKG & EMPA). Enhancements of CH_4 and CO are observed during July 17-21, 2011.